Technical Report

TR-00-11

A natural analogue for copper waste canisters: The copper-uranium mineralised concretions in the Permian mudrocks of south Devon, United Kingdom

A E Milodowski, M T Styles, V L Hards
Natural Environment Research Council
British Geological Survey

August 2000

Svensk Kärnbränslehantering AB
Swedish Nuclear Fuel
and Waste Management Co
Box 5864
SE-102 40 Stockholm Sweden
Tel 08-459 84 00
+46 8 459 84 00
Fax 08-661 57 19
+46 8 661 57 19

A natural analogue for copper waste canisters: The copper-uranium mineralised concretions in the Permian mudrocks of south Devon, United Kingdom

A E Milodowski, M T Styles, V L Hards
Natural Environment Research Council
British Geological Survey

August 2000

Executive summary

This report presents the results of a small-scale pilot study of the mineralogy and alteration characteristics of unusual sheet-like native copper occurring together with uraniferous and vanadiferous concretions in mudstones and siltstones of the Permian Littleham Mudstone Formation, at Littleham Cove (near Budleigh Salterton), south Devon, England. The host mudstones and siltstones are smectitic and have been compacted through deep Mesozoic burial. The occurrence of native copper within these rocks represents a natural analogue for the long-term behaviour of copper canisters, sealed in a compacted clay (bentonite) backfill, that will be used for the deep geological disposal of high-level radioactive waste by the Svensk Kärnbränslehantering AB (SKB). The study was undertaken by the British Geological Survey (BGS) on behalf of SKB between November 1999 and June 2000. The study was based primarily on archived reference material collected by the BGS during regional geological and mineralogical surveys of the area in the 1970's and 1980's. However, a brief visit was made to Littleham Cove in January 2000 to try to examine the native copper in situ and to collect additional material. Unfortunately, recent landslips and mudflows obscured much of the outcrop, and only one new sample of native copper could be collected.

The native copper occurs as thin plates, up to 160 mm in diameter, which occur parallel to bedding in the Permian Littleham Mudstone Formation at Littleham Cove (near Budleigh Salterton) in south Devon. Each plate is made up of composite stacks of individual thin copper sheets each 1–2 mm thick. The copper is very pure (>99.4% Cu) but is accompanied by minor amounts of native silver (also pure - >99%) which occurs as small inclusions within the native copper. Detailed mineralogical and petrological studies of the native copper sheets, using optical petrography, backscattered scanning electron microscopy, X-ray diffraction analysis and electron probe microanalytical techniques, reveal a complex history of mineralisation and alteration that can be related to the burial and diagenetic history of the Permian strata.

The native copper mineralisation exhibits close temporal association with the formation of uraniferous and vanadiferous concretions (known as "fish-eyes") in the same rocks. Petrographical relationships indicate that both the copper and the "fish-eye" concretions formed during burial diagenesis but before the maximum compaction of the host mudstone and siltstone. The regional burial history Wessex Basin (Chadwick, 1985), indicates that the maximum compaction of the Permian strata would have been achieved by at least the end of the Lower Jurassic (possibly even in the Triassic). Therefore, the native copper mineralisation is older than 176 Ma.

The native copper sheets display a complex sequence of alteration and subsequent mineral growth of minerals on their surfaces. The earliest alteration was to copper oxides – principally cuprite with minor tenorite, indicating a change to more oxidising groundwater conditions. The dissolution of native silver and the growth of fringes of copper arsenides followed this. Nickel arsenides and chalcocite, associated with the precipitation of uranium silicates occurred in the later stages of alteration. This suggests a return to a more reducing porewater environment. Again, petrographical relationships indicate that this alteration and subsequent mineralisation is geologically old (i.e. Lower Jurassic or older).

Secondary malachite, intimately intergrown copper sulphate and copper oxides, copper chloride, copper-uranium arsenate and uranium vanadates have formed as late-stage alteration products of the native copper and earlier diagenetic cuprite, chalcocite, copper-nickel arsenide and uranium silicate alteration and mineralisation. This late-stage alteration is most probably attributable to near-surface weathering processes.

Although the native copper is affected by corrosion, the study has shown that a significant proportion (30–80% of the original thickness) of the copper sheets has been preserved in the saturated compacted clay environment of the Littleham Mudstone for many millions of years, at least since the end of the Lower Jurassic. Apart from the recent weathering effects due to exposure at outcrop, most of the observed corrosion and alteration of the native copper is geologically old and also occurred before the end of the Lower Jurassic. This demonstrates that the native copper can remain stable in a saturated and compacted clay environment for geological timescales (over 176 Ma) well in excess of the timescales considered for Performance Assessment. Since the copper sheets found in the Littleham Mudstone Formation are very thin (1–2 mm) and have survived over this long time, waste canisters – which will be made from much thicker copper – would be expected (by comparison) to show greater performance.

Contents

List of plates

List of figures

Chapter 2

Chapter 5

1 Introduction

The Swedish concept for the geological disposal of spent fuel and high-level radioactive wastes (HLW) at depths of up to 700 m in crystalline basement rocks envisages the use of a multi-barrier engineered repository system. The waste form is planned to be encapsulated in a corrosion-resistant canister, surrounded by a compacted bentonite buffer, which will act to seal and isolate the waste canisters from the adjacent environment within a granitic host rock /Werme, 1998/. The design of the disposal system intends that the canister will prevent all dispersal of radioactivity to the surrounding rock mass, as long as it remains intact, whilst the other components of the barrier system (the bentonite buffer backfill and the repository host rock itself) can retard and attenuate radionuclide dispersal to acceptable levels if the canister starts to leak /Werme, 1998/. Ideally, the canister should be sufficiently resistant to corrosion in order to contain and isolate the waste for at least 100 000 years – the timescale considered in Performance Assessment (PA) for the radioactivity to decay to levels that are compatible to the acceptable target risk for the various radiotoxicological components of the waste /Werme, 1998/. In addition, neither the canister material nor its corrosion products should have deleterious effects on other barrier components, in order that these components remain effective in retarding or attenuating radionuclide migration should canister failure and leakage occur /Werme, 1998/.

Various metals have been considered for use in canister construction but copper metal has been selected by Svensk Kärnbränslehantering AB (SKB) as the most suitable, on the basis of its cost and corrosion resistance /Werme, 1998/. Copper has similarly been selected in the design concepts for canister construction in the Canadian and Finnish radioactive waste disposal programmes /Johnson et al, 1994; King, 1995/. In the United Kingdom, British Nuclear Fuels Limited at one time also considered employing copper waste canisters to isolate glassified HLW for potential sea-bed disposal options /Tylecote, 1979/.

Experimental and theoretical studies suggest that copper has a wide stability range and that corrosion effects will be small in the mildly alkaline, reducing groundwater environment that is anticipated will persist during much of the lifetime of a potential Swedish repository /Werme, 1998 and references therein/. Of principal concern to the stability of the copper is the potential presence of dissolved sulphides in the groundwater, which can enhance copper corrosion, or the formation of sulphides as a result of the activity of sulphate reducing bacteria. Both dissolved sulphide concentration in groundwater, and the potential activity of sulphate-reducing bacteria within the compacted backfill around the canisters are considered likely to be minimal within the current SKB repository design concepts /Werme, 1998/. However, because geological systems often involve complex interrelated processes that occur over extremely long time scales, these processes often cannot be adequately reproduced or represented in short-term laboratory experiments. Therefore, long-term predictions of the performance of the repository system are subject to uncertainty if they are based solely on theoretical calculations using information derived from short-term experimental observations. These uncertainties can be reduced by studying the processes operating in natural systems of a broadly equivalent nature (“natural analogues”) that can be demonstrated to have been operative over a long period of time /Chapman and McKinley, 1987; Miller et al, 1994/. Natural analogues can serve to:

(i) identify important long-term processes that might influence the behaviour of the repository system;

(ii) test whether models of processes that underpin PA for the behaviour of repository components, waste form dissolution or radionuclide-rock interactions are adeuate and realistic;

(iii) provide illustrative material to demonstrate our degree of understanding of long-term processes, thereby building public and peer confidence in PA for a repository.

There have been several natural analogue investigations relating to the corrosion and longevity of copper. Most of these have involved the study of buried archaeological artefacts (e.g. coins, ingots, scrap metal, sculptures, weapons, axes and other tools) composed of copper or tin-bronzes /Tylecote, 1979; Bresle et al, 1983; Miller et al, 1994/. However, the chemical composition of the artefacts and the environment in which they are found are seldom representative of real repository materials and geochemical conditions /Miller et al, 1994/. Studies of copper corrosion rates have also been made on buried lightning conductor plates /Hallberg et al, 1984/. A particularly detailed study of copper corrosion in relation to waste canister behaviour is that carried out on a bronze cannon recovered from the wreck of the Swedish man-of-war "Kronan", which sank in the Baltic Sea during the Battle of Öland in 1676 /Hallberg, 1988; Miller et al, 1994; King, 1995/. The cannon was partially buried in a vertical position in tightly packed, seawater-saturated clay sediments containing montmorillonite. The vertical redox profile through the sediments provided the opportunity to study corrosion in an environment that is broadly analogous to copper canisters surrounded by bentonite buffer in the SKB repository design. However, the environment of the Kronan cannon is considered to be generally more oxidising than is anticipated within a HLW repository /Miller, 1994/.

Whilst observations on buried industrial and archaeological artefacts provide valuable information on processes operating over the 10 to 10^3 year timescale, observations from geological analogues are also required to evaluate processes that operate over the longer timescales required in PA, and validate model predictions. Copper occurs naturally as a native metal and, therefore, can be stable in certain environments over geological timescales. However, the fact that most copper deposits are hydrothermal in origin demonstrates that copper can also be extremely mobile in some groundwater systems /Miller et al, 1994/. Marcos /1989, cited by Miller op.cit./ examined copper from a range of different geological associations, as natural analogues for copper waste canisters. She found that native copper metal remained stable under a broad range of hydrogeological environments, but none of these are really representative of a repository environment.

In relation to this, the British Geological Survey (BGS) was commissioned by SKB to undertake a small-scale pilot study of the mineralogy and alteration characteristics of native copper occurring together with unusual uraniferous concretions in the Permian mudrocks of south Devon (United Kingdom). These copper occurrences and uranium-rich concretions represent a potential natural analogue for the long-term behaviour of copper waste canisters surrounded by a bentonite buffer - as envisaged in the SKB design for a HLW repository. This report describes the work carried out by the BGS for this study, under SKB Purchase Order No. 2248/1, between November 1999 and May 2000.

2 Geological setting

2.1 General geology

Native copper, closely associated with uranium, vanadium, nickel, cobalt, copper, lead, silver, barium, selenium, arsenic and sulphide mineralisation, occurs within complex diagenetic concretions in the Permian Littleham Mudstone Formation of south Devon in southwest England. These mudstones are best exposed in the cliffs between the western end of Littleham Cove (National Grid Reference ST 037 795) and the town of Budleigh Salterton (National Grid Reference ST 060 816), approximately 4 km east of Exmouth and the estuary of the River Exe (Figure 2-1). The geology of the area is summarised in Figures 2-1 and 2-2.

The area lies close to the western margin of the Wessex Basin. This major sedimentary basin consists of a system of post-Variscan sedimentary depocentres and intra-basinal highs that developed across central southern England and adjacent offshore areas /Underhill and Stonely, 1998/. It represents a series of extensional sub-basins that form part of an extensive network of Mesozoic intracratonic basins that covered much of NW Europe /Ziegler, 1990/. The basin was initiated in the Permian and, except for localised volcanic rocks at the base of the Permian sequence (Exeter Volcanic Series), the basin was essentially filled by a thick sequence of Permian to Tertiary (Oligocene) sedimentary rocks. The western margin of the basin is delineated by the unconformity between the Permo-Triassic rocks and the underlying Variscan basement rocks, comprising deformed and metamorphosed Devonian and Carboniferous strata intruded by a major granite batholith (the Dartmoor Granite).

The Permo-Triassic rocks are continental (red-bed) sediments /Allen and Holloway, 1984; Underhill and Stonely, 1998, and references therein/. West of the Exe Estuary, the Permian strata rest unconformably on the Variscan basement /Bateson, 1987/. They comprise basal breccias and conglomerates succeeded by sandstone (Exmouth and Dawlish Beds) interbedded with thin lavas (Exeter Volcanic Series). These were deposited on a deeply dissected basement surface in a number of east-west trending intramontaine basins which opened into the broader Wessex Basin to the east /Allen and Holloway, 1984; Underhill and Stonely, 1998/. The strata represent locally derived detritus deposited as interdigitating alluvial fans with some aeolian sands, and were probably deposited under a hot semi-arid environment /Henson, 1970; Smith et al, 1974/.

The basal Permian strata are overlain, to the east of the Exe Estuary, by a dominantly argillaceous sequence – the Aylesbeare Mudstone Group (Figure 2-1). These have gentle regional dip of 5-10° to the east. In south Devon (south of Aylesbeare) these strata can be subdivided into two discrete units /Tandy, 1974; Harrison, 1975; Bateson, 1987, and references therein/: the Exmouth Mudstone and Sandstone Formation (lower unit) and the Littleham Mudstone Formation (upper unit). Further north, this lithological distinction within the Aylesbeare Mudstone Group cannot be made.

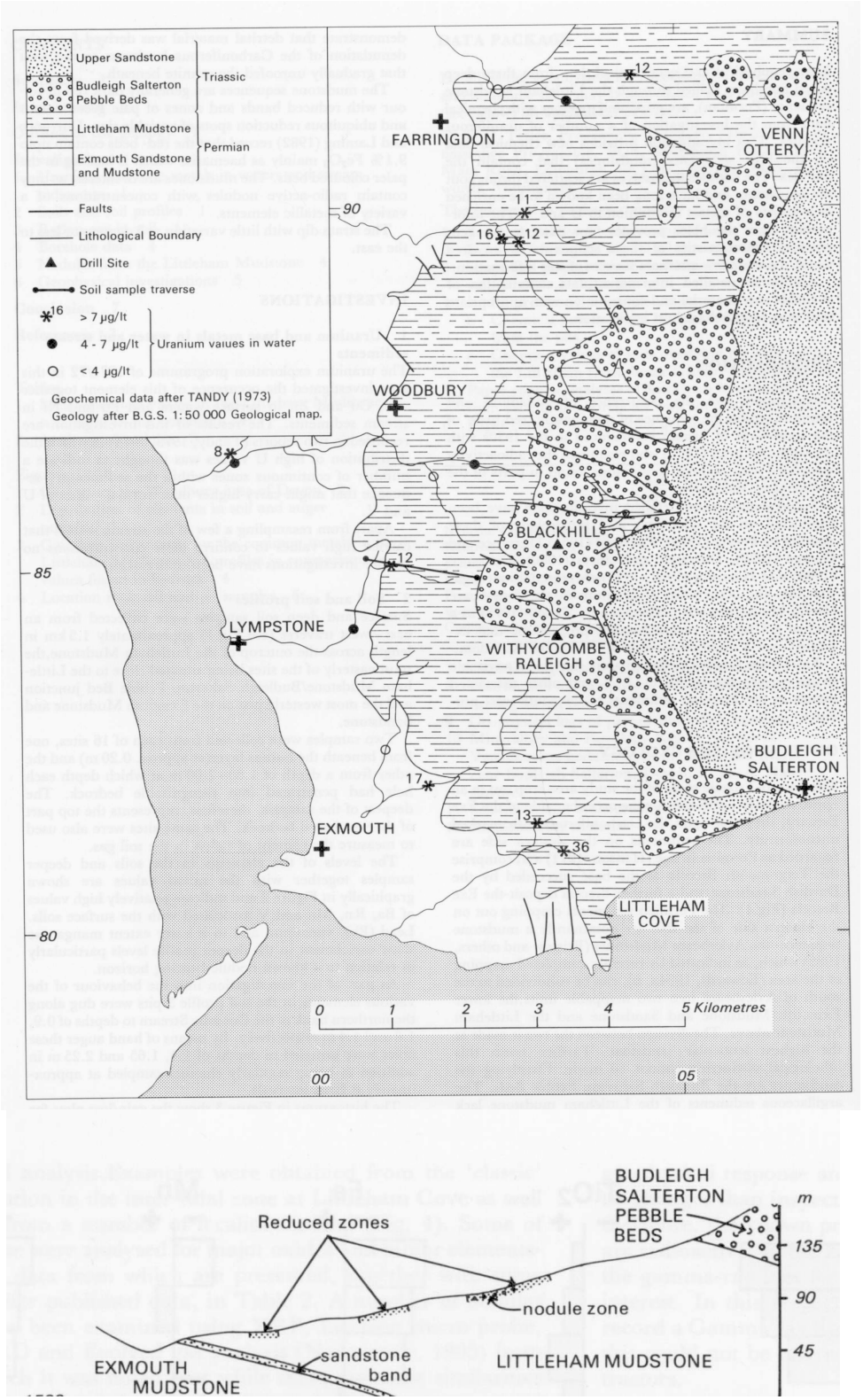

Figure 2-1. *Geological map and cross-section of the Littleham Cove-Budleigh Salterton area /taken from Bateson, 1987/.*

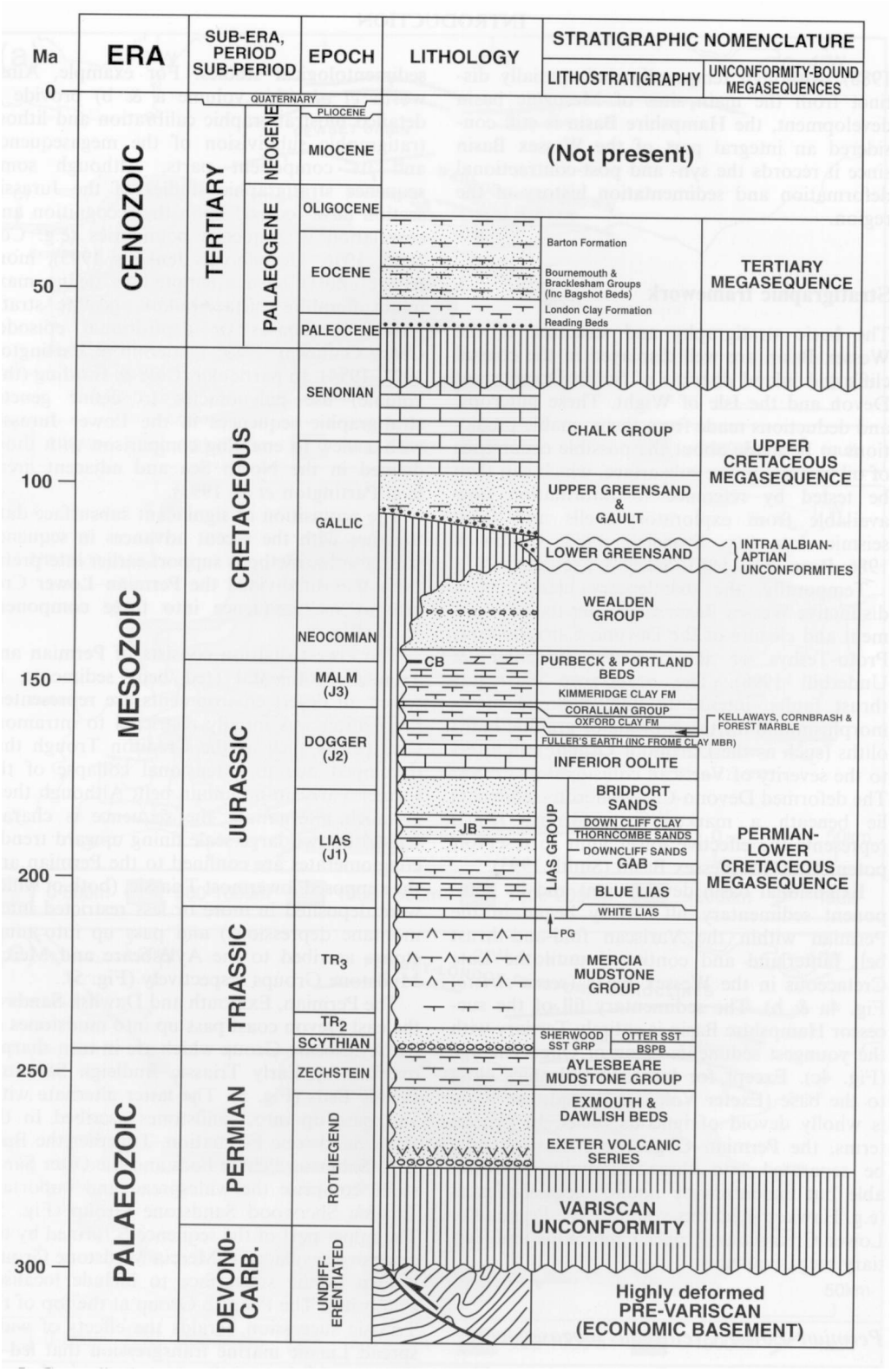

Figure 2-2. *Generalised stratigraphical sequence for the Wessex Basin /taken from Underhill and Stonely, 1998/.*

The Exmouth Mudstone and Sandstone Formation is exposed along the coast between Exmouth and Littleham Cove (Figure 2-1). The unit is characterised by a cyclic sequence of thick reddish-brown current-bedded and channel sandstones (>1.25 m thick) near the base, and reddish-brown mudstones and siltstones with numerous thin and lenticular sandstones, often cut by sandstone dykes. The rocks commonly display greenish or "bleached" horizons, lenses and greenish reduction spots. The distinct "bleached" band, mainly in the coarser sandstones, is often stratiform although there are also non-stratiform zones of bleaching and reduction /Harrison, 1975/. The bleaching is due to the reduction and dissolution of fine-grained disseminated ferric oxides in the rocks /Harrison, 1975/.

The Littleham Mudstone Formation is generally finer grained and comprises a sequence of blocky and laminated red-brown mudstones intercalated with numerous thin but persistent olive-green silty sandstone and sandy siltstone beds. It is exposed between the western end of Littleham Cove and approximately 1 km west of Budleigh Salterton (Figure 2-1). The formation is estimated to have a maximum thickness of about 115 m /Tandy, 1974/, although extensive and severe landslips, mudslides and cliff falls obscure much of the outcrop.

The Aylesbeare Group is considered to be probably of Zechstein (Upper Permian) age. The strata are interpreted as an alluvial floodplain or flood basin complex /Henson, 1970; Allen and Holloway, 1984/. The coarser sandstones and gravels formed as channel deposits, whilst the finer silty sandstones, siltstones and mudstones represent deposition as overbank flood deposits, levee and crevasse splay deposits /Henson, 1970; Tandy, 1974/. The formation of ephemeral lakes is indicated by ripple bedding and infilled abandoned channels represent transitional sedimentation. Channel deposits dominate the Exmouth Mudstone and Sandstone Formation, whereas flood deposits are predominant in the Littleham Mudstone Formation.

To the east, approximately 1 km west of Budleigh Salterton, the Littleham Mudstone Formation is unconformably overlain by the Budleigh Salterton Pebble Bed (Figure 2-1). This conglomeratic formation is considered to represent the basal Triassic. In turn, this is overlain by the Sherwood Sandstone Group (Otter Sandstone Formation), which represents a very thick sequence of fluvial-dominated red-bed sandstones that extends throughout much of the Wessex Basin /Allen and Holloway, 1984; Underhill and Stonely, 1998/.

A coastal section between Exmouth and Littleham Cove is cut by several approximately N-S and NW-SE faults, often showing evidence of small normal displacements, mostly with downthrows to the east. However, in some cases, these faults may display strike-slip /Harrison, 1975/ or even reversed movement.

2.2 Occurrence of uraniferous, vanadiferous and copper-bearing concretions

Unusual nodules or concretions, enriched in uranium, vanadium, lead, nickel, cobalt, chromium, copper, silver, zinc, arsenic and selenium, occur abundantly in localised horizons within the Littleham Mudstone Formation. Small amounts of copper mineralisation (chalcopyrite and secondary copper carbonates/ have also been recorded as

minor matrix cements, and as coatings on joints and along bedding planes, from the Exmouth Mudstone and Sandstone Formation between Exmouth and Littleham Cove /Carus-Wilson, 1913/. The uraniferous-vanadiferous nodules are most abundantly developed at the south-western half of Littleham Cove, between Straight Point and just west of the base of West Down Beacon /Harrison, 1975/. Here, nodule-rich horizons are seen in the base of the cliffs and, at the western end, in the wave-cut platform that is exposed at low tide.

To date, investigations of these concretions have focused on the uraniferous-vanadiferous concretions, locally referred to as "fish-eyes" /Craik-Smith, 1999/. These concretions were first recognised by Carter /1931/, from a brick pit at Withycombe Rayleigh and from the coastal section at Littleham Cove. The brick pit at Withycombe Rayleigh has subsequently been backfilled and built over by modern housing development and is no longer exposed. Subsequently, detailed mineralogical studies of the nodules were made by Perutz /1939/ and Ponsford /1955/. More recently, the concretions have been examined as a result of exploration and assessment of potential uranium and vanadium resources in the United Kingdom /Tandy, 1973; Tandy, 1974; Harrison, 1975; Bateson, 1987/, and as potential sources for the localised concentrations of radon found in stream waters, groundwaters and soils of southeast Devon /Durrance, 1978; Durrance and George, 1976; Durrance et al, 1980/.

Morphologically and mineralogically, the uraniferous-vanadiferous nodules are very complex /Perutz, 1939; Harrison, 1975; Durrance and George, 1976/. They range in size from 1 mm to 10 cm diameter. Their morphologies include: (i) irregular black concretions, with irregularities being filled by grey clay; (ii) spheroidal-asteroidal concretions consisting of a black core surrounded by grey clay and in turn, by black material, which on its outer surface extends as radial fins away from the centre of the concretion; to (iii) concentric spherical concretions consisting of a black core (which is often irregular) surrounded by successive concentric bands or "shells" of siltstone impregnated by fine black mineralisation separated by lithified grey siltstone. The black bands are enriched in vanadium and contain up to 14% V_2O_3 /Harrison, 1975; Durrance et al, 1980; Nancarrow, 1985/, which may be present as authigenic montroseite (VO.OH) and vanadian mica (possibly roscoelite). Within these bands and in the cores of the nodules, a wide variety of authigenic minerals have previously been identified /Perutz, 1939; Harrison, 1975; Durrance et al, 1980; Nancarrow, 1985/, and principally include (note: ideal mineral chemical formulae shown):

Sulphides:

bornite (Cu_5FeS_4),
chalcocite (Cu_2S)
chalcopyrite ($CuFeS_2$)
covellite (CuS)
digenite (Cu_9S_5)
galena (PbS)
pyrite (FeS_2)
sphalerite (ZnS)
molybdenite (MoS)

Arsenides

algodonite (Cu_6As)
maucherite (Ni_3As_2)
modderite ($Co_{0.36}As$)
niccolite (NiAs)
rammelsbergite ($NiAs_2$)
safflorite ($CoAs_2$)
skutterudite ([Ni, Co, Fe]As_3)

Selenides

clausthalite (PbSe)

Carbonates

malachite ($CuCO_3.Cu[OH]_2$)

Silicates

coffinite ($USiO_4$)
vanadian mica – roscoelite $KV_2[OH]_2AlSi_3O_{10}$)

Oxides

montroseite (VO.OH)

Vanadates

metatyuyamunite ($Ca[UO_2]_2[VO_4]_2.3\text{-}5H_2O$)

Many of the minerals are disseminated as fine grained phases throughout the nodules. However, the metallic sulphide and arsenide minerals commonly form discrete segregations, often fringing the black vanadiferous haloes /Harrison, 1975/. The nickel arsenides sometimes form dense concentric zones within the cores of the nodules /Harrison, 1975/.

In detail, the origin and paragenesis of the nodule mineralisation is not fully understood. The nodules are clearly post-depositional (i.e. authigenic) in origin. Harrison /1975/ considered that they were associated with deep-sourced regional hydrothermal solutions related to the waning phases of the metalliferous mineralisation in southwest England. He considered that the mineralisation was controlled by the percolation of acidic mineralised fluids through the more permeable strata horizons and structures. Mineral deposition then occurred principally at the interfaces between permeable and impermeable layers. However, Durrance and George /1976/ suggested that precipitation and nodule nucleation was controlled by the distribution of fragments of organic (plant) detritus deposited within the sediments. The decomposition of the organic detritus during diagenesis created localised reducing porewater conditions that resulted in bleaching and reduction of ferric oxides in the adjacent sediment /Durrance et al, 1978/, and the precipitation of metals from the pore fluids migrating through the rocks.

Similar uraniferous concretions have been described from Permo-Triassic rocks elsewhere in the United Kingdom /Harrison et al, 1983/ and in Switzerland /Hoffman et al, 1987; Hoffman, 1990/. In both cases, the uranium, copper, nickel and arsenide mineralisation are closely associated with localised reduction around organic nuclei. Recent studies of red-bed hosted copper-mineralisation in the Cheshire Basin show that metalliferous pore fluids, rich in copper, lead, arsenic, vanadium and other base metals, can

readily be generated from within the Permo-Triassic red-bed sediments themselves, by leaching during diagenesis /Plant et al, 1999/. Therefore, it is not necessary to invoke extraneous hydrothermal sources /cf. Harrison, 1975/, to explain the mineralisation in the Littleham Mudstone Formation. K-Ar radiometric dating of the authigenic vanadian mica (roscoelite) in similar concretions from the Permo-Triassic red beds of northern Switzerland gave ages ranging from Lower Cretaceous to Lower Jurassic age /Hoffman, 1987/. These ages are consistent with the estimated burial depth at the time of nodule formation in the Swiss occurrences, of between 500 and 800 m, based on the state of the sediment compaction fabric preserved in the concretions /Hoffman, 1987; Hoffman et al, 1990/. The copper carbonates /Harrison, 1975/ and metatyuyamunite /Durrance and George, 1976/ reported from the nodules are clearly secondary alteration products, and have been identified along cracks and other surfaces where the nodules have been exposed to recent weathering and associated oxidation.

Harrison /1975/ also described the stratiform occurrence of sheet-like native copper, accompanied by traces of native silver, in the Littleham Mudstone Formation at Littleham Cove. This type of mineralisation is rare, although it appears to be closely associated with similar uranium, vanadium, cobalt, nickel and arsenic mineralisation described from the more common “fish-eye” concretions described above. The copper was reported to occur as thin discoidal plates up to 160 mm by 90 mm in diameter, and up to 4 mm thick. Harrison (op. cit.) described these plates as being aligned with bedding planes within grey silty marl, and comprised flakes of native copper intercalated with laminae of grey marl and black concentrations of uranium, vanadium and other minerals similar to those seen in the “fish-eye” type concretions. Recently, Craik-Smith /1999/ also briefly reported the occurrence of plates of native copper (with visible native silver) from the Littleham Mudstone Formation at the same locality. He observed them occurring as “stringer-like formations”, often associated with rhomb calcite, and also with reduction zones in the greenish-grey marl bands. Evidence for the paragenesis of the native copper is fragmentary. Harrison /1975/ concluded that it was preceded by, although possibly closely related to, the precipitation of nickel arsenides and coffinite. However, it should be noted that this is the reverse of the conclusions reached from the present study (described in the following sections). The native copper is superficially altered to malachite where it has been exposed to weathering.

Native copper associated with uraniferous-vanadiferous concretions has been reported from other Permo-Triassic and red-bed sequences /Beddoe-Stephens, 1980; Hoffman et al, 1987; Hoffman, 1990/. However, it occurs only as disseminated fine grains. Its paragenesis appears to be closely related to the uranium, vanadium, and sulpharsenide mineralisation. The occurrence of relatively large sheet-like plates of copper appears to be very rare and, so far, has only been described from the Littleham Mudstone Formation at Littleham Cove /Harrison, 1975; Craik-Smith, 1999/.

3 Samples and field observation

The BGS holds a large reference collection of uraniferous-vanadiferous concretions from Littleham Cove and elsewhere in south Devon. These have been acquired as a result of systematic regional geological mapping undertaken by the BGS, and from a series of mineral reconnaissance programmes funded by the UK Department of Trade and Industry (DTI). The early investigations undertaken for the DTI in the 1970's focused on potential uranium resources /Tandy, 1973, 1974, Harrison, 1975/ . Further samples were obtained from the area during the 1980's as part of a subsequent DTI exploration programme for vanadium and base metal (nickel, cobalt) mineralisation /Nancarrow, 1985; Bateson, 1987/ . The BGS reference collection also includes the original concretions and associated copper sheets described by Harrison /1975/.

The samples contained within the BGS reference collection were briefly evaluated to identify appropriate samples of native copper for detailed mineralogical and petrographical examination for the present study. Four samples of plate-like or sheet-like native copper from the Littleham Mudstone Formation of Littleham Cove were identified. One of these – reference sample E42682 (referred to here as block "e4") was originally described by Harrison /1975/ . This had been cut in half and the cross section prepared as three polished blocks which are referred to in this report as blocks e4 a, b and c. The other three plates (referred to as blocks "B1", "B2" and "B3") were preserved intact as collected. One of these – "B1" – was figured but was not petrographically examined by Harrison /1975, Plate 2a, p. 23/ . Polished sections were prepared from these three copper plates.

As part of this study, the BGS also undertook a short reconnaissance field visit between 10–14 January 2000, to examine the Littleham Mudstone Formation sequence exposed between Exmouth and Budleigh Salterton. The purpose of the visit was to try to evaluate the geological relationships between the copper mineralisation and other features, and to attempt to collect further samples of native copper. The full sequence of the Exmouth Mudstone and Sandstone Formation and the Littleham Mudstone Formation (Figure 2-1) was systematically examined, from Exmouth in the west to 1 km west of Budleigh Salterton.

Scattered and localised reduction spots, and bleached horizons (irregular, stratiform, and along joints and fractures) were observed throughout the Exmouth Mudstone and Sandstone Formation. However, no concretions associated with native copper were found, and only trace amounts of secondary blue-green copper hydroxycarbonates or hydroxychlorides were seen as surface stains on some exposed vertical joints in sandstone near Orcombe Point, close to Exmouth.

Much of the exposure of the Littleham Mudstone Formation in Littleham Cove was found to be badly obscured by cliff falls, and landslipped material. Exceptionally heavy rainfall during December 1999 and early January 2000 resulted in the liquefaction of much of the landslipped material with the development of extensive and dangerous deep mudflows. These prevented access over large parts of the landslipped area and to exposures of the Littleham Mudstone Formation in the slip faces of the cliffs above. The accessible outcrops of the formation, together with fallen blocks of mudstone and

siltstone in the landslips and mudflows on the beach were examined. The uraniferous concretions and reduction spots (often with black cores) were readily seen as scattered occurrences and in concentrations along certain horizons within the Littleham Mudstone Formation (Plate 3-1). In many cases, the nodules and reduction spots appear to be randomly disseminated within the rock matrix along certain horizons. However, in other cases nodule development is clearly concentrated along the fractures (Plate 3-2). Similarly, reduction and bleaching of the red mudstones often appears to occur along more permeable siltstone and sandstone bands, whilst in other cases, bleaching often picks subvertical fracturing in the mudstone (Plate 3-3). Many of these fractures are associated with damage zones around several small normal faults seen cutting the Littleham Mudstone Formation. Although minor copper mineralisation was often seen as blue-impregnations within thin horizons of permeable sandstone and siltstone in the upper part of the mudstone sequence, no concretions containing native copper were identified in situ. However, one small copper plate (referred to here as block “b4”) was found lying partially buried in the surface of a mudflow deposit. This sample was prepared as a polished section and examined in detail as part of this study.

Plate 3-1. *Dark uraniferous concretions surrounded by a pale green grey bleached halo in red silty mudstone, exposed at low tide in the wave-cut platform at Littleham Cove. The concretions are developed along a thin horizon of silty mudstone that displays patchy bleaching. Littleham Mudstone Formation..*

Plate 3-2. *Concentration of uraniferous nodules along irregular fractures in red silty mudstone exposed at low tide in the wave-cut platform at Littleham Cove. The fractures also display a thin zone of bleaching in the adjacent wallrock. Littleham Mudstone Formation.*

Plate 3-3. *Pale green-grey reduction bands developed along thin siltstone and sandstone beds, and along the margins of sub-vertical hairline fractures in red mudstone. Littleham Mudstone Formation, Littleham Cove.*

4 Analytical methods

4.1 Optical petrography

Segments of the native copper sheets from the BGS reference collection, together with the new sample collected during the January 2000 field visit, were embedded in epoxy resin then sawn and prepared as polished blocks. The blocks were cut so as to intersect the copper sheets and any adjacent enclosing mudstone or siltstone matrix. The polished section blocks were examined by reflected light optical microscopy, to characterise the petrography and mineralogy of the ore mineral assemblage. Reflected light petrographical observations were made before coating the sections with carbon for backscattered scanning electron microscopy and electron microprobe analysis.

4.2 Backscattered scanning electron microscopy

After preliminary optical microscopic examination the polished sections were examined by backscattered scanning electron microscopy (BSEM), to provide high-resolution mineralogical and spatial information on mineral relationships and rock microfabric. Prior to examination in the scanning electron microscope, the polished sections were coated under vacuum with a thin film of carbon approximately 25 nm thick (using an EMITECH 960L carbon evaporation-coating unit), to provide them with an electrically conductive surface. Semi-quantitative microchemical information obtained by energy-dispersive X-ray microanalysis (EDXA) – recorded simultaneously during BSEM observations – was used to identify minerals on the basis of their chemistry.

BSEM-EDXA analyses were performed using a LEO 435VP, variable pressure digital scanning electron microscope, fitted with an Oxford Instruments ISIS 300 digital EDXA system and a KE-Developments four-element solid-state backscattered electron detector. BSEM-EDXA observations were typically made using 10-20 kV electron beam accelerating potential and 100 to 800 pA beam currents. The instrument was operated under high-vacuum mode (i.e. $<10^{-4}$ torr) for the purposes of this study.

4.3 Electron microprobe studies

4.3.1 Microchemical mapping

The large-scale distribution of the main chemical components was investigated by making microchemical X-ray maps on the Cameca SX50 electron microprobe. The maps were made on a grid of 1024 x1024 pixels, using an electron beam defocused to 6μm and on a spacing of 6 μm achieved buy moving the specimen stage. This gives continuous coverage of an area approximately 6 mm square, large enough to be representative of a significant part of the sample. Dwell time at each point was 60 msecs, giving detection limits around 1 wt%; a set of 3 maps takes approximately 16 hrs to collect. Maps were made for copper, sulphur, arsenic, nickel, uranium and silicon for all

areas and additionally cobalt, silver and phosphorus in some areas. The results are presented as colour maps with a rainbow scale where magenta shows low concentrations and red high concentrations. The scale is a relative scale, to suit the range of counts in each map and absolute concentrations vary from map to map. As not all maps show features of interest, only selected maps are shown in this report.

Rapid maps of smaller areas were made of features of particular interest. These cover smaller areas as they are made by scanning the electron beam, and as accumulation times are only a few minutes detection limits are higher. They are used to study the major components.

4.3.2 Electron microprobe point analysis

A small number of point analyses were made by electron microprobe analysis (EPMA) to try to identify the main mineral phases identified from optical examination and microchemical mapping. These analyses were also carried out by wavelength dispersive analysis, using Cameca SX50 electron microprobe instruments. The instrument was calibrated using a range of pure metal, synthetic compounds and well-characterised minerals as reference materials. The analyses are described and discussed in the following sections, according to the mineral species rather than from each sample examined.

4.4 X-ray diffraction analysis

Three samples of silty mudstone from Littleham Mudstone Formation associated with uraniferous and vanadiferous concretions were taken for analysis from the BGS reference collection. All three samples were originally collected from Littleham Cove. The samples were selected to provide an indication of the bulk and clay mineralogy of the background red silty mudstone host rocks (Reference Collection No. KH1346/Lab Number F666) and the grey bleached haloes associated with mineralised reduction spots (Reference Collection No. HBR8014/Lab Number F664 and Reference Collection No.HBR8026/Lab Number F665). Representative sub-samples (~30 g) of each were first taken, and crushed in a pestle and mortar to <2 mm. This material was then further subdivided for subsequent analysis.

For whole rock (bulk) analysis, a sub-sample of the coarsely crushed material (c.5 g) was taken from each sample and ground to a coarse powder (<125 μm) in an automatic pestle and mortar. A representative sub-sample of the ground material (c.3 g) was subsequently micronised under acetone for ten minutes in order to produce a uniform particle size. The resultant powders were then dried at 55°C before being back-loaded into standard aluminium sample holders.

In order to study the clay minerals present, a fine (<2 μm) fraction oriented mount was prepared. A sub-sample (c.20 g) of the coarsely crushed material was taken and dispersed in 150ml of deionised water by shaking for 2 hours on a reciprocal shaker and subsequent treatment with ultrasound for approximately 3 minutes. The resultant suspensions were then sieved on 63 μm and the <63 μm fraction placed in a 250 ml measuring cylinder and allowed to stand. To prevent flocculation 1ml of 0.1M ‘Calgon’

(sodium hexametaphosphate) was added to the suspensions. After a period dictated by Stokes' Law, a nominal <2 μm fraction was removed and dried at 55°C. 100mg of the <2 μm material was then re-suspended in a minimal amount of distilled water and pipetted onto a ceramic tile in a vacuum apparatus to produce an oriented mount. The clay mounts were then Ca-saturated using 2 ml 1M $CaCl_2 \cdot 6H_2O$ solution and washed twice to remove excess reagent before being allowed to air-dry.

XRD analysis was carried out using a Phillips PW1700 series diffractometer using Co-K_α radiation and operating at 45kV and 40mA. For bulk analysis the micronised powder mounts were scanned over the range 3–50°2θ at a scanning speed of 0.7°2θ/minute. The oriented mounts were scanned over the range 1.5–32°2θ in both air-dried and ethylene glycol-solvated states, and after heating at 550ºC for 2 hours at a scanning speed of 0.5°2θ/minute. Diffraction data were analysed using the PC-based Phillips X'Pert software coupled to an International Centre for Diffraction Data (ICDD) database.

5 Observations and results

5.1 Mineralogy of the Littleham Mudstone Formation host rocks

The results of both bulk and fine (clay) fraction XRD analyses are summarised in Table 5-1, below. The XRD results show that the silty mudstones are composed of major quartz with a clay mineral assemblage dominated by major mica (illite) or smectite. Minor components include calcite, chlorite, orthoclase and plagioclase (nominally identified by XRD as “albite" (Table 5-1). Although only a very limited study of the mineralogy of the Littleham Mudstone Formation has been undertaken, the results suggest that there may be a difference in the mineralogy of the red host rock and the bleached/reduced zones. Smectite, which forms the major clay mineral in the back-ground host rock, is absent in the two bleached mudstone samples (where mica/illite is the dominant clay mineral). Similarly, hematite which is seen as a minor component in the red mudstone, is much reduced and only present in trace amounts in the reduced mudstone haloes. Pyrite is also seen as a trace component of the reduction haloes whereas it is not identified by XRD in the red host rock.

Table 5-1. Summary of XRD results.

Sample	Description	Analysis	Major	Minor	Trace
F664	HBR 8014	Bulk	Quartz	Calcite, mica*, chlorite, orthoclase	?Albite, ?hematite/pyrite
		Clay	Mica	Chlorite	
F665	HBR 8026	Bulk	Quartz	Calcite, mica, chlorite, albite, orthoclase	Hematite/pyrite
		Clay	Mica	Chlorite	
F666	KH1346	Bulk	Quartz	Albite, mica, chlorite, calcite, hematite	?Orthoclase
		Clay	Smectite	Mica, chlorite	

*An undifferentiated species giving a 10Å basal spacing.

5.2 Petrographical examination

5.2.1 Sample e4

This sample was collected by Harrison and is figured and referred to in his paper /Harrison, 1975/, where the full specimen number E 42682 is used. The sample is roughly circular and around 6cms in diameter. It is unusual in that the Cu plate is totally enclosed in sediment giving an overall shape of a disc about 1 cm thick (Plates 5-1 and 5-2). The bright blue colour is oxidative alteration that has occurred since the sample

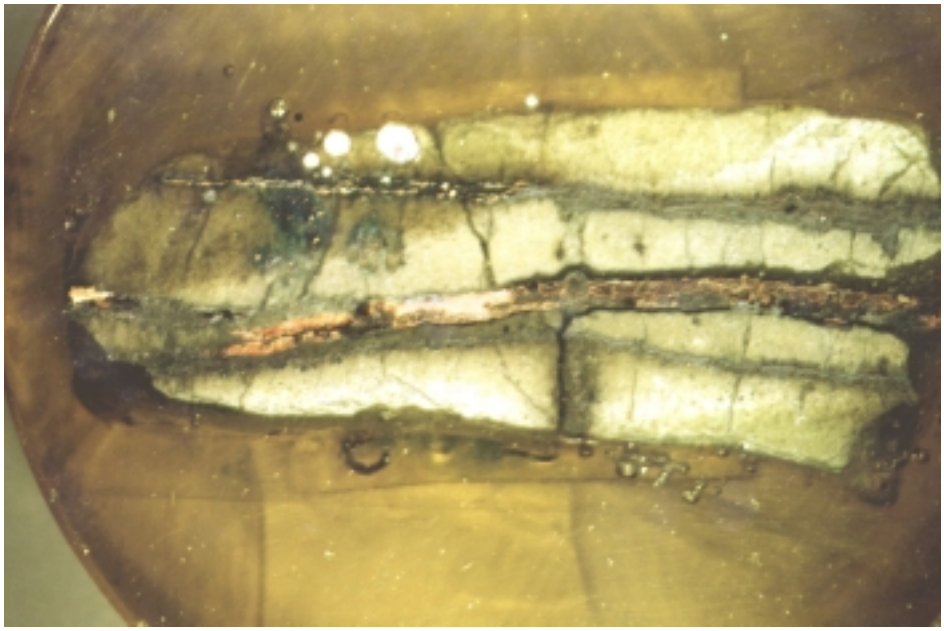

Plate 5-3. *Left hand end of plate e4, block e4a.*

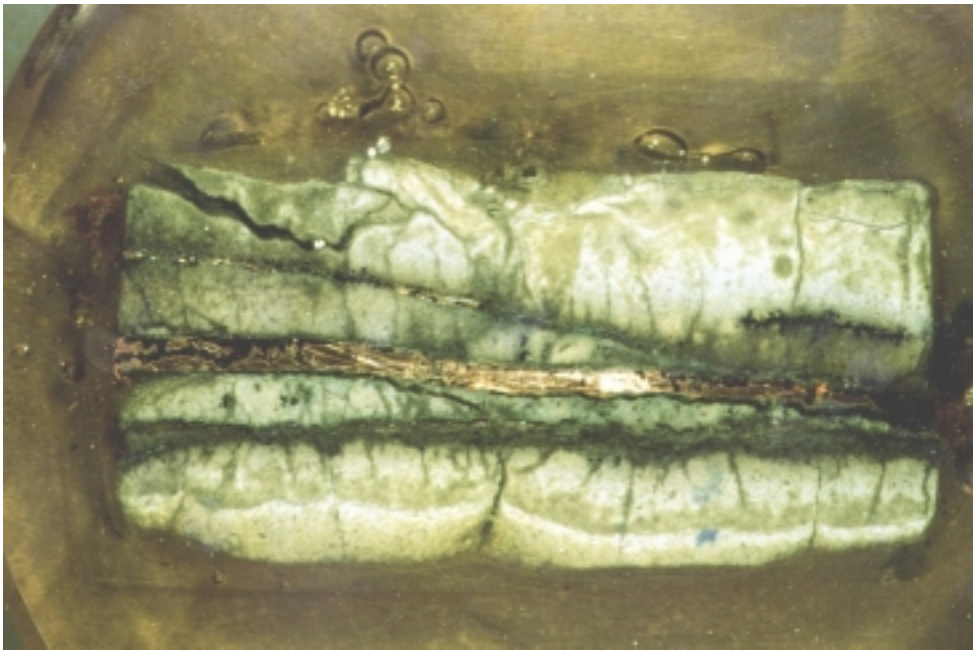

Plate 5-4. *Centre part of plate e4, block e4b.*

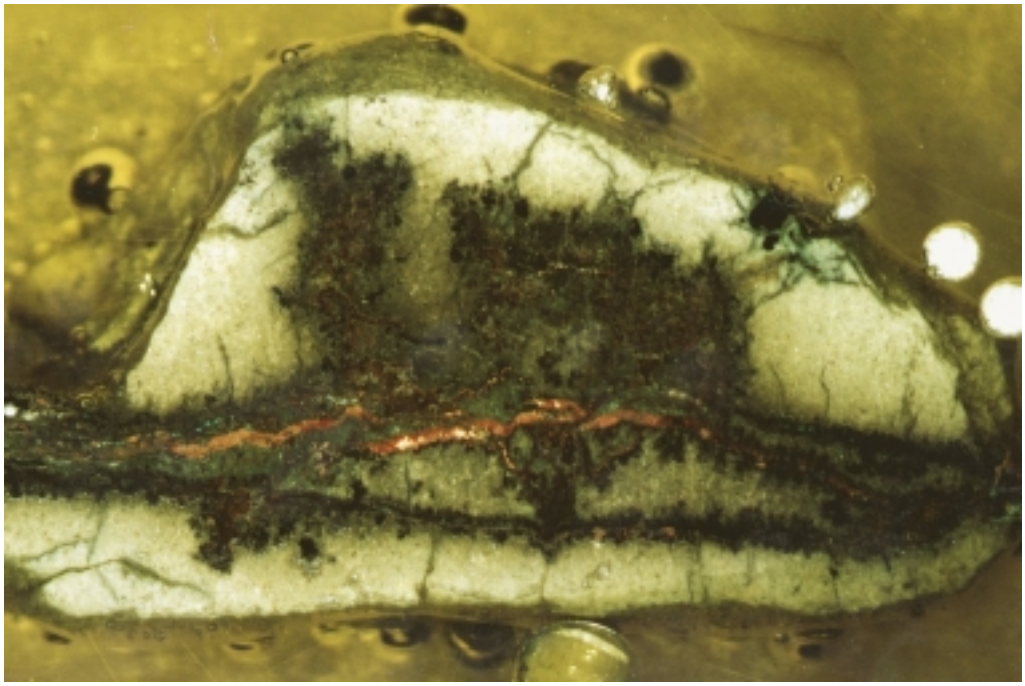

Plate 5-5. *Plate e4 right hand side, block e4c.*

In several places the alteration of the metal–rich layer is markedly asymmetrical, with alteration affecting only one side of the plate (Plate 5-6). The orientation of this asymmetry is consistent throughout the sample.

Examination in reflected light confirms the observations under the binocular microscope. It shows that most of the alteration of the Cu-plates is to a dull grey poorly polished mineral, that could not be identified optically (this will be referred to as oxide/sulphate and the details of its composition are discussed in Section 5.3) with only minor amounts of cuprite (Cu_2O) remaining (Plate 5-7). At one end of the plate, however, block e4c, the alteration is largely to cuprite with minor amounts of the sulphate. In several places thin stringers of a bright , yellow-white, high-reflectance nickel arsenide mineral are present. It forms thin films, 10-20 μm thick around the outer surfaces of the plates (Plate 5-8) and thin veins through the sediment (Plate 5-9).

Detailed BSEM-EDXA generally confirms the reflected microscopy observations above but also reveal a number of additional features. Minor amounts of native silver are also present as inclusions within the copper metal sheets (Plate 5-10). In some cases, silver appears to have possibly coprecipitated with the copper along grain boundaries. However, in most cases, the silver grains are subhedral crystals (Plate 5-10), which appear to be partially embayed and corroded by the copper, implying that they preceded copper growth. Along the altered surface of the copper sheet, the silver grains have been partially dissolved, leaving pores which have subsequently been mineralised by a thin film of copper arsenide. It should be noted that the copper arsenide is absent from the interface between the copper metal and intact silver grains (Plate 5-10). This indicates that the copper arsenide is later than either the silver or the copper, and post-dates or is associated with silver dissolution. The thin film of nickel arsenide, seen in reflected

Plate 5-6. *Plate e4, asymmetrical alteration of Cu sheet. Field of view 5 mm.*

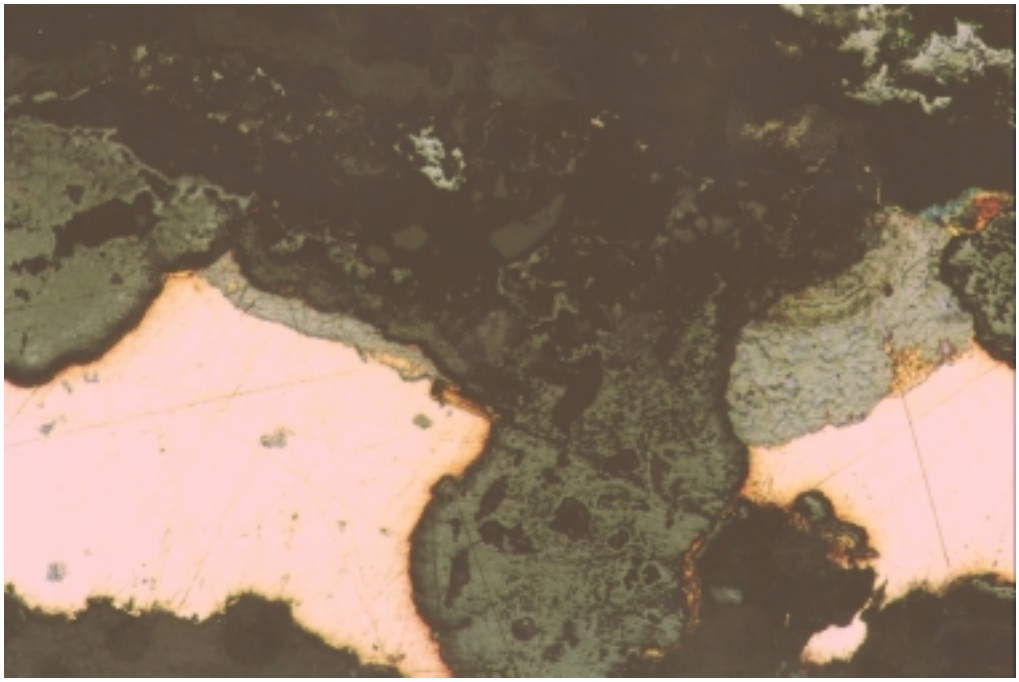

Plate 5-7. *Block e4b, showing alteration of Cu metal to colloform cuprite (pale grey) and later Cu-oxide/sulphate (dark grey), which cuts across both the oxide and copper metal. Field of view 1.3 mm.*

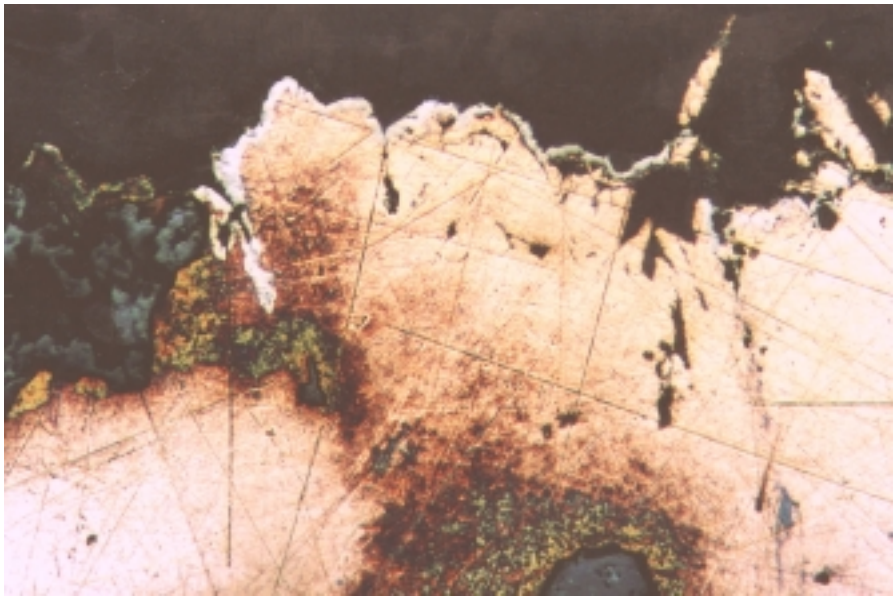

Plate 5-8. *Peripheral arsenides (white) on Cu metal, some at the left-hand side has altered to oxide/sulphate. Field of view 0.6 mm.*

light resting on earlier copper oxide, is also evident under BSEM. Locally this also appears to overgrow a thin veneer of copper arsenide Plate 5-11. A similar relationships between the copper arsenide and nickel arsenide are much better seen in the other samples of native copper. Relicts of microcrystalline chalcocite (Cu_2S) can be found encrusting the surface of the copper oxide alteration (Plate 5-12). Most of the chalcocite has been oxidised and replaced by an intimate intergrowth of copper oxide (probably cuprite) and copper sulphate or oxysulphate. This is further described in Section 5.3.1 – The nature of the oxide/sulphate alteration. The chalcocite is either intergrown with the late nickel arsenide. or occurs beneath a layer of nickel arsenide.

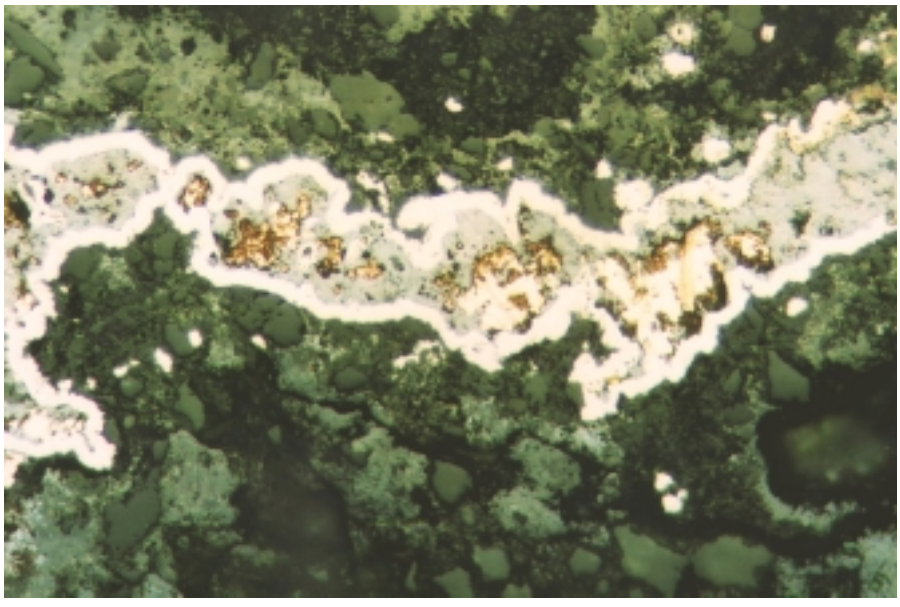

Plate 5-9. *Arsenides surrounding Cu-oxide with remnants of Cu-metal. Field of view 0.6 mm.*

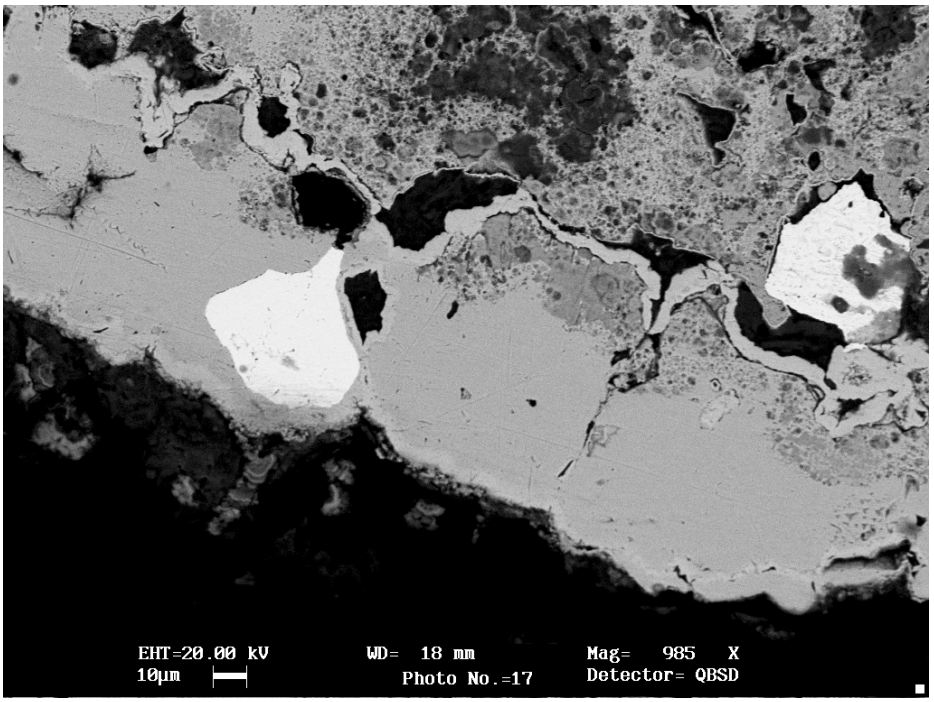

Plate 5-10. *BSEM image of the altered edge of copper plate e4, showing bright inclusions of native silver. The copper metal (duller mid grey) is extensively altered to a spongy matrix of copper oxide with relict copper metal. Voids created by the dissolution of the silver (black) are lined by a thin film of copper arsenide (lighter mid-grey).*

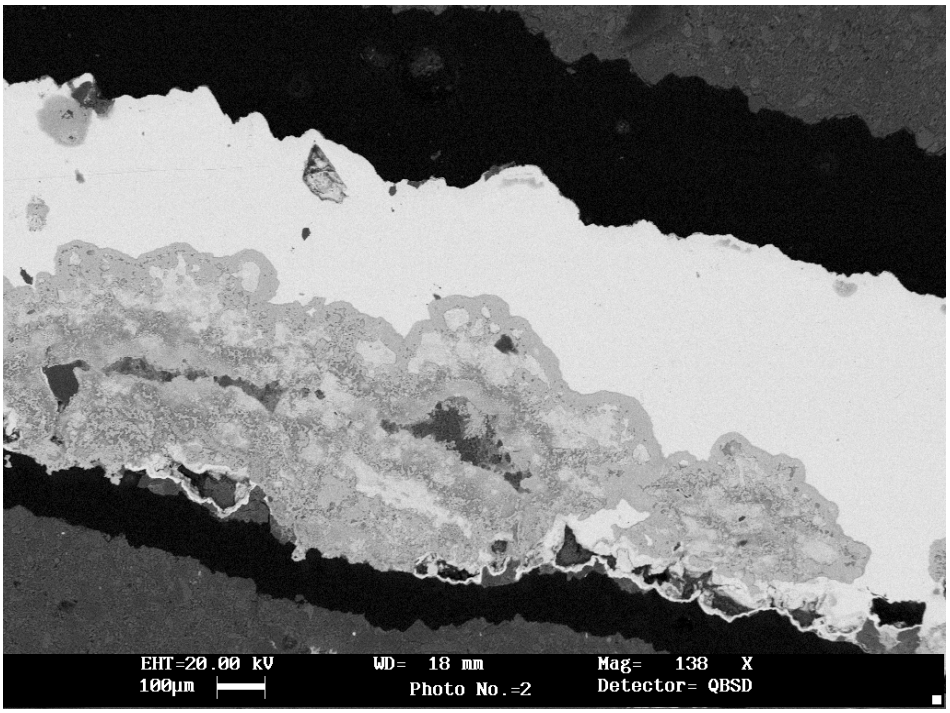

Plate 5-11. *BSEM image of the altered edge of copper plate e4, showing bright fringe of nickel arsenide resting on spongy copper oxide and sulphate alteration (dull grey). Dark areas within this alteration represent vanadian illite or mica. Sample e4.*

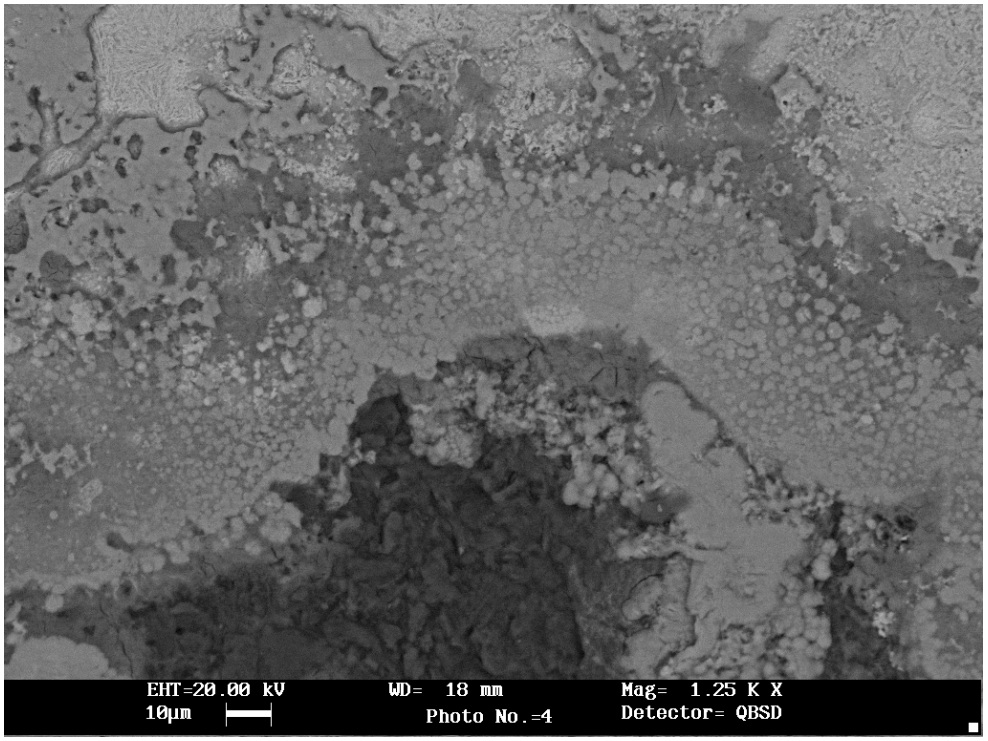

Plate 5-12. *BSEM image of relict microcrystalline chalcocite fringe on the outer surface of copper oxide alteration layer. The chalcocite can be seen as brighter relicts within the mid-grey microcrystalline material, which appears to be partially altered to copper sulphate. Sample e4.*

BSEM observations also reveal that the copper metal forming the sheets contains corroded relict grains of detrital quartz and feldspar. This suggests that in part the copper has grown by replacement of the sedimentary host rock, and not simply as a fracture filling. Authigenic vanadian illite or vanadian mica are also seen to be intergrown with the copper metal (Plate 5-11). Minor fine grained uranium silicate (possibly coffinite) occur in close association with the nickel arsenide. The extent of the corrosion of the copper shows no geometric relationship to the proximity of the uranium minerals.

5.2.2 Sample B1

This sample is roughly 8 cm x 6 cm and a maximum thickness of about 4 mm where there is a small amount of sediment adhering (Plate 5-13). It clearly shows the curled up edges that are a feature of many of these plates. As with the corrosion effects seen in many of the copper sheets and subsheets, the folding of the sheet edges is typically only in one direction. The polished block B1 was cut from the central part with significant amounts of sediment. The block shows there are two main sheets with several offshoots and bifurcations (Plate 5-14).

Plate 5-13. *Plate B1, showing grey siltstone adhering, and dark uraniferous nodule in centre.*

Plate 5-14. *Cross section of plate B1, showing slightly darker faint outline of the halo around the nodule, centre, which is below the plane of the block surface.*

The ‘lower’ layer in Plate 5-14 is Cu metal that is little altered while the adjacent ‘upper’ layer is largely grey arsenide[1] with remnants of Cu metal (Plate 5-15). The offshoot layers are largely grey arsenide.

The reflected light examination confirms previous observations. This shows how there is minimal alteration of the metal sheet, just a little peripheral oxide (Plate 5-16) and grey arsenide, while the adjacent layers are extensively altered to grey arsenide (Plate 5-17). A small amount of Ag metal is present within the Cu sheets and a little white arsenide occurs around the margins and in the sediment.

The copper sheet in B1 is also complexly intergrown with a small uranium-enriched “fish-eye” concretion. This dark uraniferous concretion can just be seen exposed in the surface of the mudstone adhering to the surface of the copper sheet seen in Plate 5-13. Unfortunately, this uraniferous nodule was just missed by the original polished block prepared from the sample. However, the surface of the counterpart rock slice cuts directly through the concretion. This was, therefore, polished (section B1a) and examined in detail by BSEM-EDXA. The alteration characteristics of the copper sheet are essentially similar to that described from section B1; however, section B1a reveals a complex relationship between the native copper and the growth of the concretion. Copper sheets developed outside of the concretion have been deformed by compaction around the concretion margins, whilst those passing through the centre of the concretion are largely undeformed (Plates 5-18 and 5-19). This implies that the native copper

Plate 5-15. *B1, Cu metal layers adjacent to arsenide layers (grey-green). Field of view 3.3 mm.*

[1] The term grey arsenide is used for a mineral that has a grey colour and low reflectance that later electron microprobe analysis showed to be a nickel arsenide.

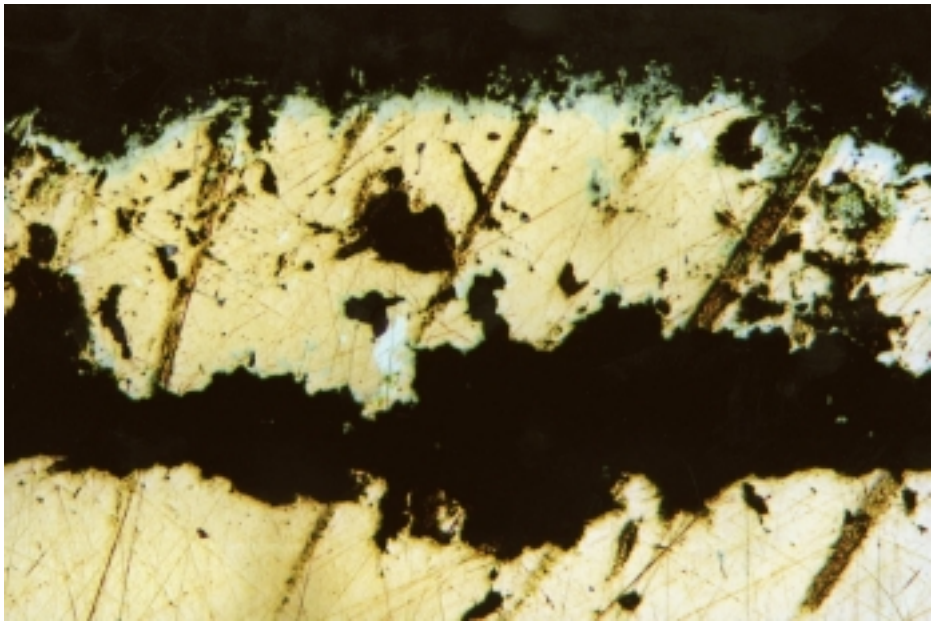

Plate 5-16. *B1, Copper sheet with silver metal (white) with peripheral alteration to cuprite (grey), brown lines are scratches. Field of view 6 mm.*

sheets started growing before being enclosed by the concretion; however, the copper sheets are considerably thinner where they pass through the centre of the nodule than within the enclosing sediment. This suggests that the growth of the copper sheets was arrested by being enclosed in the nodule, but continued to develop and thicken outside of the nodule.

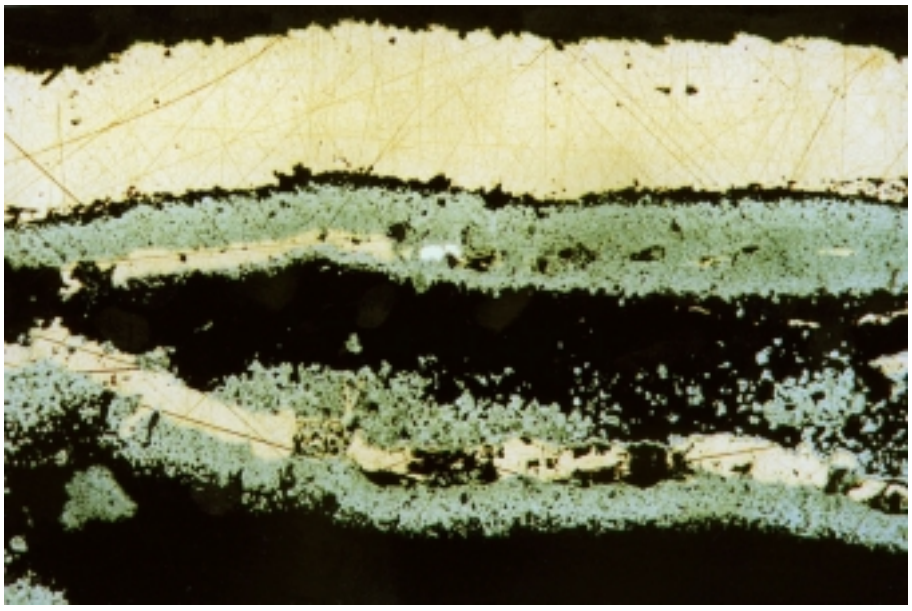

Plate 5-17. *B1, Extensive grey arsenide 'alteration' in layers adjacent to fresh layers. Silver metal (white) is present in the arsenide. Field of view 2.6 mm.*

Plate 5-18. *Photomicrograph of B1 (block B1a) showing compactional deformation of copper sheets around the outside of a concentrically banded "fish-eye" concretion. Thin pink sheets of copper can be seen to traverse across the centre of the nodule, and are much thinner than the sheets in the adjacent sedimentary matrix. The dark core of the nodule comprises mainly vanadiferous illitic clay with disseminations of fine native copper, copper oxide and uranium silicate. This is enclosed by a dense rigid shell of grey metallic nickel arsenide. External dark vanadium-rich haloes surround the arsenide shell.*

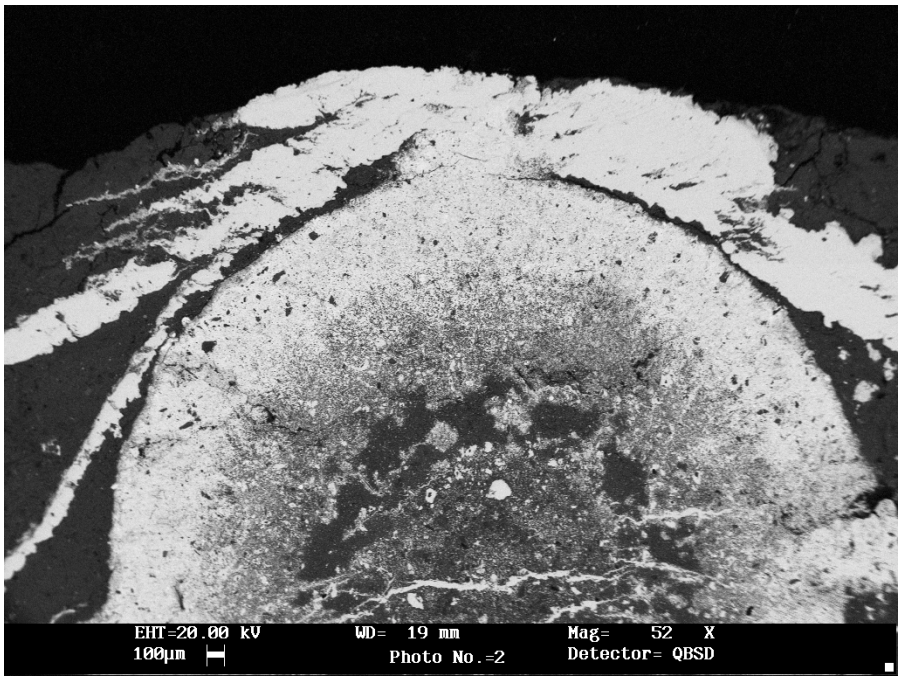

Plate 5-19. *BSEM image showing detail of deformation of copper sheets (bright) around spherical banded "fish-eye"concretion. The bright outer shell of the concretion comprises dense nickel arsenide developed around a core of vanadian illite (black) with disseminated grains of copper associated copper oxide alteration and uranium silicate.*

The concretion itself has a concentric growth fabric. The dark core of the nodule (Plate 5-18) contains discrete disseminated grains of native copper within a siliceous matrix of fine-grained vanadian illite (Plate 5-19). The grains of native copper show a similar alteration to the cooper sheets. They are highly corroded and fringed by platy copper oxide alteration (Plate 5-20). Fine grained uranium silicate is intimately associated with, or nucleates upon, the copper oxide. The outer part of the concretion comprises largely dense nickel arsenide. This cements and partially replaces the original sediment matrix. Disseminated grains of chalcocite and uranium silicate are common within the nickel arsenide shell of the concretion (Plate 5-21). The relict sediment preserved within the nickel arsenide cement displays a relatively open and uncompacted grain framework (Plate 5-21), in contrast to the enclosing host mudstone. This implies that the nodules formed early during the diagenesis of the host rock, before significant burial compaction had taken place.

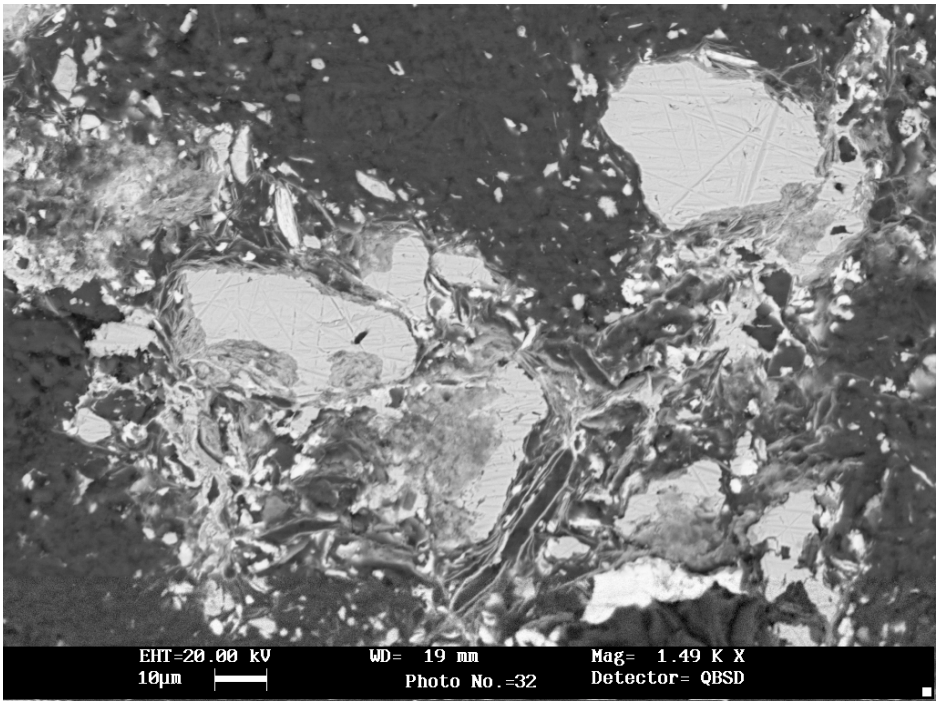

Plate 5-20. *BSEM image of the core of the "fish-eye" concretion in B1a, showing corroded grains of native copper enclosed within platy copper oxide alteration products. Bright grains of authigenic uranium silicate are seen closely associated with the copper oxide alteration. The dark matrix comprises vanadium-rich illitic clay.*

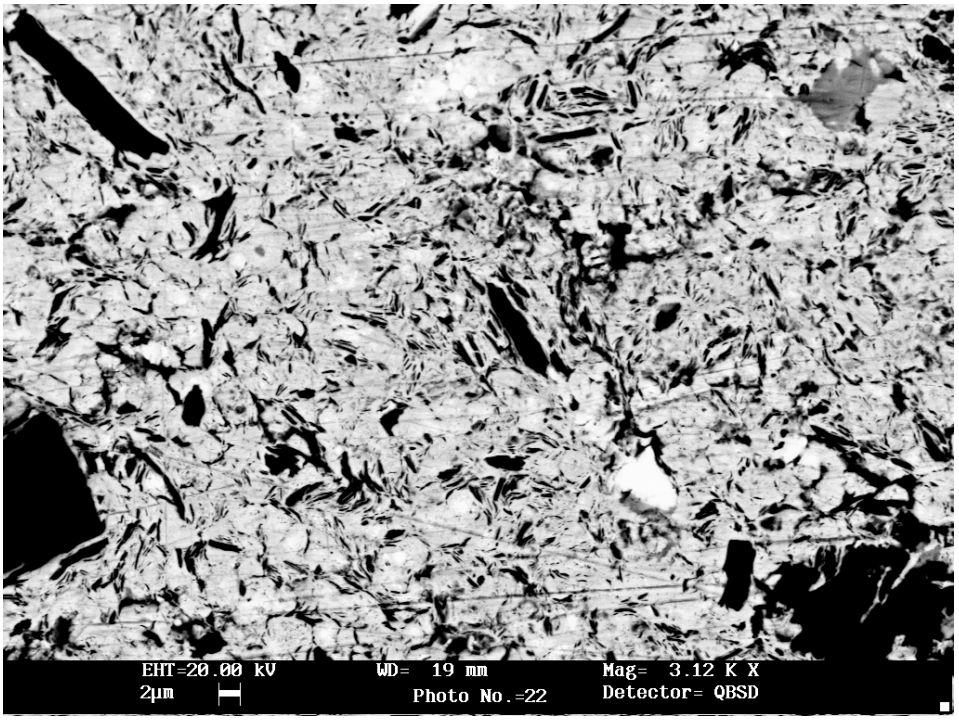

Plate 5-21. *BSEM image showing relict uncompacted mudstone fabric (black) within nickel arsenide shell (mid grey) of concretion in B1a. Minor uranium silicate (bright) and chalcocite (dull grey) are intergrown with the nickel arsenide cement.*

5.2.3 Sample B2

This sample is slightly larger, 11 x 7 cm and around 2 mm thick, as there is only a little sediment adhering (Plate 5-22). Again the curled up edges are present (Plates 5-22 and 5-23). The block shows that it is composed of four interleaved sheets, each around 0.5 mm thick (Plate 5-23). Most of the layers show only minor alteration but there are three much thinner layers, below layer 1, below layer three and above layer 4 (number from base upwards) which show extensive alteration to grey nickel arsenide. There is again a suggestion of asymmetric alteration patterns. Examination in reflected light confirms the previous observations, particularly the dramatic differences in alteration between the different layers, layer two shows only very slight peripheral alteration (Plate 5-25) while the thin uppermost layer is very extensively altered to grey nickel arsenide (Plate 5-26). Higher resolution BSEM observations reveal that copper arsenide (similar to that identified in block e4) predates the nickel arsenide, forming a thin discontinuous layer along the interface between the nickel arsenide and the copper metal. In part, the copper arsenide appears to have been replaced by the nickel mineral. Minor to trace amounts of uranium silicate occur as tiny inclusion grains (< 2 µm) within the outer edge of the nickel arsenide layer.

BSEM observations revealed the presence of relict calcite vein mineralisation within the central copper sheets. This calcite preserves a bedding-parallel cross-fibre fabric which is indicative of formation by a incremental opening and vein infill by a multistage crack-seal mechanism /cf. Ramsey, 1980; Barker, 1990/. The development of the copper sheet appears to have utilised the calcite veining, and the copper metal has largely overprinted and replaced the calcite, so that original calcite is now preserved only as corroded relict inclusions in the copper.

Plate 5-22. *Plate B2 showing copper sheet with curled-up edges, with grey siltstone-mudstone still adhering to the surfaces of the copper plate. Field of view = 14 cm.*

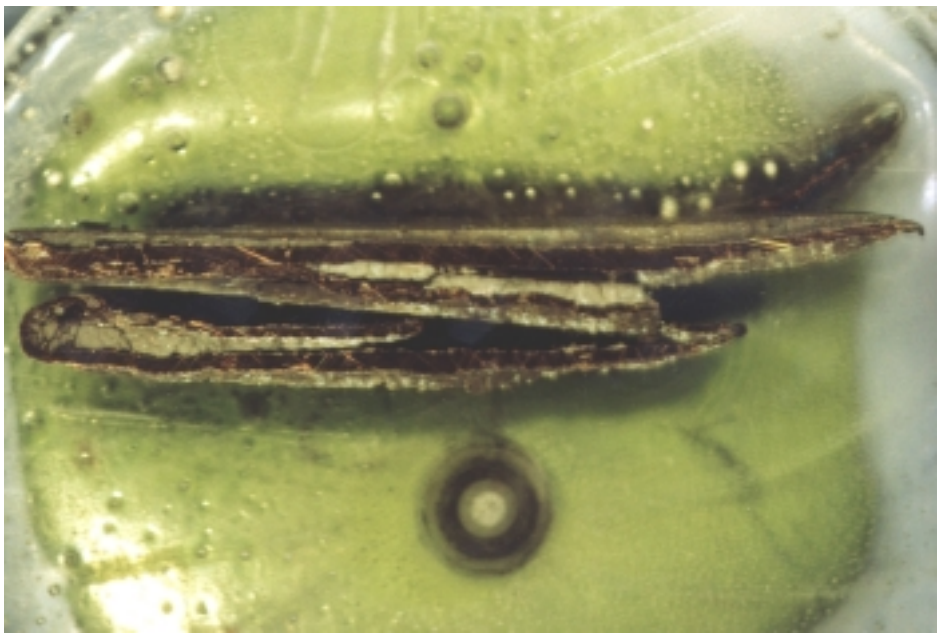

Plate 5-23. *Cross section of B2 showing the copper plate to comprise a stack of close-spaced thin copper sheets.*

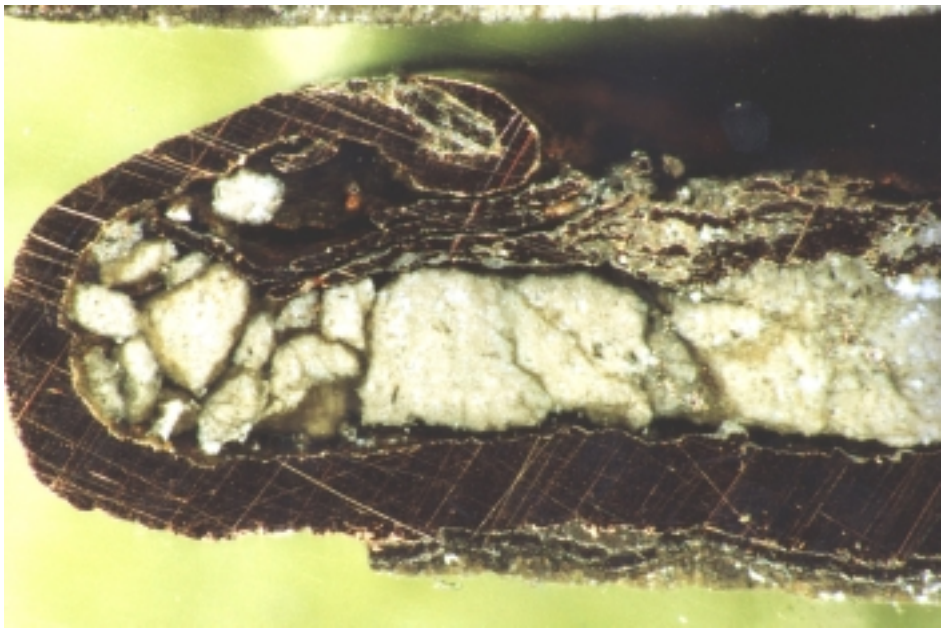

Plate 5-24. *Detail of the curled edge of the copper sheet in B2.*

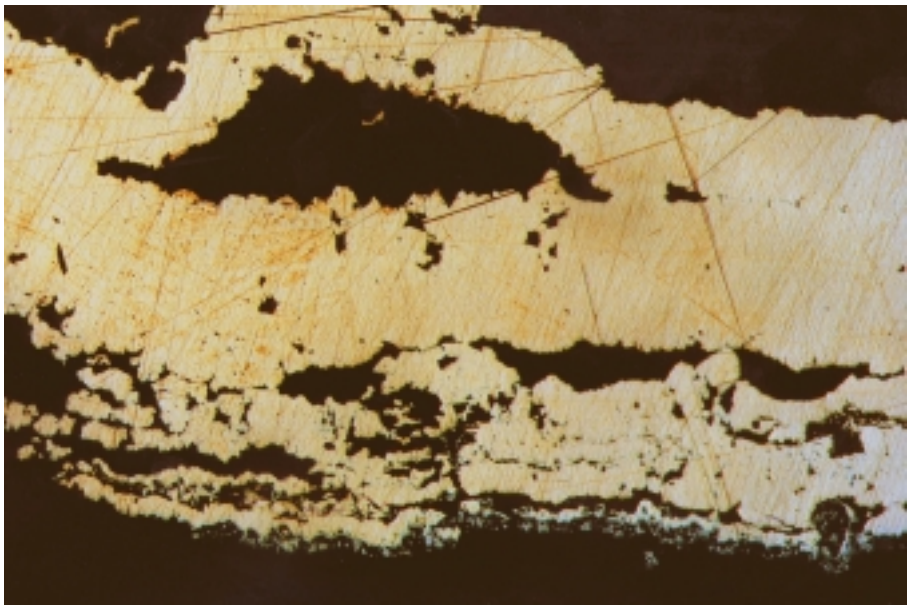

Plate 5-25*. Cu metal layer showing only slight peripheral alteration to grey arsenide (grey). Field of view 2.6 mm.*

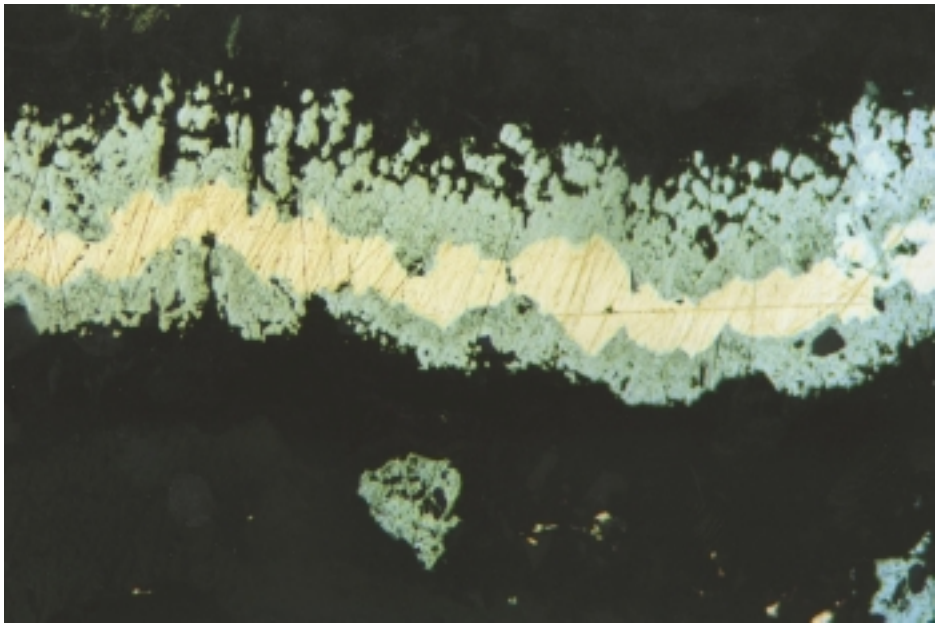

Plate 5-26*. Extensive alteration to grey arsenide. Field of view 2.6 mm.*

5.2.4 Sample B3

This sample is roughly circular, about 7 cm in diameter and has very little adhering sediment and is around 3 mm thick. Again curled up edges are present (Plate 5-27). The block shows that it is composed of four thin interleaved sheets with some cross-cutting Cu veins at one end (Plate 5-28).

The lower three layers are relatively fresh but with marked minor alteration along the lower surface of plates one and two (Plate 5-29), while the uppermost layer is extensively altered to grey arsenide. There is much more extensive alteration at the edge of the sample where there are cross-cutting veins (Plate 5-30).

Reflected light examination confirms these observations and shows that there is some early alteration to cuprite and later alteration to grey arsenide and earthy Cu-oxide[2]. There are also thin stringers of white arsenide along the margins of some of the plates (Plate 5-31). The detail of the cross-cutting vein in Plate 5-30 shows that it is extensively altered but where it crosses the other plates there is apparently no alteration of the other plates. (Plate 5-32).

[2] The term earthy copper oxide is used to describe a very fine-grained substance that in reflected light is grey with low reflectance and bright orange-red bireflectance. Individual crystals cannot clearly be seen and it is often porous. Optically it resembles limonite but qualitative microanalysis shows only the presence of Cu and it is assumed to be Cu oxide or hydroxide.

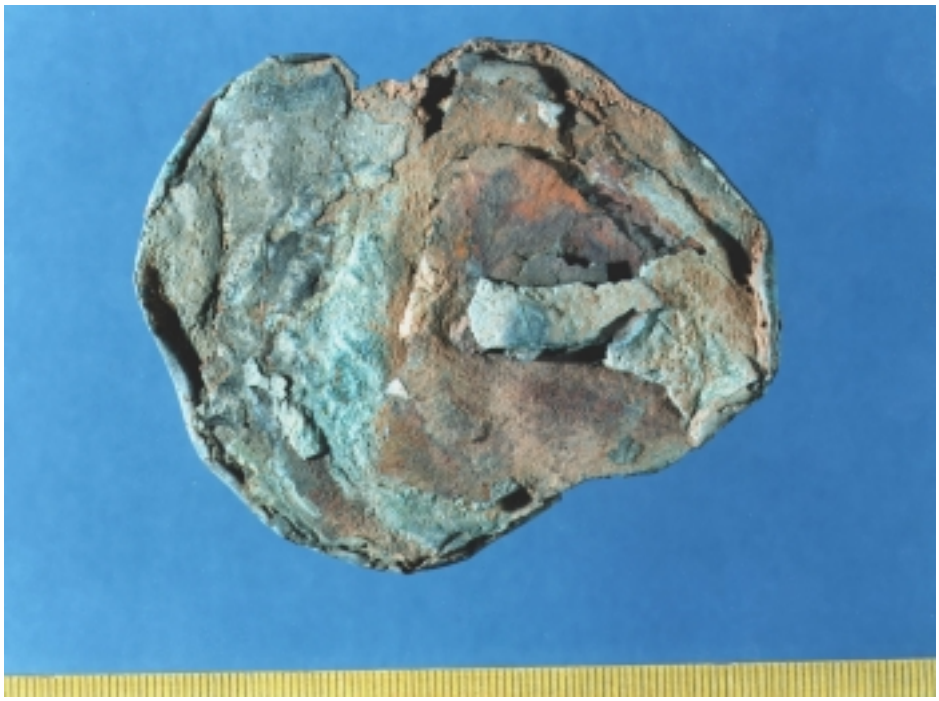

Plate 5-27. *Sample B3.*

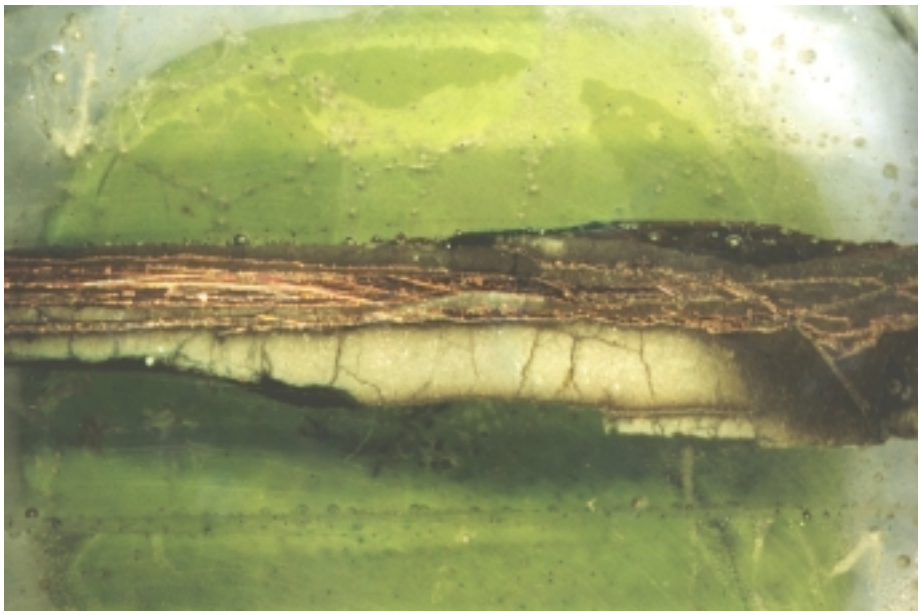

Plate 5-28. *Cross section of B3.*

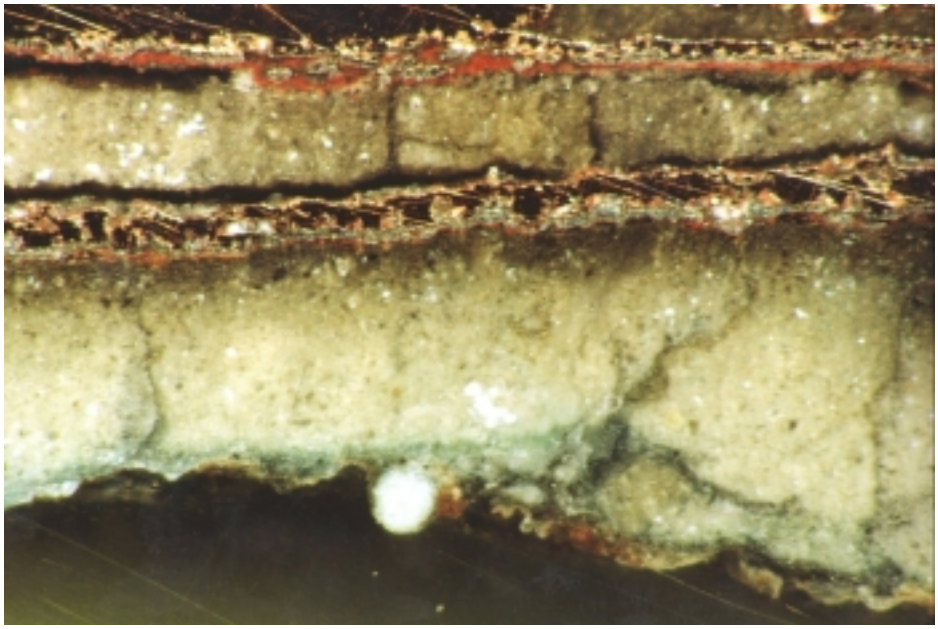

Plate 5-29. *B3 asymmetrical alteration to grey arsenide in central layer.*

Plate 5-30. *Cross cutting 'veins' of grey arsenide.*

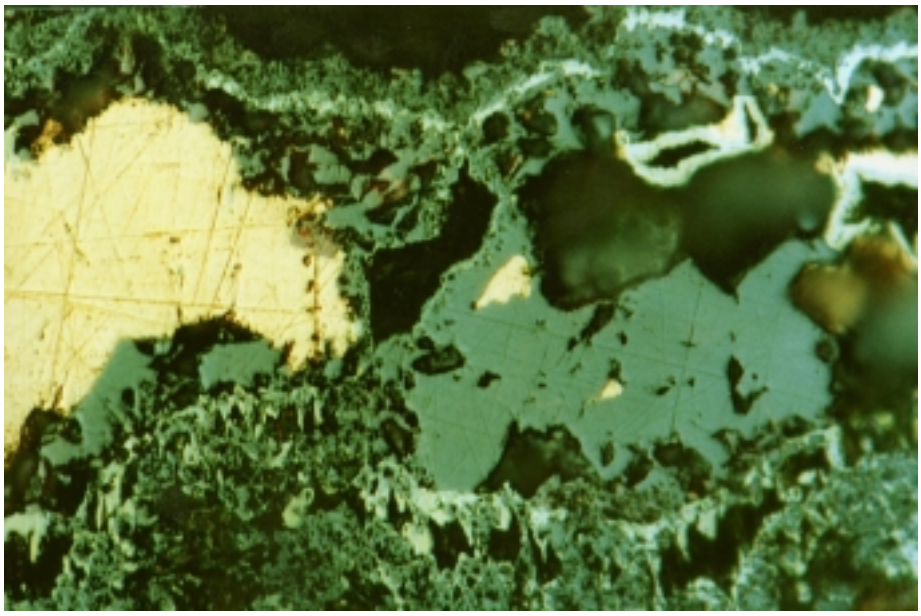

Plate 5-31. *Alteration to cuprite (grey, large crystals) with later grey arsenide and white arsenide (pale grey) and earthy Cu-oxide (grey porous). Field of view 0.25 mm.*

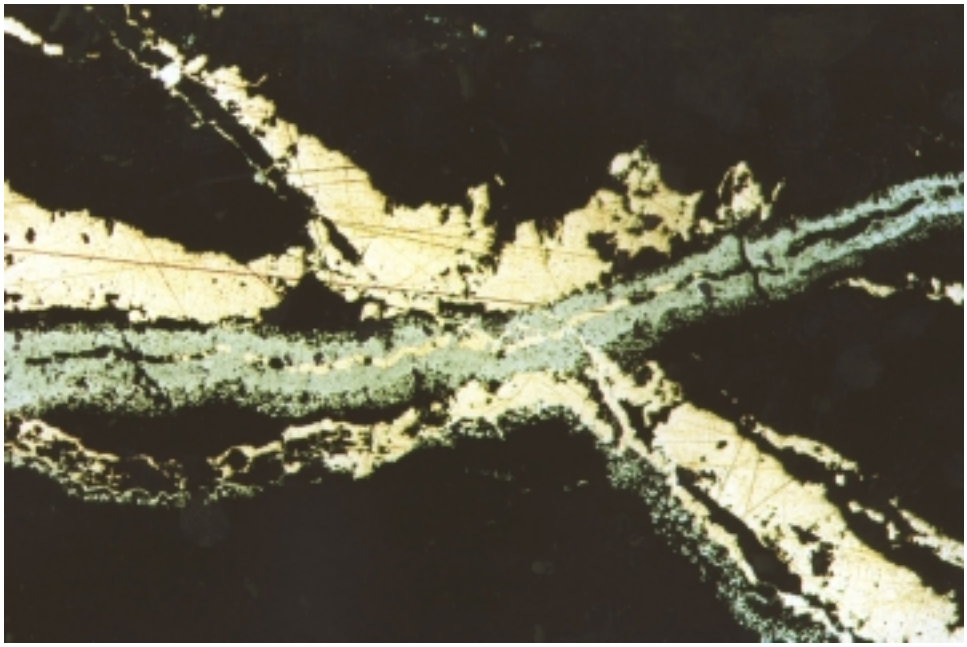

Plate 5-32. *Detail of cross-cutting veins showing the grey arsenide crossing the unaltered copper. Field of view 1.3 mm.*

5.2.5 Sample B4

This is the sample that was collected in January 2000, and is roughly 3 cm x 2cm in size and 3 mm thick (Plate 5-33). The block shows that it appears to consist of a single sheet that bifurcates but is joined at both edges (Plate 5-34). There is very little sediment but that present on the upper surface has a lot of red coloured alteration and that on the lower surface is fractured and veined by bright green malachite (Plate 5-35). The copper sheets have a lot of a pink-brown alteration product, a contrast to the grey arsenide in most samples.

Reflected light examination confirms that the main alteration is to coarse crystals of cuprite and fine-grained earthy cuprite with only very minor grey arsenide. The alteration is particularly around the outer surfaces in some plates but on both inner and outer surfaces on others. White arsenide minerals are present around the outer surface in many places. (Plate 5-36). The sequence of alteration can clearly be seen in Plate 5-37 and 5-38. The Cu is first altered to coarse cuprite (grey Plate 5-37, deep red Plate 5-38) veined along fractures by the arsenides (yellow-white Plate 5-37), enclosed by earthy cuprite (orange-red Plate 5-38) followed by malachite (green Plate 5-38).

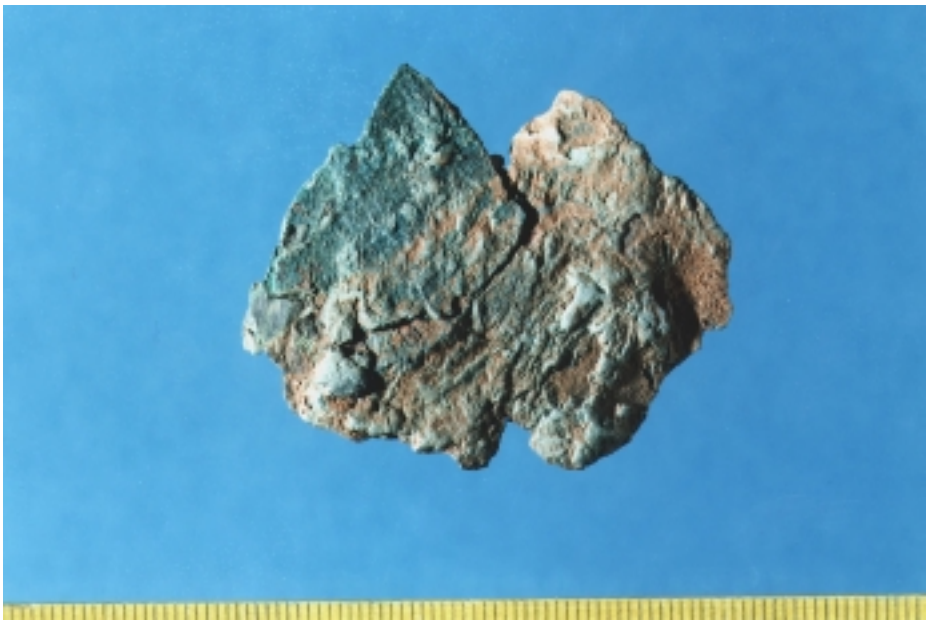

Plate 5-33. *Plate B4. Field of view 25 mm.*

Plate 5-34. *Cross section to B4.*

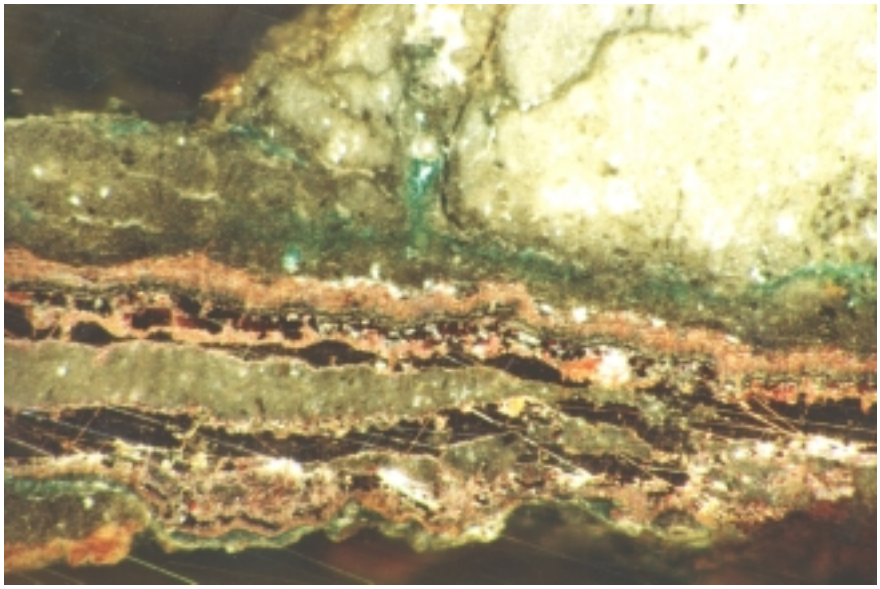

Plate 5-35. *Oxide alteration of B4 showing pink and red Cu oxides and green malachite.*

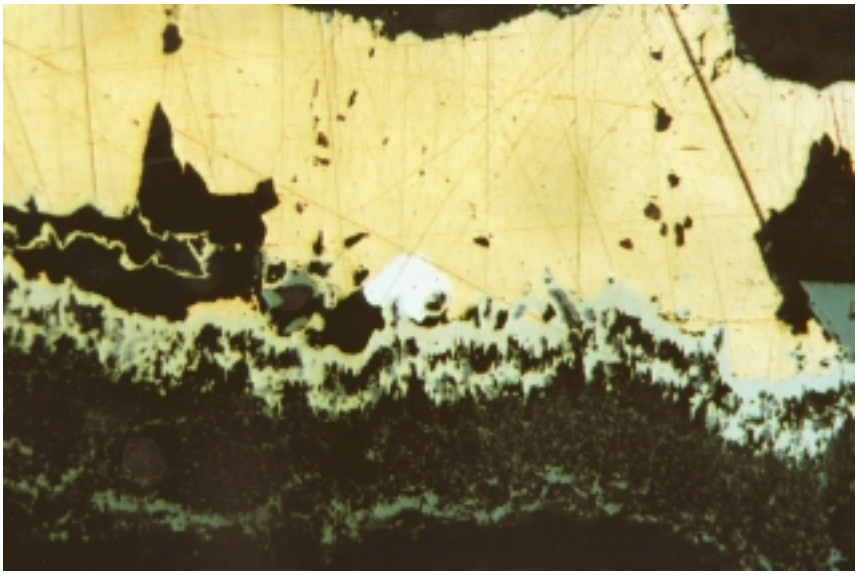

Plate 5-36. *Cu metal with small Ag metal (white centre), grey-white arsenides around margin. Field of view 0.65 mm.*

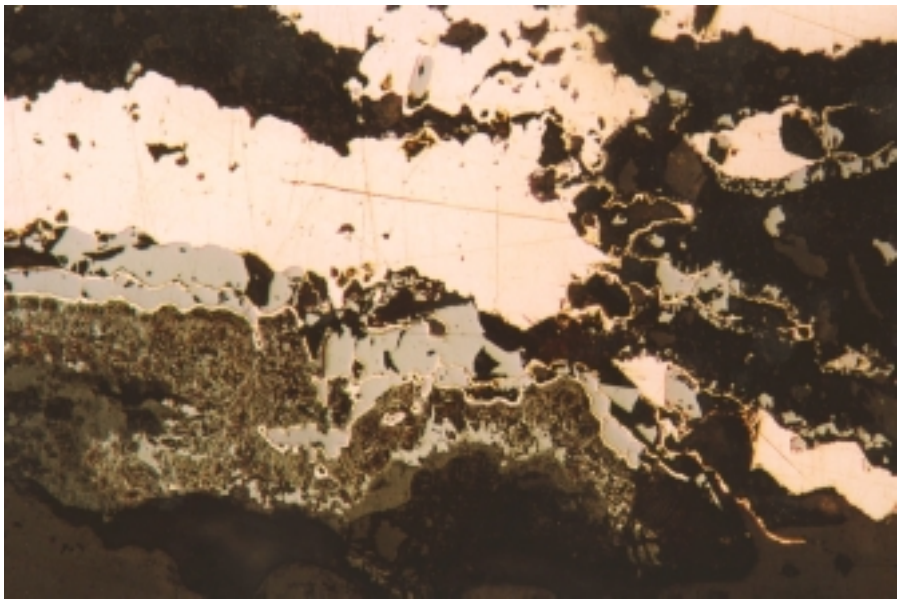

Plate 5-37. *Plate B4, showing Cu metal with coarse Cu oxide (grey), earthy Cu-oxide (grey-brown) and malachite (dull grey-brown). Field of view 0.65 mm.*

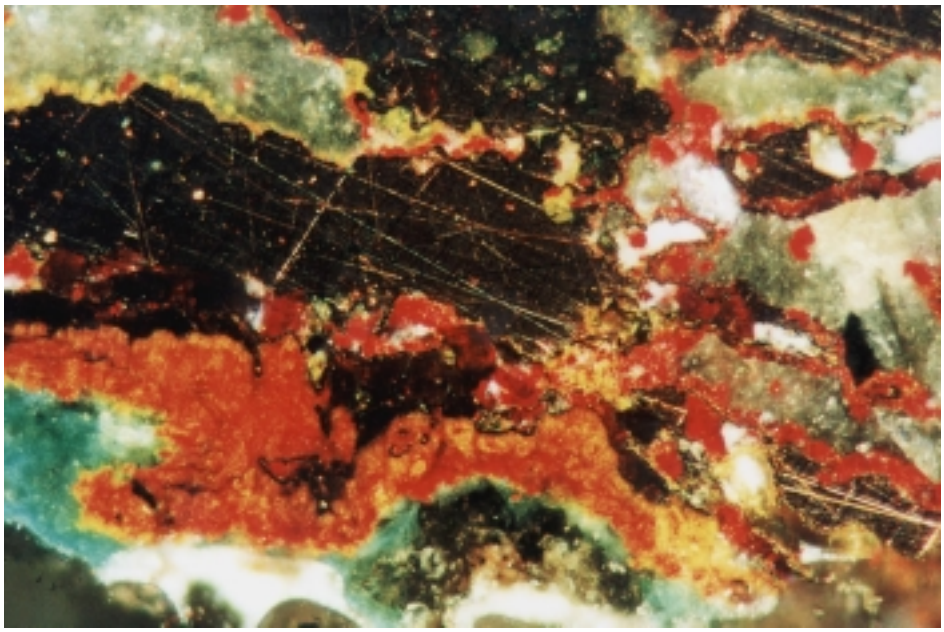

Plate 5-38. *As plate 5-37, cross polarised light. Cuprite is deep red in coarse grains and orange-red in fine earthy form.*

5.3 Electron microprobe studies

5.3.1 Microchemical mapping

Sample e4b central part

This is an area in the block cut from the central part of sample e4 and shows three plates with complex and intimately intergrown assemblage of largely copper oxide and copper sulphate-type alteration. The map for Cu (Figure 5-1) shows the three plates, the central plate is largely Cu metal which shows in yellow-orange colours, while the upper and lower plates are altered to a fine intergrowth of copper oxides and copper sulphate or oxysulphate, and hence have lower Cu contents giving blue-green colours. A map of the same area but processed to enhance the lower Cu values suggests that low levels of Cu may be present at considerable distances away from the actual sheets (Figure 5-2).

The map showing the distribution of S (Figure 5-3) shows the area where the plates have been altered to a complex intergrowth of copper oxide and copper sulphate or oxy-sulphate. This occurs only around the margins of the central plate but is very extensively developed in the upper and lower plates. The sulphur content is very variable from one place to another suggesting that the composition of the oxide/sulphate phase varies from place to place. The S does match very closely with Cu showing that only significant amounts of Cu-rich S-bearing phases are present.

The map for As (Figure 5-4) shows abundant As minerals around the lower Cu layer and on the upper side of the upper layer. Again there are several colours indicating several As contents and different As-bearing minerals.

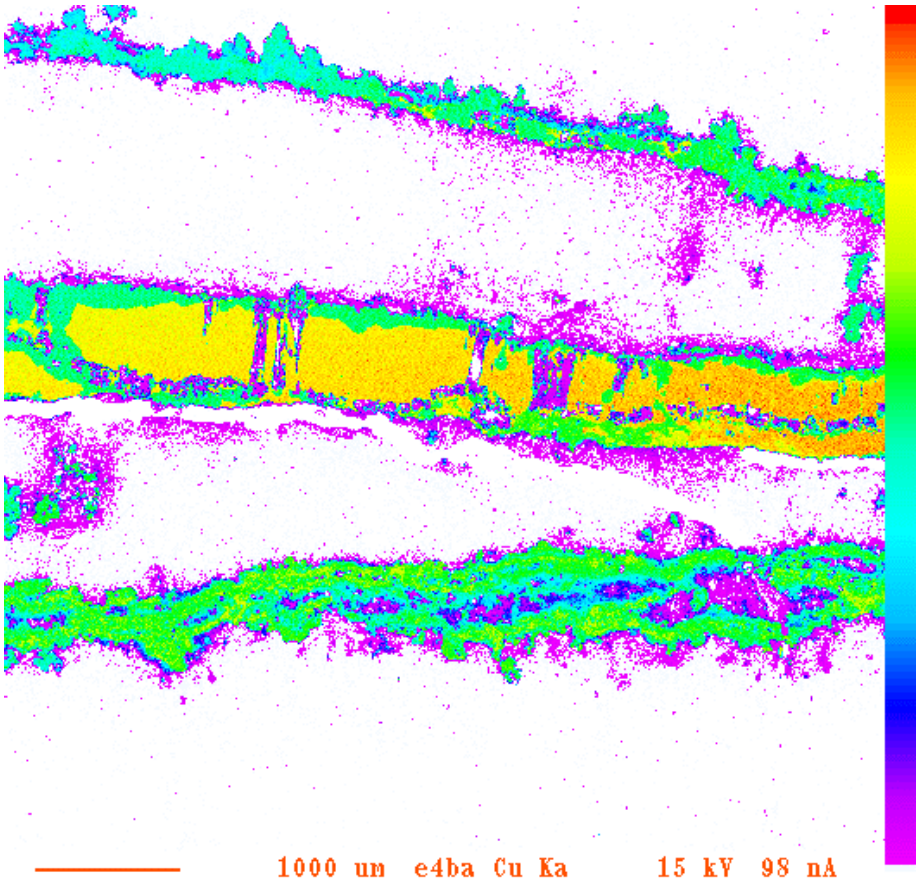

Figure 5-1. *Map of central part of block e4b showing the distribution of Cu. Low values are shown in magenta, high values in bright red.*

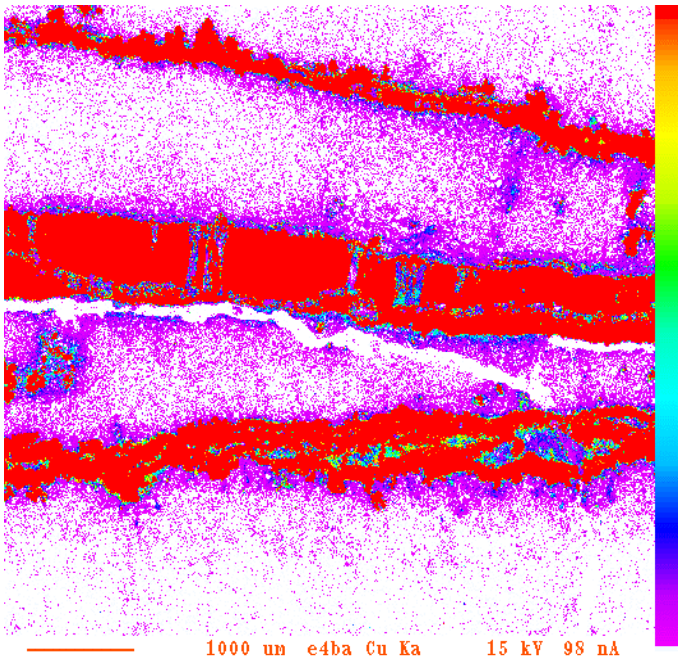

Figure 5-2. *Map as Figure 5-1 but enhancing the low values of Cu.*

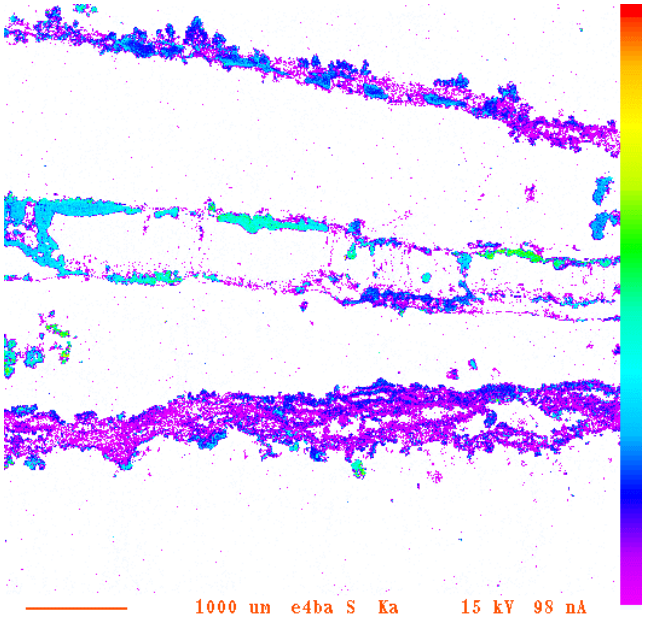

Figure 5-3. *Map for S of the central part of block e4b.*

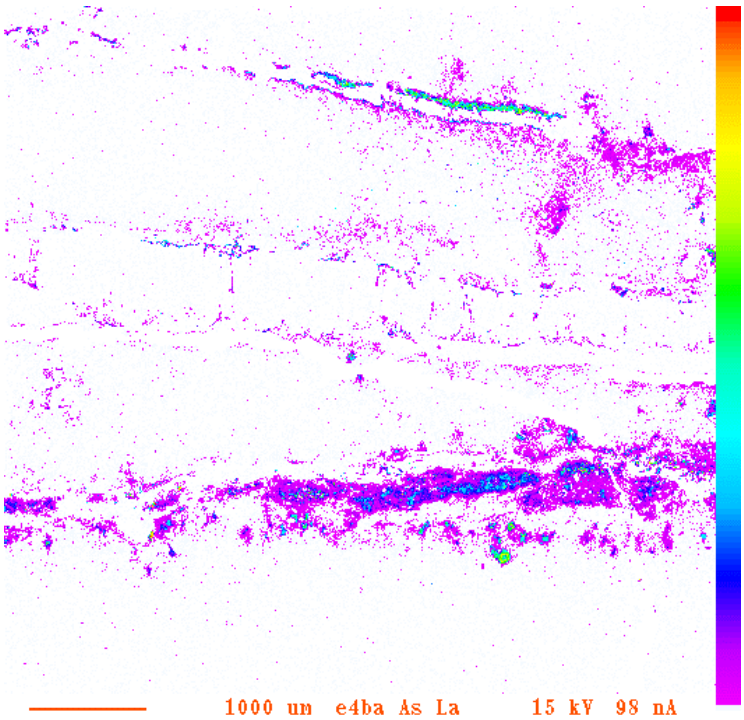

Figure 5-4. *Map for As of central part of block e4b.*

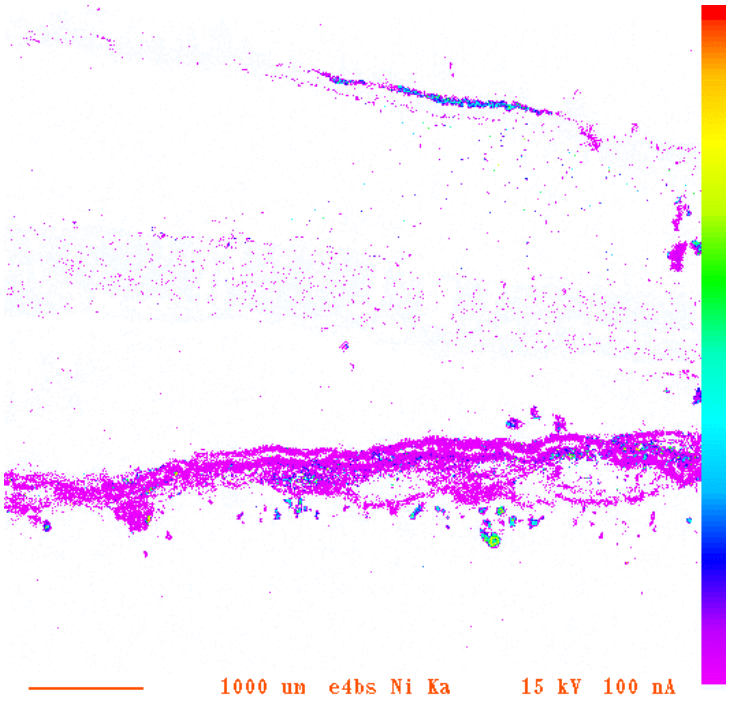

Figure 5-5. *Map for Ni for the central part of blocke4b.*

Ni and Cu arsenides are known to be present from previous studies and the map for Ni (Figure 5-5) shows that there are several grains with high Ni, shown in green-light blue which are probably Ni arsenides. The very distinct As-rich area within the lower Cu plate does not contain Ni but corresponds to moderate Cu and is a Cu arsenide. The very thin layer on the upper side of the upper Cu-layer has moderate Ni and Cu and is a CuNi arsenide. The lower oxide/sulphate layer contains low levels of Ni, shown in magenta while the upper layer does not. This suggests that they are either a different mineral or formed by a different process.

The map for U (Figure 5-6) shows that there are a number of small U-rich minerals present, particularly along the lower surface of the lower Cu layer. There is also a clear association with the Ni-arsenide minerals.

The map for Si (Figure 5-7) shows the coarser quartz (SiO_2) grains as individual particles in yellow-green and the finer ‘clay’ matrix in blue. The epoxy resin that is used to impregnate the voids in the sample during preparation shows on magenta.

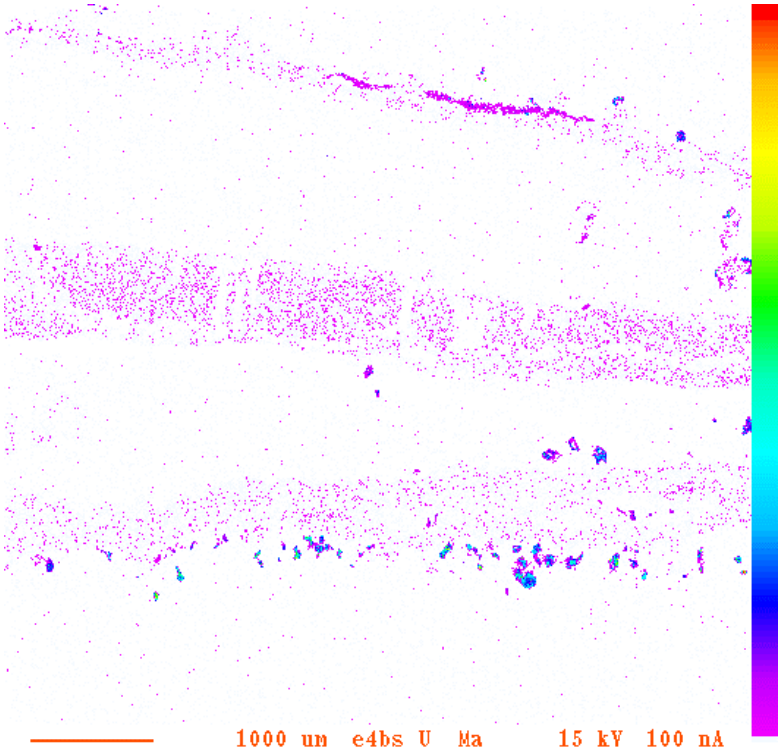

Figure 5-6. *Map for U for central part of block e4b.*

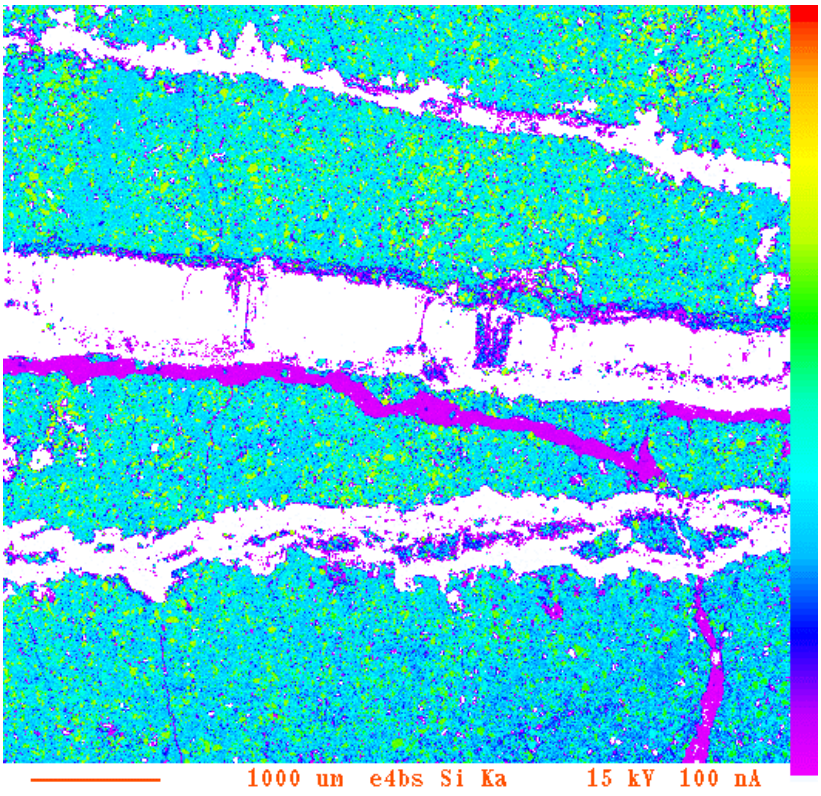

Figure 5-7. *Map for Si for centre of block e4b.*

Sample e4b right hand part

This part of the sample shows many features that are similar to the central part but there are some differences of detail. The map for Cu (Figure 5-8) shows that the upper two layers in the previous are coalesced and that there is a different upper layer. The central layer is again largely Cu metal with oxide/sulphate alteration that is very markedly along the upper surface. Towards the right hand side the oxide/sulphate completely penetrates the Cu sheet and on the right shoulder there is an area that is yellow-green rather than the darker green of the main sulphate. This is cuprite (Cu_2O) and is shown in Plate 5-6. The upper and lower layer are extensively altered but with colours varying from blue to yellow-green indicating variations in composition.

The map for S again (Figure 5-9) shows considerable variation in the S contents indicating several different minerals, both replacing the central layer and within the other layers. The lower layer in particular shows only minor amounts of S in most places and high S only along the margins of the layers. The fact the Cu is high within these areas suggests that the layer is largely a Cu oxide mineral with minor sulphate apart from around the margins.

The Ni and As maps show almost identical features to the central area. The map for U (Figure 5-10) shows a concentration of particles below the lower layer and again there is an association with Ni-arsenide particles.

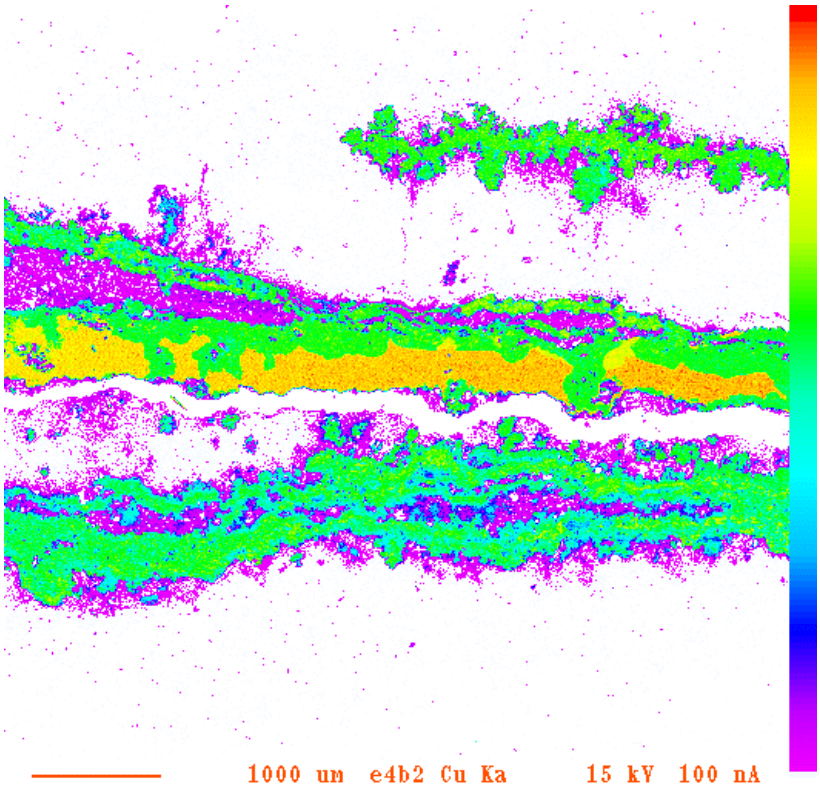

Figure 5-8. *Map for Cu for right hand part of block e4b.*

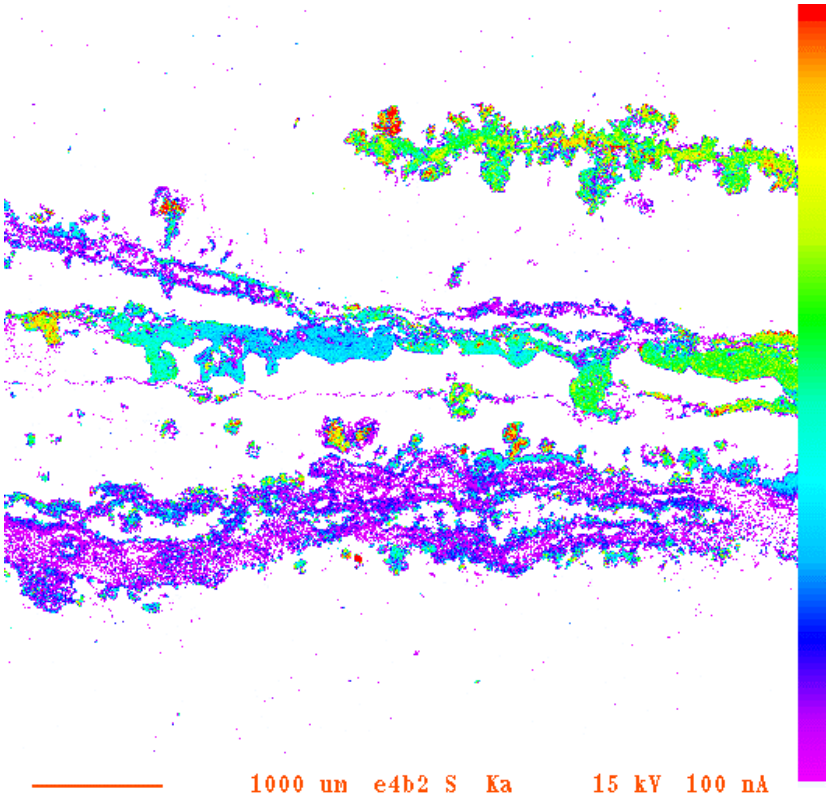

Figure 5-9. *Map for S for right hand part of block e4b.*

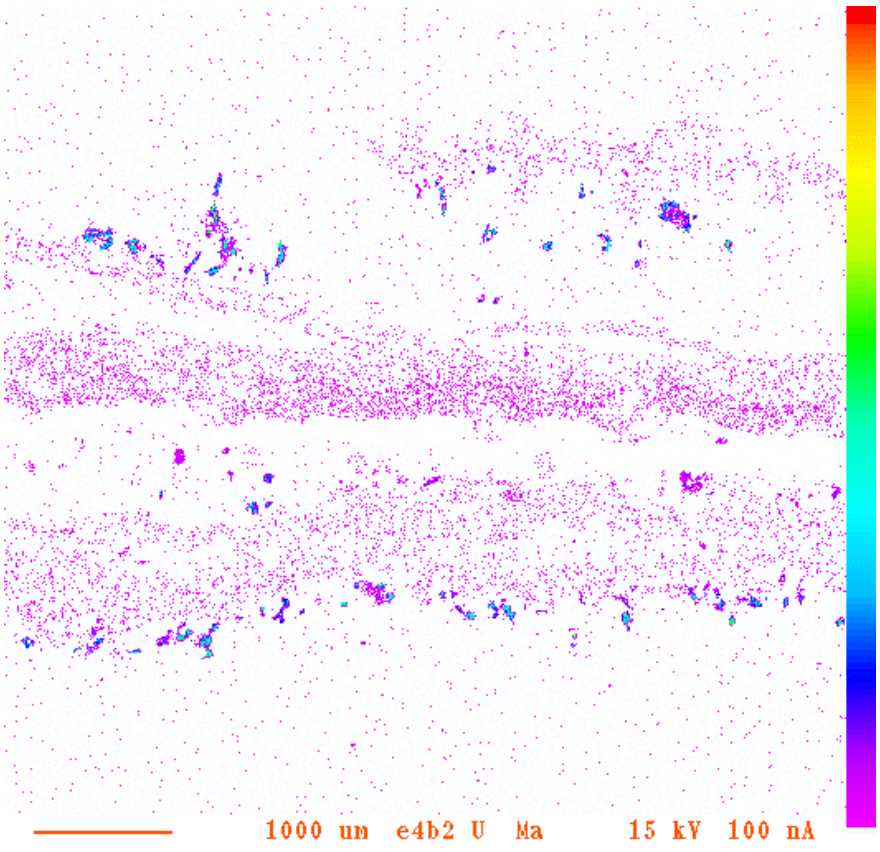

Figure 5-10. *Map for U for the right hand part of block e4b.*

Sample e4c left hand part

These maps cover the left hand part of the block shown in Plate 5-2. The map for Cu (Figure 5-11) shows two diverging plates and a more diffuse area above. The upper plate has an area showing yellow, which on the photos (Plate 5-2) can be seen to be metal, while the rest is alteration products.

The map for S (Figure 5-12)shows that most of the altered Cu contains little S, which confirms the optical observation that it is largely oxide. Sulphate, shown in blue, is largely around the margin of the oxide and there is apparently less variation in composition than in the previous sample b.

The map for Ni (Figure 5-13) shows areas of high Ni which also contain high As and are Ni-arsenides but there are also areas of the Cu oxide that also contain low levels of Ni, such as the areas to the top centre and lower left. It is noticeable that not all the areas assumed to be Cu oxide contain Ni.

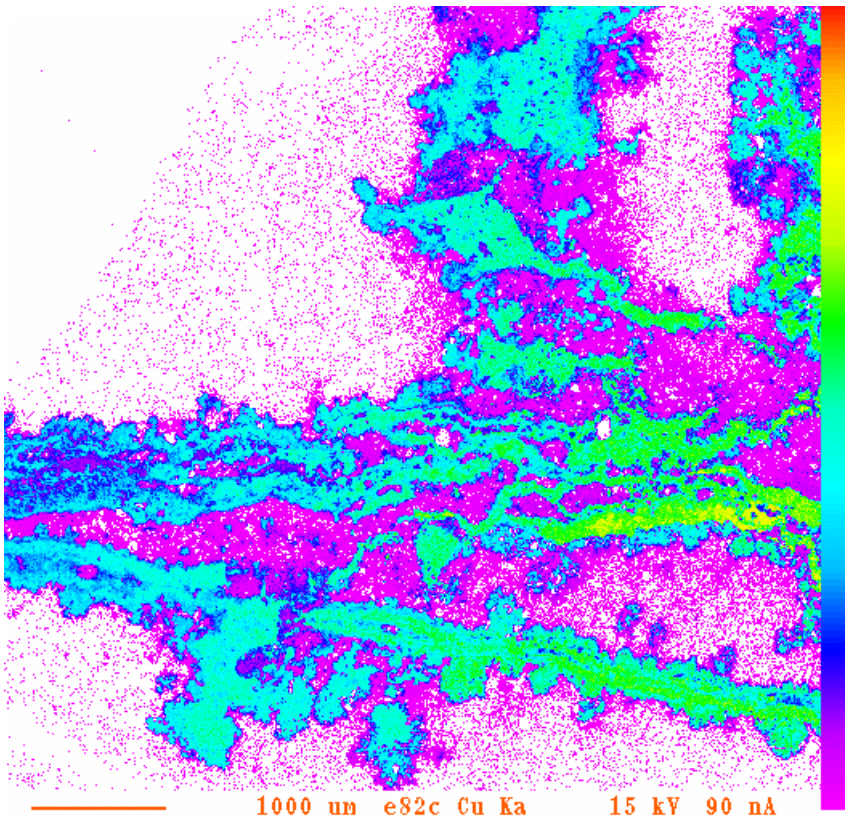

Figure 5-11. *Map for Cu of the left hand part of block e4c.*

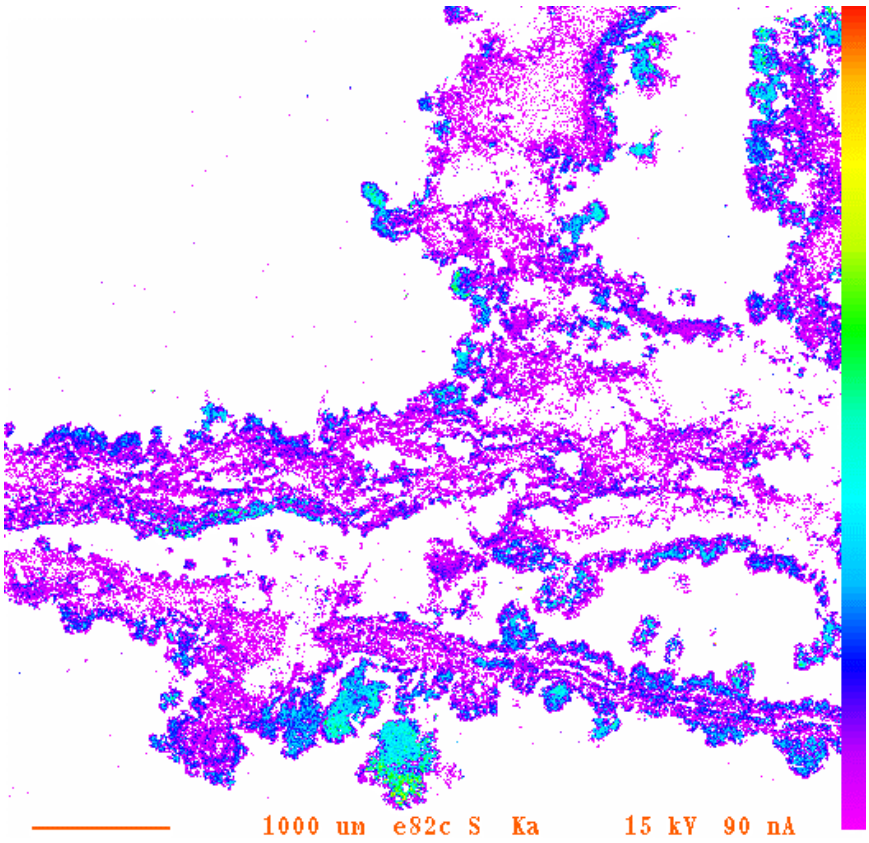

Figure 5-12. *Map for S for left hand part of block e4c.*

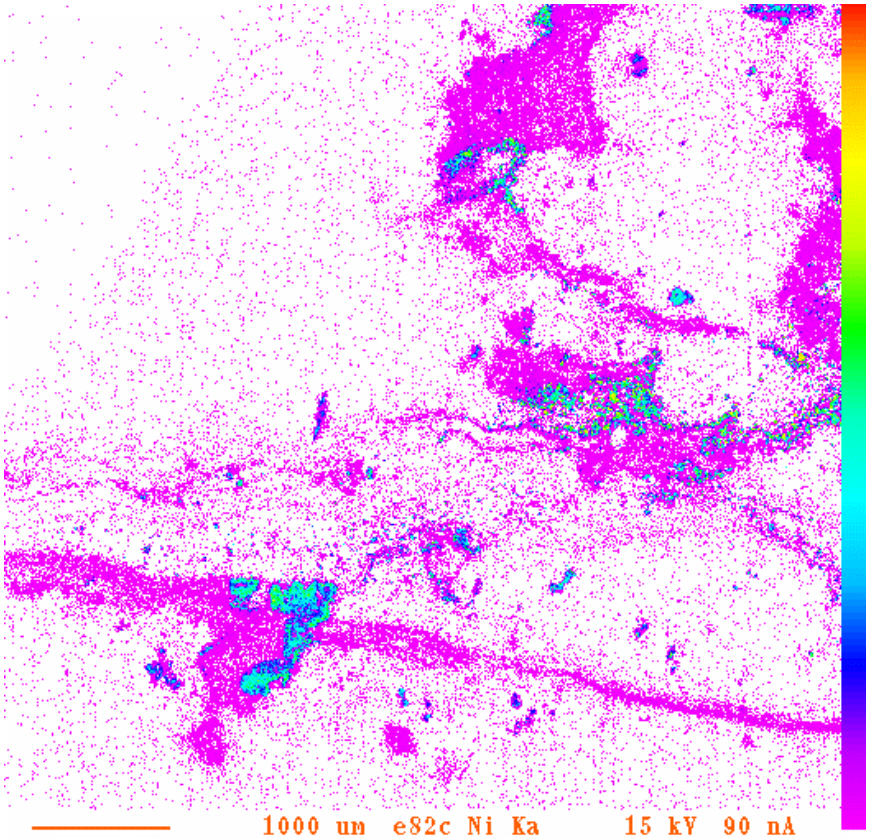

Figure 5-13. *Map for Ni of the left hand part of block e4c.*

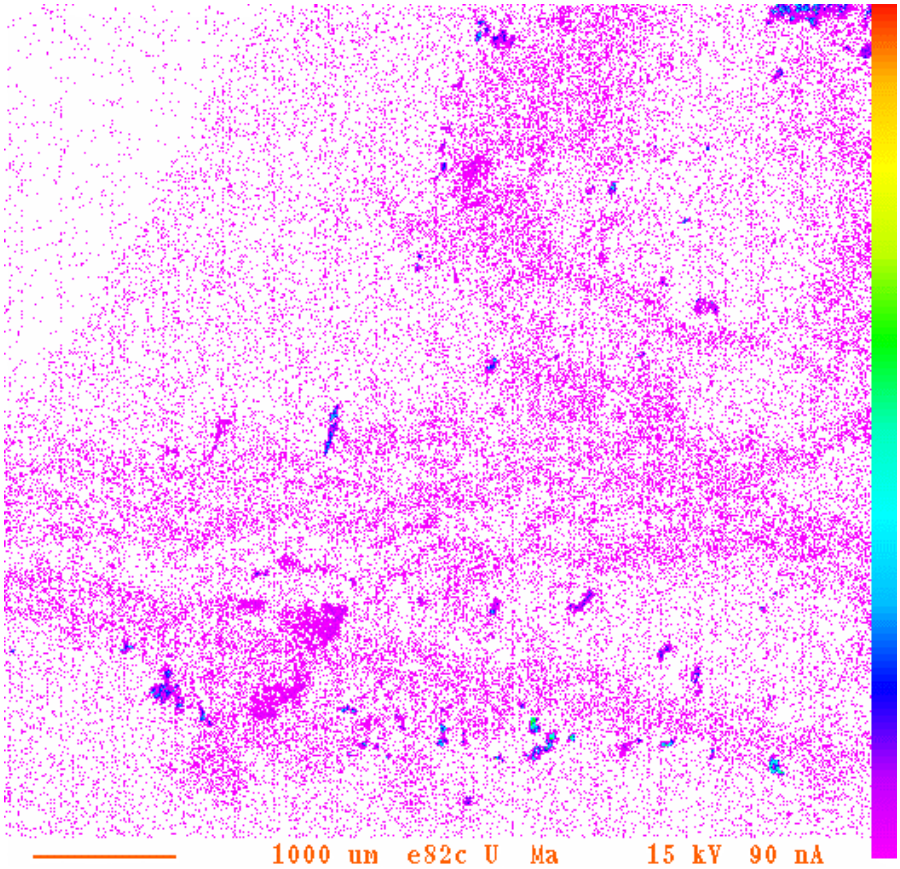

Figure 5-14. *Map of U in the left hand part of block e4c.*

The map for U (Figure 5-14) shows that there is a concentration of grains along the lower surface of the lower layer and around the margin of the upper Cu area. There is some association with the smaller Ni-arsenide grains.

Sample e4c right hand part

The maps for Cu and S (Figures 5-15 and 5-16) for the right hand part show similar features. The Cu map shows oxide and remnants of metal in yellow-green and the sulphate in blue-green. The marginal alteration to oxide/sulphate is even more distinct.

The map for Ni (Figure 5-17) shows the high-Ni arsenide particles and the low-Ni area and ‘veins’ where Ni is present in the Cu oxide phase. The As map (Figure 5-18) shows several areas with numerous small arsenide particles. Some, such as that at the upper left correspond to high Ni and high Cu and are CuNi arsenides, that near the centre is high Ni and low Cu, Ni arsenide, while that at the lower right is high Cu and low Ni, Cu arsenide.

There is little U in this area, mostly around the margin of the Cu in the upper part.

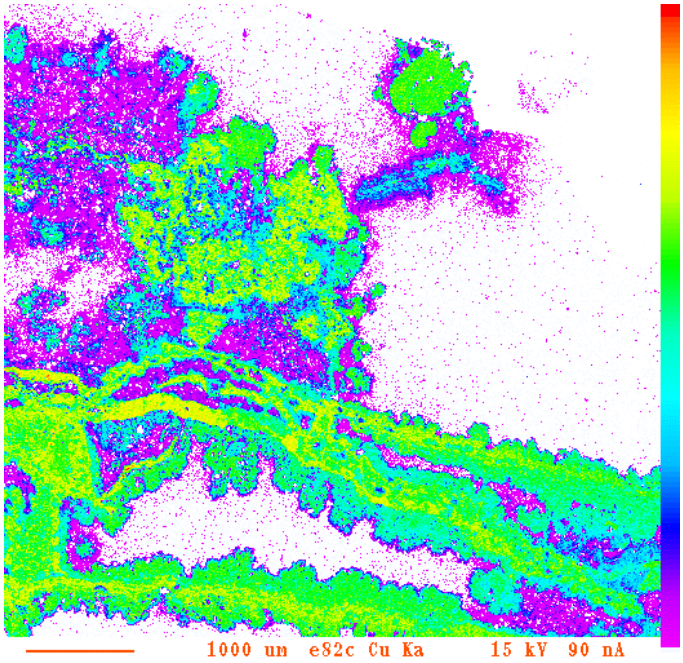

Figure 5-15. *Map for Cu for right hand part of block e4c.*

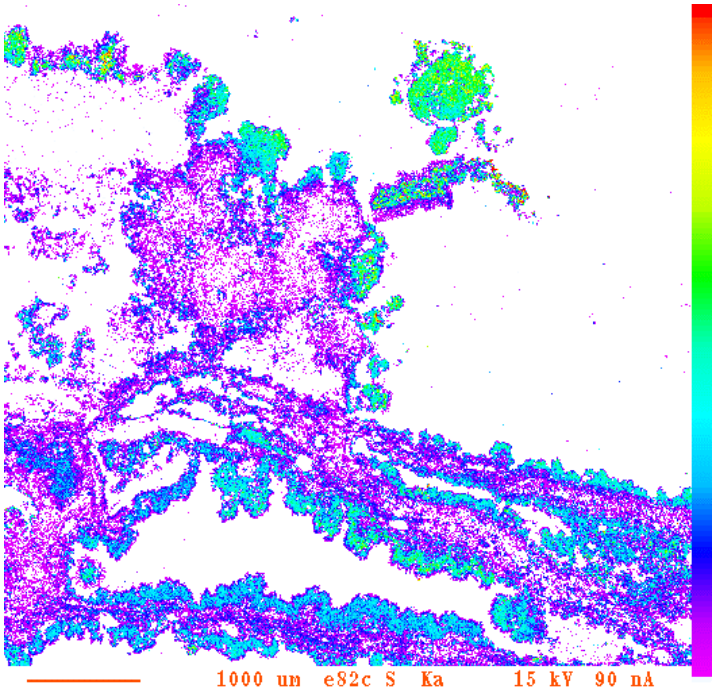

Figure 5-16. *Map for S for right hand part of block e4c.*

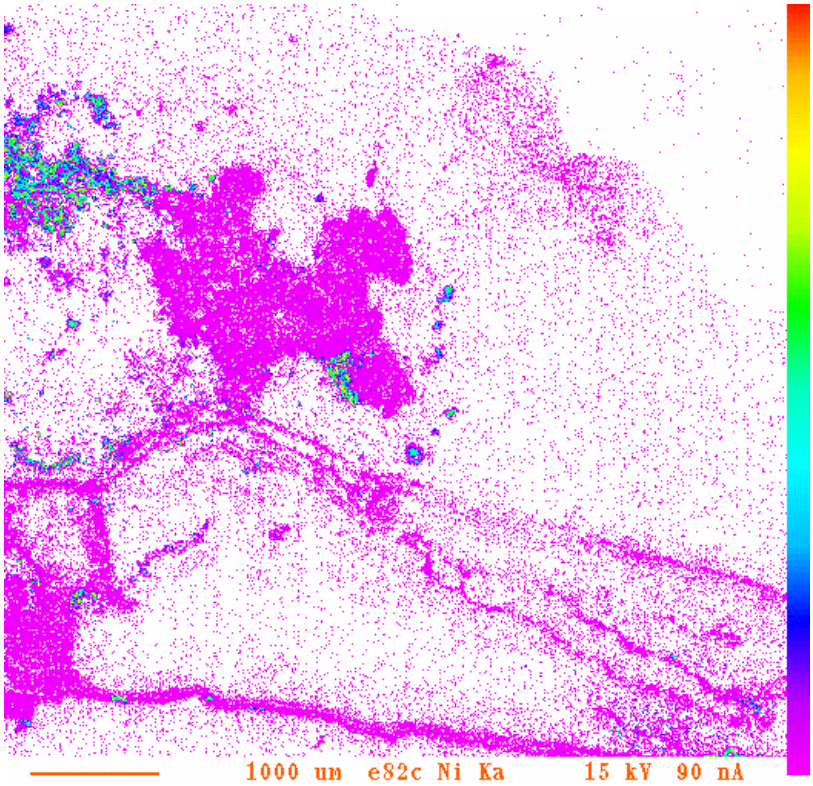

Figure 5-17. *Map for Ni for right hand part of block e4c.*

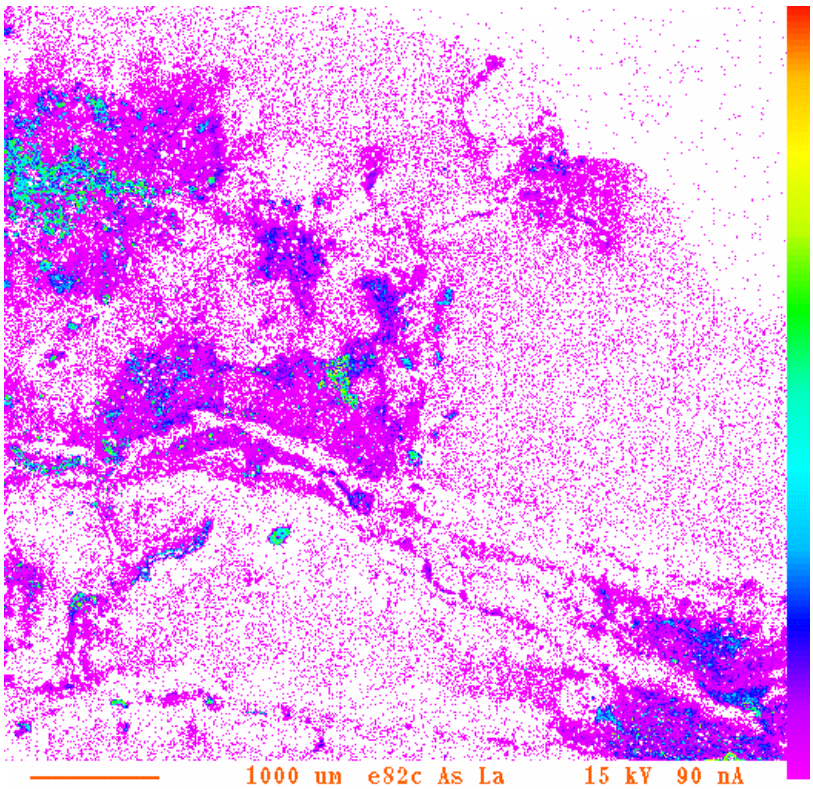

Figure 5-18. *Map for As for right hand part of block e4c.*

The nature of the grey arsenide 'alteration'

The grey arsenide alteration particularly affecting the copper sheets in blocks 1-3 has been investigated in more detail to identify the minerals involved and the process taking place. In some places the grey arsenide appears to be corroding the margins of the copper and in many places appears to have largely replaced the copper leaving just a few remnants (Plates 5-11, 5-16, 5-22). The relationship between copper sheets and arsenides was briefly investigated using rapid maps of smaller areas. These maps are in groups of four where the caption lists the elements in the order top left, top right, bottom left, bottom right.

The thick unaltered copper sheets can be seen at the top left and bottom right of the Cu map (Figure 5-19) with the altered sheet through the centre. This map also shows that there is very little Cu within the main arsenide zone but there are a few 'intergrowths of Cu-rich mineral which proved to be CuS, chalcocite. Outside the main arsenide zone fine Cu-arsenide grains are present.

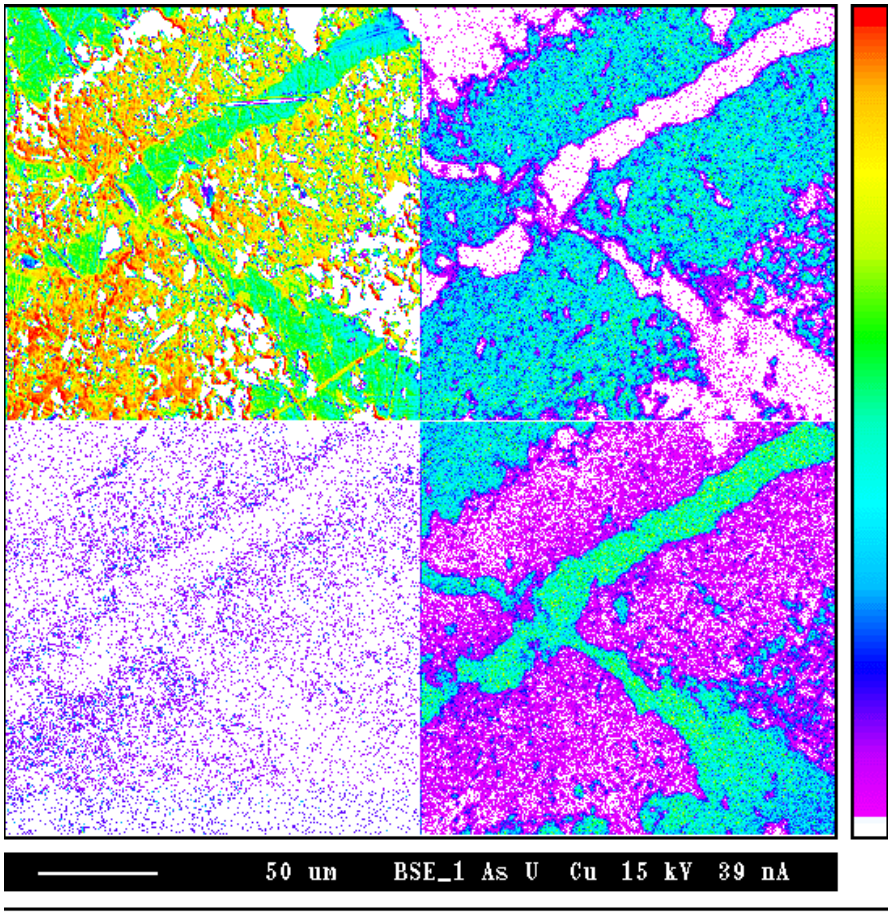

Figure 5-19. *X-ray maps of the cross-cutting layers in B3 shown in Plate 5-22.*

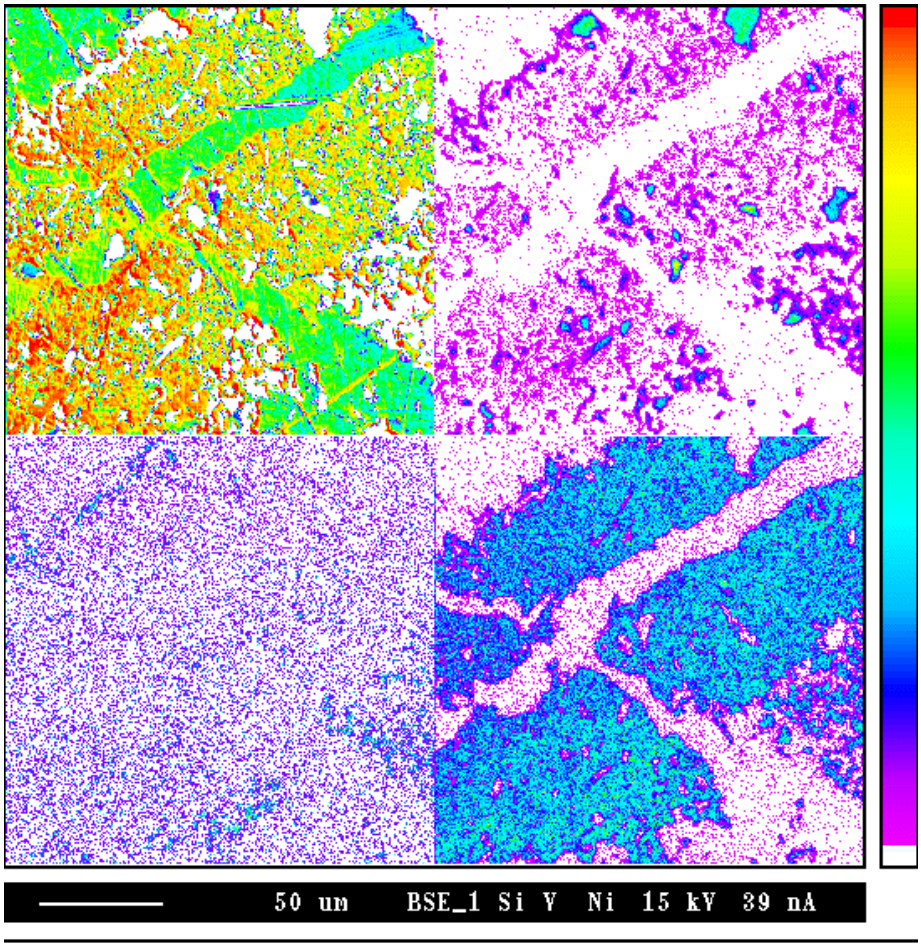

Figure 5-20. *X-ray maps of the cross-cutting layers in B3 shown in Plate 5-22.*

The map for Ni (Figure 5-20) shows that the main component is Ni-arsenide which analysis showed to be chemically similar to maucherite ($Ni_{11}As_8$), but optically it is very different. Maucherite is white with high reflectance whilst this is grey with low reflectance, virtually the same as the included chalcocite. The distribution of silica is very interesting, as it shows a large number of quartz particles within the Ni-arsenide. Numerous quartz particles are not seen inside the copper sheets so this suggests that the arsenide is growing in the sediment around the copper sheet rather than extensively replacing it. The amount of corrosion and replacement of the copper sheet in this area appears to be quite small.

The U Ni As association

Several of the larger scale maps show an association between U and Ni-arsenides and this has also been further investigated.

The maps in Figure 5-21 show a Cu oxide/sulphate particle with a partial rim of Ni arsenide. The U closely follows but not quite exactly the Ni arsenide suggesting they may not actually be in the same mineral.

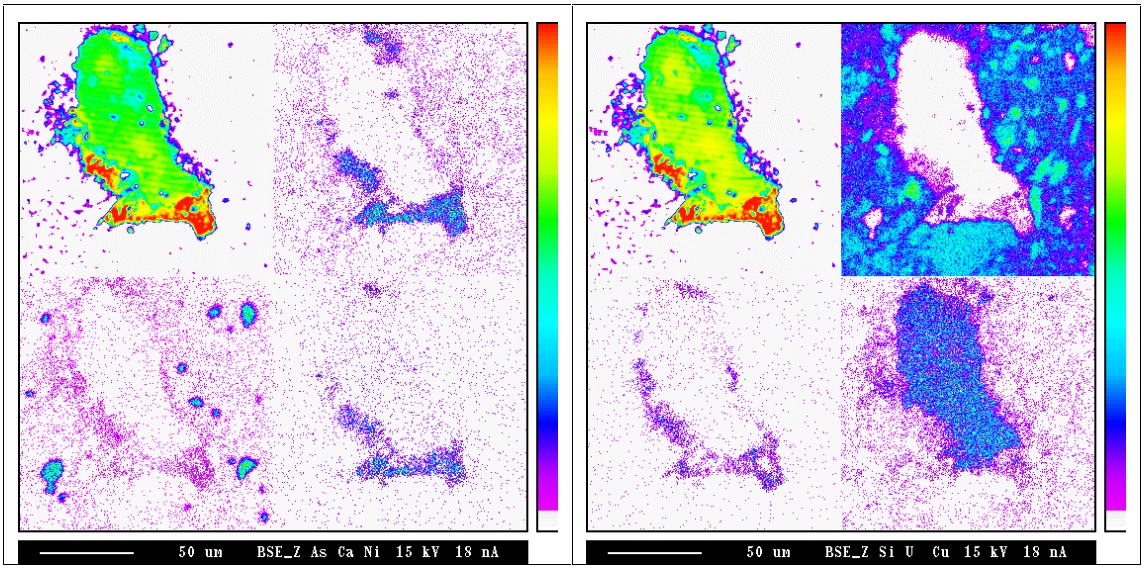

Figure 5-21. *Maps of particles from block e4b.*

The maps in Figure 5-22 are of different particles at a higher magnification. These maps suggest there may be two types of U mineral, one which is indistinguishable from the Ni arsenide grains and another, in the central part which does not contain Ni and As but has Ca and P and minor Si (not shown).

The largest of the NiAs-U particles below the lower Cu layer, shown on the maps Figure 5-23 lower right was examined. This proved to be a mini-nodule.

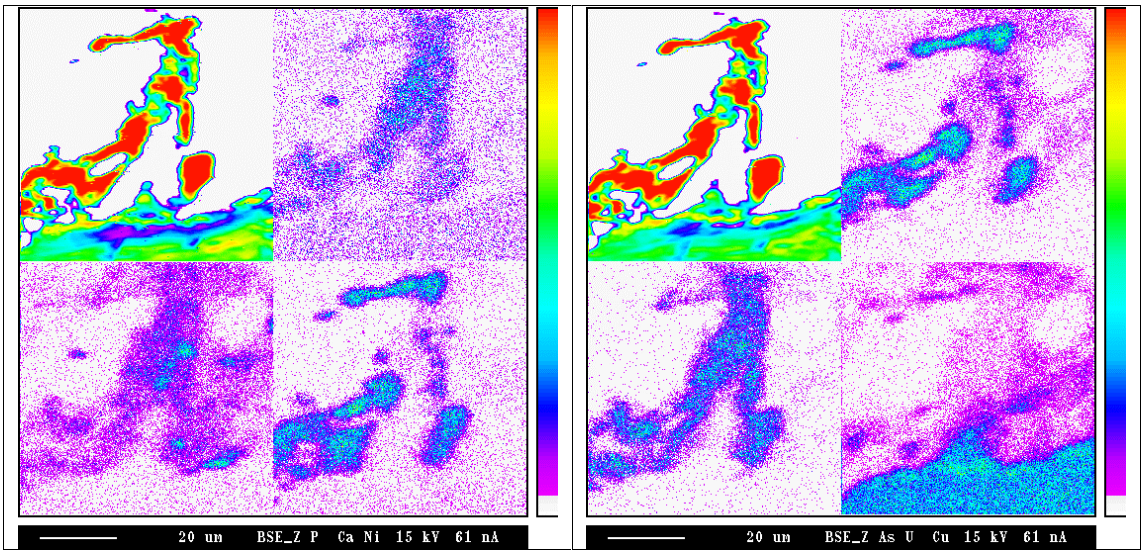

Figure 5-22. *Maps of particles from block e4b.*

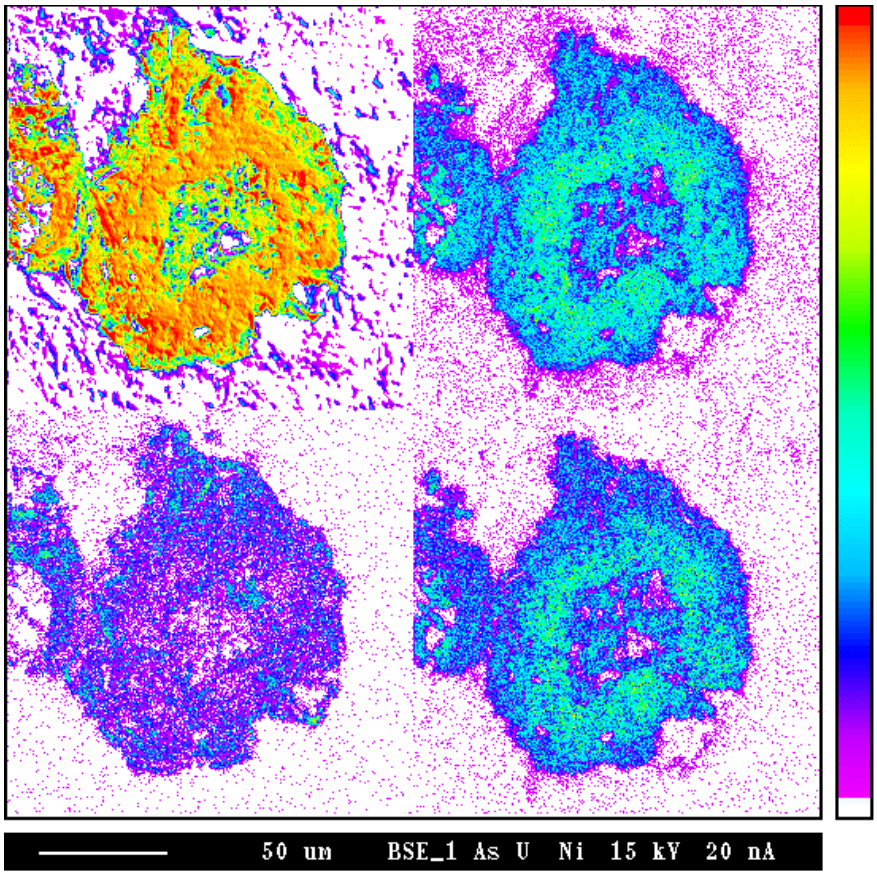

Figure 5-23. *Elemental maps showing annular structure of the "mini-nodule" in sample e4b.*

It consists of a concentric annular body of NiAs with abundant U. The distribution of U is very inhomogeneous and is particularly abundant around the outer margin and also the porous centre. This suggests that the U mineral is depositing around the NiAs at a late stage.

Examination of the distribution of U in the grey arsenide rims in block 2 sheds further light on the association.

The maps in Figure 5-24 show similar features of the arsenide 'overgrowth' on the copper sheet with Uranium distributed around the margin and in the interstices of the arsenide. This suggests that the U is as a fine-grained phase that is growing around the arsenide at a late stage of the depositional history. Also of interest in these maps is the abundance of V around the outer parts of the layer. This is a V-rich mica like mineral that is found in many of the samples.

From this limited investigation it is clear that U is commonly closely associated with Ni arsenide. In some cases it is not possible to ascertain whether it is actually in the Ni arsenide, but in others it is a separate very fine-grained phase that is forming around the margins of the NiAs. U is also present as a separate phosphate-like mineral. The grain size of these minerals is very small, only up to 2 or 3 microns and hence accurate identification will be very difficult.

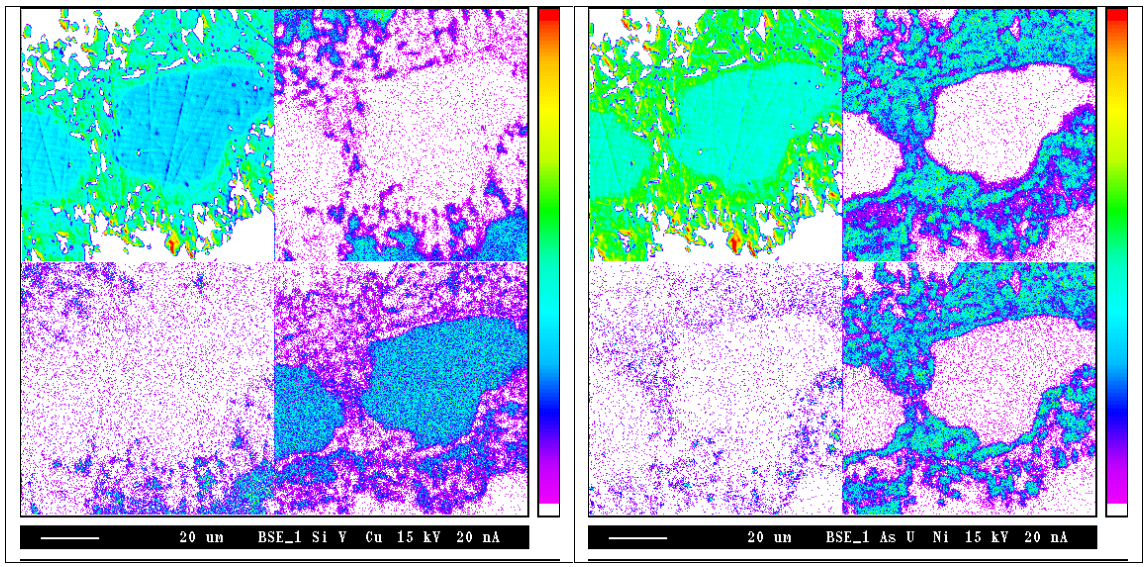

Figure 5-24. *X-ray maps of part of block 2.*

The nature of the oxide/sulphate alteration

Complexly and intimately intergrown oxide-sulphate type of alteration is the most common in block e4 but not found in the other samples. Its appearance under the reflected light microscope is a massive homogenous phase with some porosity that replaces both the Cu metal and Cu-oxide alteration (Plate 5-7). It has a very low reflectance, lower than cuprite and is softer and does not polish as well as cuprite. The nature of this alteration is very complex and the best information to date is from a detailed BSEM examination of the same area as covered by Plate 5-7 and shown in Plate 5-39.

A higher magnification view (Plate 5-40) of the central part of the oxide/sulphate shows a polygonal–like or microbotryoidal (microcolloform) structure which contains Cu, S and O (probably a sulphate or oxysulphate) with interstitial areas, slightly darker that contain little or no S (oxide). At the highest resolution it can be seen that there is a sub-micron scale zonation to the microcolloform structures (Plate 5-41). The polygonal structure is often indicative of formation from a gel.

The alteration in the area on the left side of the oxide/sulphate embayment shows slightly different features Plate 5-42. An area in the oxide/sulphate close to the oxide interface preserves small spherical structures, around 1 μm in diameter. Such structures are often associated with sulphides and particularly those with a biogenic origin. These are perhaps relics after sulphide similar to that found in another area of the sample (Section 5.2) and shown in Plate 5-12. It is possible that earlier Cu-oxide alteration has been attacked by sulphur reducing bacteria to form a layer of Cu-sulphide. This sulphide was subsequently oxidised to form a gel of sulphate, possibly hydrated sulphate and oxide.

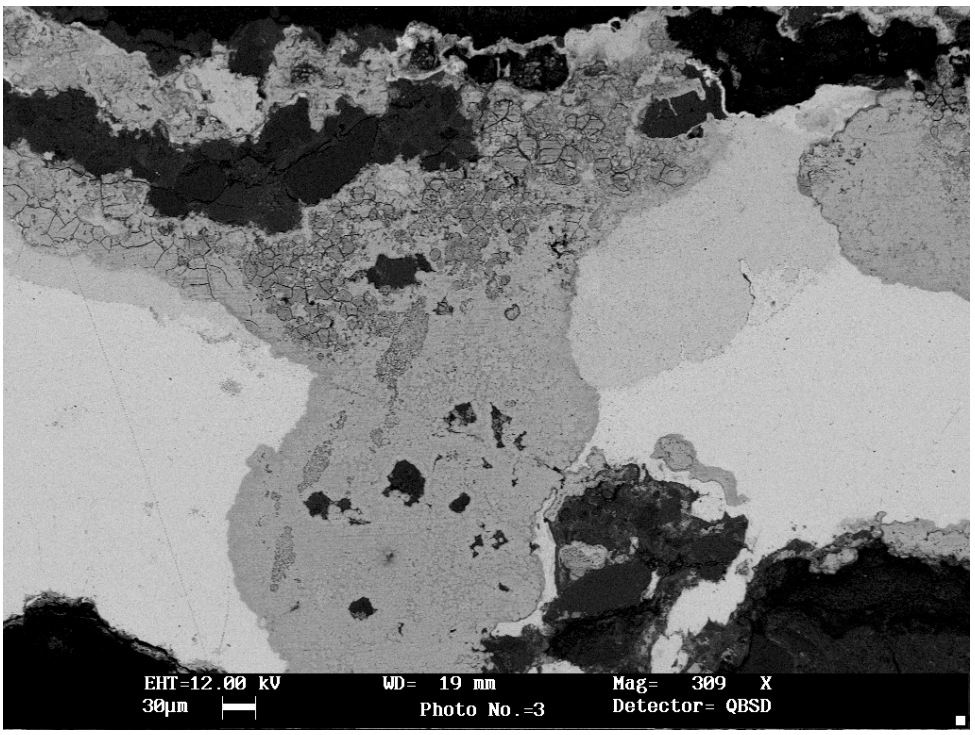

Plate 5-39. *BSEM image of part of e4b showing Cu-metal (white), cuprite (light grey), oxide/sulphate alteration (mid-grey) ?oxide/chloride alteration (dark-grey) and sediment (black).*

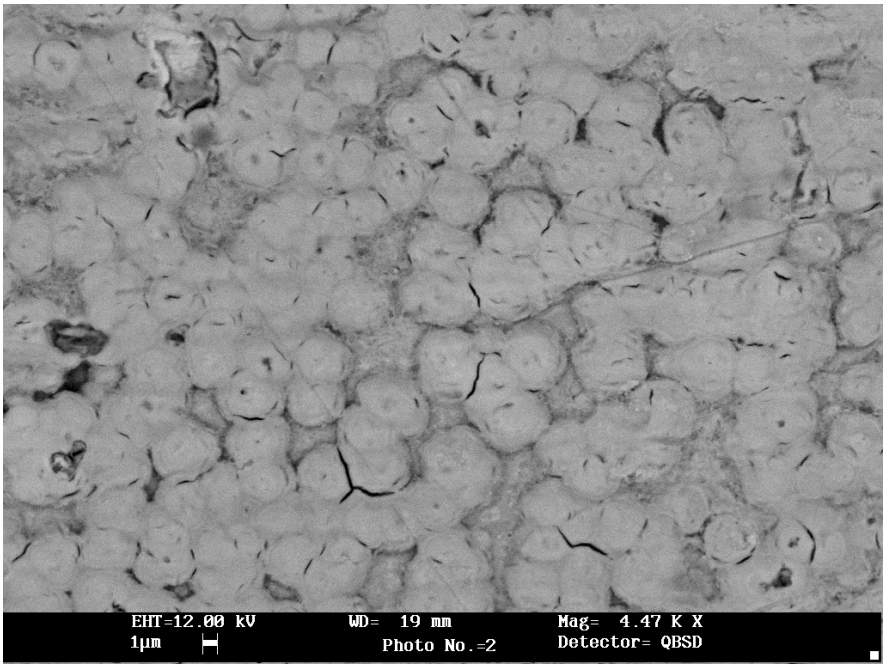

Plate 5-40. *BSEM image showing a polygonal-structure to the oxide/sulphate area consisting of S-rich lighter areas and S-poor interstitial darker areas.*

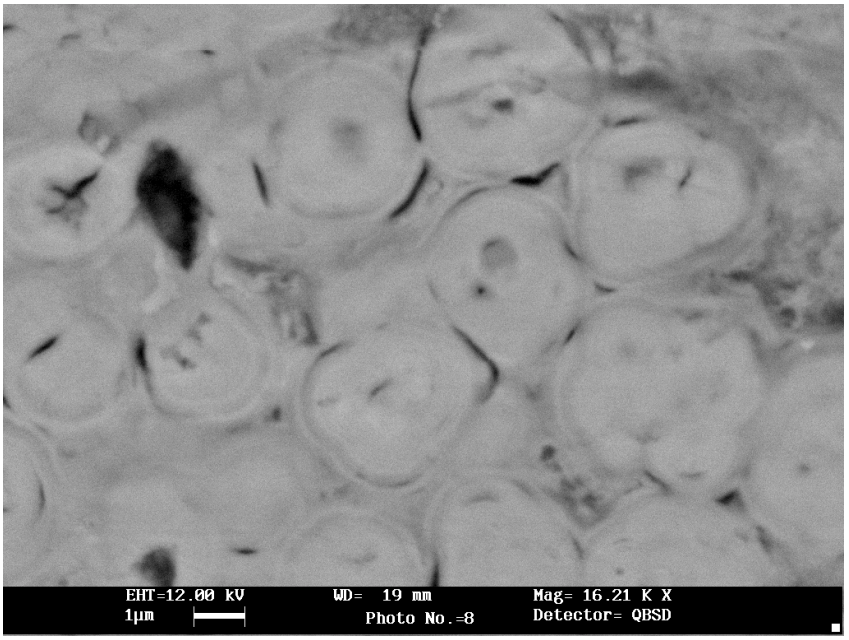

Plate 5-41. *Submicron-scale zonation in sulphate polygonal structures.*

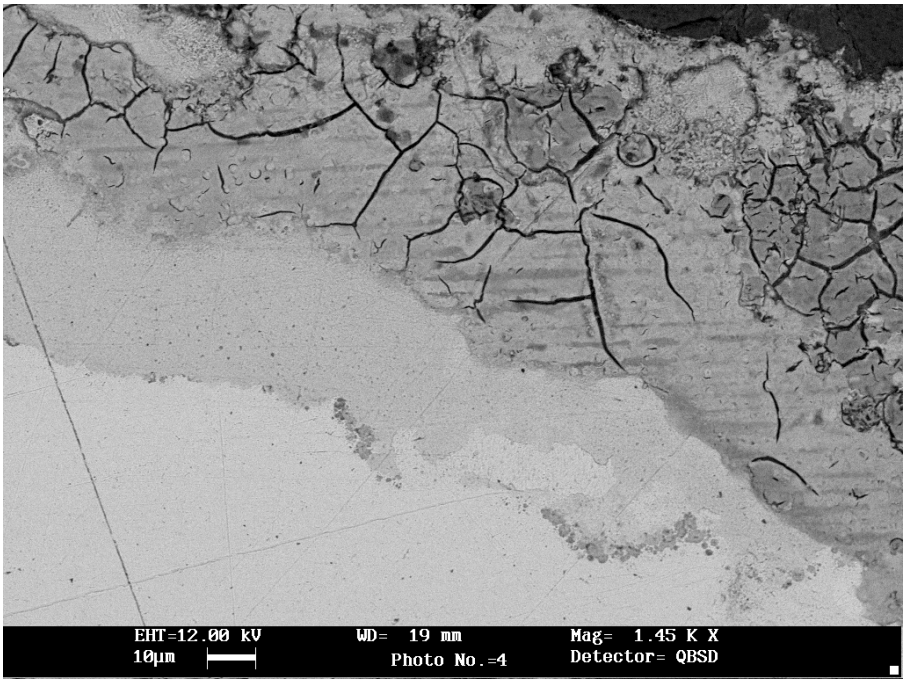

Plate 5-42. *Alteration at the edge of the Cu-sheet showing Cu-metal (white) cuprite (light grey), oxide/ sulphate (mid-grey), oxide/chloride (dark-grey very marked polygonal cracks). Along the interface between the metal and the cuprite is a slightly darker oxide phase that is probably tenorite (CuO). The stripes across the oxide/sulphate are damage from electron probe microchemical mapping.*

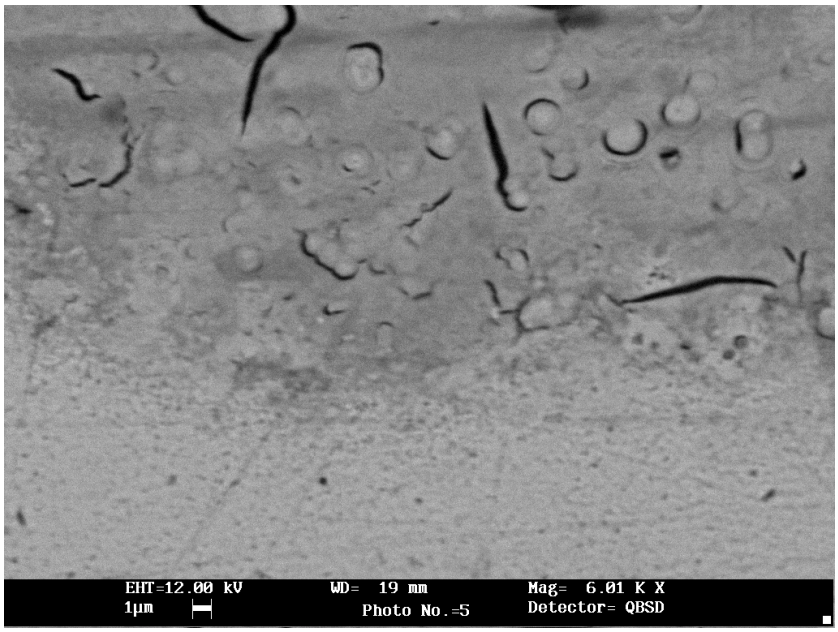

Plate 5-43. *Small spherical structures in the oxide/sulphate alteration.*

Some areas of the oxide/sulphate show marked polygonal cracking, as distinct from growth structures which indicates dehydration and shrinkage. This possibly formed during sample preparation either due to the exothermic reactions of epoxy resin setting or from heating the samples during impregnation and resin curing. The areas with the most intense cracking show traces of Cl. It is not known at present if this is natural or from resins and reagent used during sample preparation.

Fast beam microchemical maps Figure 5-25 show that in some places the sulphate/oxide appears relatively homogeneous but in others it is highly inhomogeneous with a pattern matching the polygonal structure described above. The polygonal structures are higher in S than the matrix matching the BSEM observations.

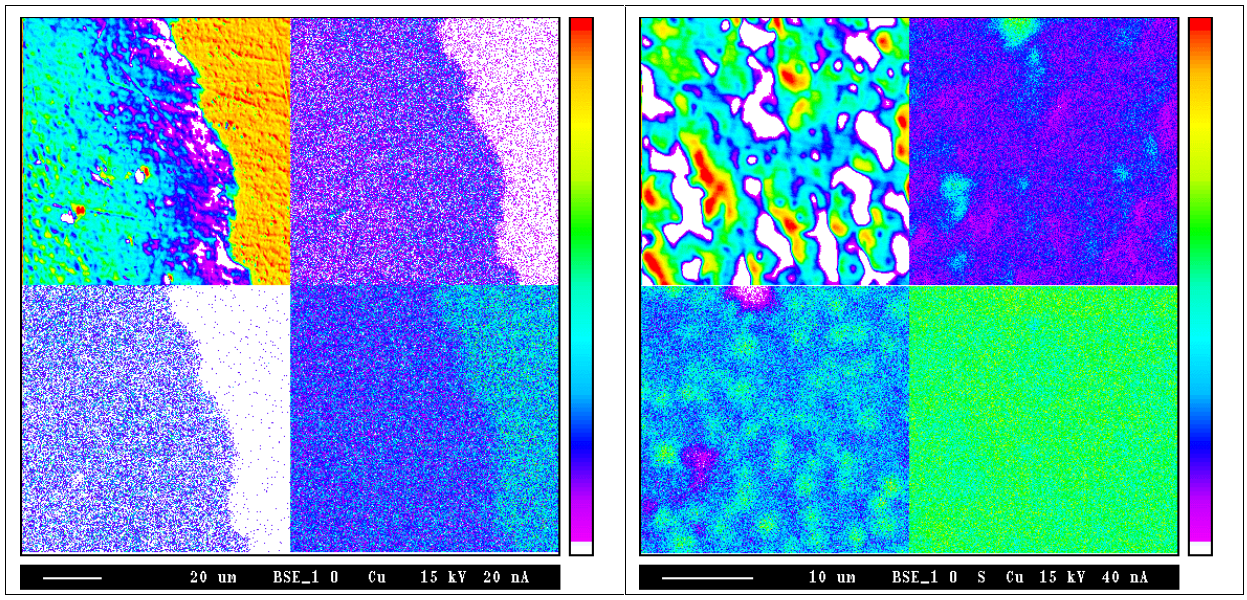

Figure 5-25. *X-ray maps showing apparently homogeneous and clearly inhomogeneous areas of sulphate/oxide alteration.*

5.3.2 Line traverse

A traverse of 200 quantitative analyses was made through the central part of block e4b in the area covered by Figure 5-1. The analyses were at a spacing of 35 μm giving a traverse length of 7 mm, which covered the three Cu-rich layers and about 2 mm either side. The electron beam was defocused to 5 μm to reduce beam damage to the sample and give a more representative analysis of the local region. The analyses were for the elements Cu, Ni, Fe, Mn, Ca, Ag, S, P, Si, and As.

The traverse (Figure 5-26) clearly shows the Cu layers with the central metal layer giving over 100% when calculated as oxide and the oxide/sulphate layers giving around 60–80%. Low levels of Cu are found throughout the matrix and this is best shown on a logarithmic plot (Figure 5-27).

This traverse shows analyses on quartz grains that contain no Cu close to the 0.01 line but the vast majority of points above 0.1, which is well above detection. There is also an increase in Cu content towards the Cu layers, which possibly indicate diffusion or redistribution mechanisms.

The values for NiO, Figure 5-28, are plotted on the same graph as Cu_2O, to give a reference. This show no Ni in the central Cu metal layer, low levels in the upper oxide/sulphate layer but relatively high values, 1–2% in the lower oxide/sulphate layer (left hand side of plot). In some places the values in the matrix seem to mirror the Cu values, e.g. around the lower layer (x –9000 to –6500), while between the central and upper layers (x –5500 to –4000) they appear to have an antipathetic relationship.

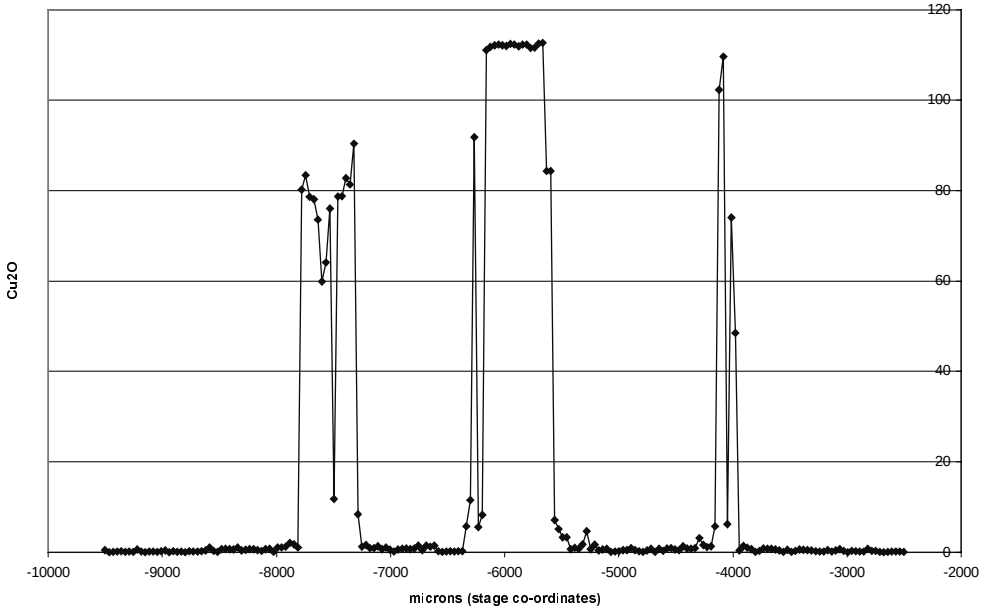

Figure 5-26. *Electron microprobe traverse across part of e4b for Cu (calculated as Cu_2O) metal shows as more than 100%.*

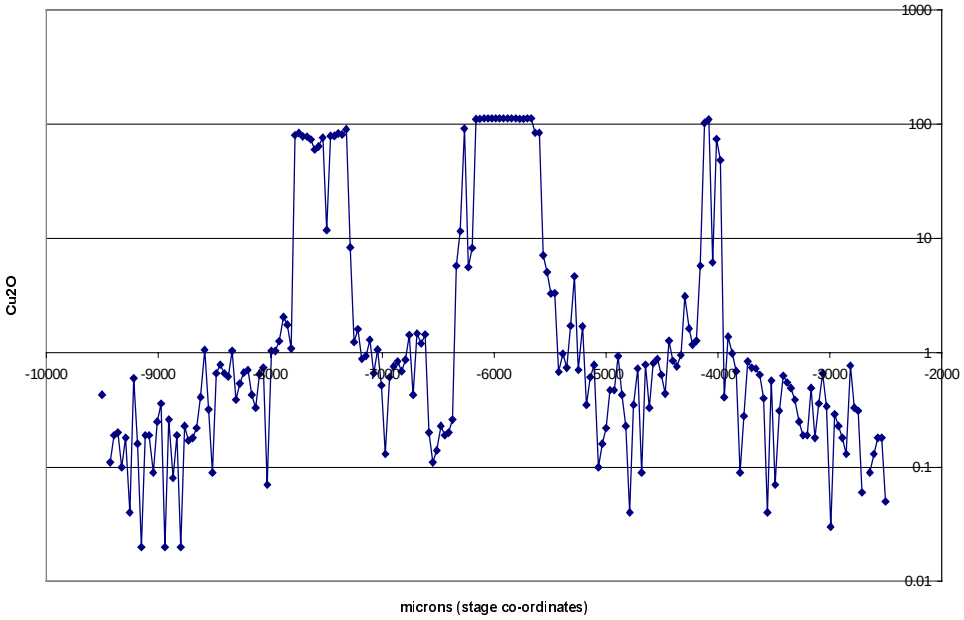

Figure 5-27. *As Figure 5-24 with Y axis on a log scale.*

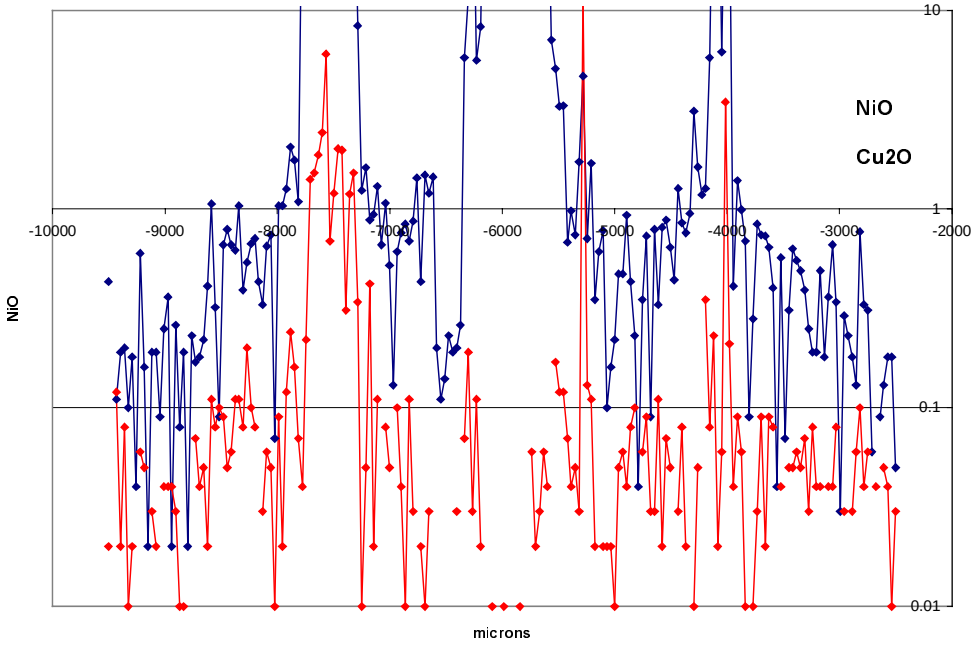

Figure 5-28. *Traverse across part of e4b, the same as Figures 5-26 and 5-27, showing Cu_2O in blue and NiO in red. The lower layer in the map, Figure 5-1, is the to left of this plot around –7500.*

5.3.3 Electron microprobe point analysis

Electron microprobe analyses of selected minerals are presented in Tables 5-2–5-5, and described briefly below.

Native metals

Native copper or copper metal is found in all the plates and most also have small inclusions of native silver or silver metal. The metals are generally very pure, the copper possibly contains traces of Ag, Cd and Ni while the silver may contain greater amounts of Cu, though some of thus could come from the surrounding copper.

Table 5-2. Electron microprobe analyses of metals (wt% element).

	S	Ag	Cd	Fe	Cu	Ni	Total
1	0.06	0.03	0.03	0.05	99.43	0.01	99.61
2	0.01	0.06	0.08	0.00	100.48	0.00	100.63
3	0.00	0.10	0.00	0.00	99.95	0.32	100.37
4	0.10	99.65	0.98	0.03	0.04	0.06	100.87
5	0.08	99.14	0.00	0.11	3.85	0.04	103.22

1–3 Native copper from block e4.
4 and 5 Native silver from block e4.

Copper oxides

Copper oxides are present as an early alteration phase of the Cu sheets. The dominant type identified from optical examination is cuprite Cu_2O but analyses show that tenorite CuO is also present. The most noticeable feature is the very variable Ni content from below detection up to 1.7%. This variation was very apparent from the maps but the reason for it is not known.

Table 5-3. Electron microprobe analyses of oxides (wt% oxide).

	As_2O_3	SiO_2	P_2O_5	SO_2	CaO	FeO	NiO	Cu_2O	Total
1	0.09	0.07	0.61	0.27	0.00	0.07	0.00	96.70	97.81
2	0.05	0.07	0.67	4.41	0.14	0.06	0.39	97.28	103.08
3	0.12	0.00	0.58	4.07	0.10	0.00	0.12	98.49	103.48
	As_2O_3	SiO_2	P_2O_5	SO_2	CaO	FeO	NiO	CuO	Total
4	0.00	0.19	0.38	0.55	0.42	0.00	1.63	94.58	97.75
5	0.36	0.14	0.08	0.70	0.33	0.21	0.83	97.43	100.08

1–3 Cuprite from block e4.
4–5 Tenorite from block e4.

Copper oxide/sulphates

Complex intergrowth of copper oxide(s) and copper sulphate or oxysulphate(s) is very common in block e4, and is the most extensive alteration product of the copper metal in this sample. The composition is very variable from place to place. Some examples are given in Table 5-4 which show that Cu varies very little but S varies substantially. The compositions determined are likely to be mixtures of several phases as indicated in section 5.3.1 – The nature of the oxide/sulphate alteration, rather than a single phase. If they do represent a single phase then the Cu:S ratios suggest a stoichiometry between Cu_4SO_4 to Cu_6SO_4. Phases of this type of composition are not known as anhydrous sulphates. There are many hydrated and hydroxysulphate minerals based on Cu_4SO_4 (e.g. brochantite $Cu_4SO_4(OH)_6$ and langite $Cu_4SO_4(OH)_6.2H_2O$). It is likely that the analyses produced here are of a phase produced by the dehydration of a hydrated sulphate during sample preparation or mixtures of a oxysulphate of a more normal Cu_2SO_5 type (dolerophane) and Cu-oxide either Cu_2O or CuO as was indicated in Section 5.3.1 – The nature of the oxide/sulphate alteration. The minerals involved in the mixture are probably largely anhydrous as they suffer only minor beam damage under the electron beam, they give analysis totals close to 100% with either a focused or defocused beam. There is, however, likely to be Cu present as both Cu_2O (cuprite) and CuO (tenorite) – as shown by detailed petrography (Section 5.3.1 – The nature of the oxide/sulphate alteration), which would raise the totals slightly. Analysis 6 gives a total well over 100% which suggests that there may be some sulphide present, rather than sulphate in this point, which could account for the higher total as some S should not have been combined with O. Detailed BSEM petrographical observations have discriminated fine grained relict chalcocite within this secondary alteration (Section 5.2).

Table 5-4. Electron microprobe analyses of oxide/sulphates (wt% oxide).

	SiO_2	SO_3	FeO	NiO	Cu_2O	Total
1	0.07	16.11	0.14	0.04	84.55	100.91
2	0.10	14.05	0.07	1.44	82.22	97.88
3	0.08	13.48	0.00	0.05	84.96	98.57
4	0.06	15.24	0.07	0.02	86.76	102.14
5	0.04	10.95	0.00	0.00	91.46	102.45
6	0.10	26.91	0.15	0.03	83.35	110.54

1–6 Copper oxide/sulphates from block e4.
4–5 Defocused beam 5 μm diameter.

Arsenide minerals

A range of arsenide minerals have been identified in a variety of modes of occurrence, including: copper arsenides – algodonite (Cu_6As) and an unidentified copper arsenide with a composition of approximately CuAs; nickel arsenides – maucherite (Ni_3As_2) and niccolite (NiAs); and mixed copper-nickel arsenides. The most abundant is the grey arsenide mineral, whose composition is similar to maucherite but which has very different optical properties.

Table 5-5. Electron microprobe analyses of arsenides (wt% element).

	As	S	Fe	Cu	Ni	Co	Total
1	48.44	0.01	0.04	48.62	1.45	2.09	100.65
2	49.81	0.00	0.03	49.46	2.29	1.18	102.77
3	28.12	0.00	0.19	73.93	0.24	0.00	102.48
4	22.17	0.01	0.04	76.61	0.06	0.00	98.89
5	48.83	0.02	0.04	2.71	45.82	2.52	99.94
6	45.18	0.07	0.17	1.24	52.96	0.00	99.62
7	35.35	0.12	0.05	34.38	27.42	1.19	98.51
8	35.25	0.06	0.11	10.42	57.02	0.08	102.93
9	32.27	0.52	0.03	43.37	19.98	0.00	96.17

1–2 Unidentified Cu arsenide, block e4.
3–4 Cu arsenide, algodonite, block e4.
5 Grey arsenide block 3.
6 Grey arsenide block e4.
7–9 Cu-Ni arsenides block e4.

6 Discussion

6.1 Diagenesis, burial history and the timing of native copper formation

The native copper mineralisation in the Littleham Mudstone Formation displays a complex relationship with the diagenesis of the mudstone-siltstone strata, and is closely associated with the development of uraniferous and vanadiferous concretions /referred to colloquially as “fish-eyes” – Craik-Smith, 1999/. These relationships enable the formation, and subsequent alteration, of the native copper to be correlated with the burial and uplift history of the Permian strata.

The earliest mineralogical phenomenon observed in these rocks is the development of minor fine iron oxide, probably largely responsible for the hematite identified in bulk XRD analyses. In the coarser silt and sand laminae, it is seen to form very fine dust rims on the surfaces of detrital quartz grains that are trapped beneath later authigenic quartz overgrowths. The iron oxide is also associated with altered detrital grains of magnetite, ilmenite, biotite and chlorite, suggesting that it is sourced from the breakdown of detrital ferromagnesian grains and iron oxides. Similar early authigenic hematite is reported from other Permo-Triassic rocks and is attributed to synsedimentary or very early near-surface diagenetic alteration – eodiagenesis (Burley, 1984; Strong and Milodowski, 1987; Strong et al, 1994/. This early hematite imparts the red colouration to the strata and is a common feature of all continental “red-bed” strata /e.g. Plant et al, 1999/.

The inclusion of detrital quartz grains with quartz overgrowths, within many of the native copper sheets, shows that the copper post-dates the quartz authigenesis. The quartz inclusions are highly corroded, indicating that the copper grew (at least partially) by replacement along coarser, and presumably more permeable, sediment laminae. Inclusions of minor amounts of native silver are associated with the copper (Section 5.2). In some cases euhedral grains of silver occur as inclusion within, therefore pre-dating, the later stages of copper growth. Elsewhere, silver is more intimately intergrown with the copper, implying that the two metals coprecipitated. Authigenic vanadian illite or white mica (probably similar to roscoelite identified in earlier studies /Harrison, 1975; Nancarrow, 1985/ occurs either as inclusions or as patchy intergrowths in the native copper, as well as within the uraniferous-vanadiferous “fish-eye” concretions, suggesting a close temporal association with the copper mineralisation.

One of the samples (block B2) was also found to contain relict cross-fibre vein calcite preserved as corroded inclusions within the copper sheets. Cross-fibre veins form by incremental crack-seal mechanism /Ramsey, 1980; Barker, 1990/, which is considered to provide strong evidence for hydrofracturing, possibly related to conditions of overpressuring /Shearman et al, 1972; Ramsey, 1980; Stonely, 1983; Barker, 1990/. The presence of this calcite within the native copper clearly demonstrates that the Littleham Mudstone Formation was buried sufficiently deep for compactional dewatering to occur, producing overpressured porewater conditions, prior to the copper mineralisation. In the case of B2, the copper-mineralising fluid re-utilised the planes of weakness along bedding that were originally opened up by hydrofracturing, accompanied by calcite veining. The development of overpressured porewaters within the Littleham Mudstone Formation also suggests that burial of the sequence was possibly quite rapid, and that

drainage of porewaters during burial and compaction was inhibited. Most probably drainage was limited by the low permeability of the mudstones and siltstone, and dewatering along the thin siltstone or fine sandstone bedding laminae offered the most permeable pathways for pore fluid movement.

Other observations from sample B1 demonstrate that significant sediment compaction was ongoing during, or continued after, native copper sheet formation. These copper sheets are extensively deformed by compaction around a competent diagenetic uraniferous "fish-eye" concretion, which is itself cemented by a complex assemblage of nickel arsenides, copper arsenide, cuprite, chalcocite, uranium silicate and vanadian illite. Native copper also occurs within the "fish-eye" concretion, both as disseminated grains and as thin sheets developed along bedding laminae. However, within the nodule the copper sheets are significantly thinner than where they extend outside the concretion. It appears that the development of the concretion inhibited further growth and thickening of copper sheets. Only copper sheets outside of the nodule continued to grow and thicken. This implies a close temporal relationship between the development of the copper sheets and the growth of uraniferous-vanadiferous concretions.

The observation of compactional deformation of the copper sheets around "fish-eye" concretions demonstrates both copper mineralisation and concretion development occurred prior to the maximum compaction of the Littleham Mudstone Formation. This has an important implication for the potential age of the native copper sheets. Within the Wessex Basin, these Permian rocks are overlain by a very thick sequence of Triassic, Jurassic and Cretaceous strata, and it is estimated that the overlying Triassic Sherwood Sandstone Group will have been buried to depths of up to 2.5 km, firstly at the end of the Jurassic and secondly at the end of the Cretaceous /Chadwick, 1985/. However, sediment compaction and dewatering occurs mainly during early stages of burial (1–2 km depth) and decreases exponentially. Sequence decompaction calculations for Wessex Basin strata /Chadwick, 1985/ suggest that Permian strata achieved maximum compaction by end-Toarcian (i.e. end-lower Jurassic). Although the Littleham Cove sequence will not have been buried as deeply as strata in the basin depocentre further east, it is probable that the main compaction effects in the mudstones will have occurred at similar times. This places important constraints on the potential age of the native copper sheets, implying they had formed at least by the end of the Lower Jurassic (176 Ma) and in reality may be somewhat older (possibly Triassic in age) since it pre-dates the main compaction effects.

The dewatering of the Permo-Triassic strata during compaction could have produced the mineralising fluids responsible for transporting the copper and associated silver, nickel, cobalt, arsenic, uranium and vanadium mineralisation. By analogy with geochemical modelling of similar metalliferous mineralisation assemblages from other red-bed sequences /Plant et al, 1999/ it also seems feasible that copper-rich solutions could have been derived through reductive leaching of the Permo-Triassic strata by these early diagenetic porewaters. The effects of leaching of the strata by reducing fluids is clearly evident from the extensive development of bleached horizons along more permeable bedding laminae and along fractures and faults in the mudstones, and reduction spots. These are associated with the reduction, leaching and loss of fine ferric oxides (hematite). Limited study of the clay mineralogy of the host rocks also indicates that the reduction and bleaching is associated with alteration of the clay mineralogy from a smectite-rich assemblage to an assemblage dominated by illite and chlorite.

It seems very plausible that reducing fluids, enriched in copper and other metals, expelled towards the basin margins during burial compaction and dewatering of the Permo-Triassic sedimentary pile were responsible for the mineralisation observed at Littleham Cove. The dewatering would have most probably have occurred both along more permeable strata (giving rise to the observed bleaching of these horizons) and through permeable fracture damage-zone networks around faults (possibly accounting for the similar bleaching observed around the faults in Littleham Cove). Localised reduction around organic detritus could account for localised reduction spot development. The mineralisation does not necessarily require an extraneous hydrothermal source such as was proposed earlier by Harrison /1975/.

6.2 Alteration of the native copper

The native copper sheets from Littleham Cove display a complex alteration sequence. Overall, the alteration is dominated by copper oxides. This is the earliest alteration product observed and comprises principally cuprite (Cu_2O), with probable minor tenorite (CuO). The cuprite forms colloform corrosion layers on the copper surface and localised lobate embayments that "eat" into the copper metal. The alteration of the copper to copper oxide(s) indicates that pore fluids moving through the Littleham Mudstone Formation became more oxidising after the formation of native copper.

Copper oxide alteration was followed by copper and nickel arsenides and sulphide (chalcocite) mineralisation. These minerals form growth fringes on the surfaces of the native copper and cuprite, partially replacing the underlying copper and cuprite substrate. Their formation indicates a return to more reducing porewater conditions. Copper arsenide (algodonite, Cu_6As) is the earliest alteration product. It also appears to be closely associated with the dissolution of native silver, where is can be found as alteration fringes on the native copper walls of dissolution cavities after native silver grains. This is followed by the deposition of often thick alteration rims of grey nickel arsenide (chemically similar to maucherite, $Ni_{11}As_8$ but which has distinctly different optical properties) with minor chalcocite. Thin alteration fringes of bright nickel arsenides (including niccolite, NiAs), sometimes accompanied by copper arsenide, copper-nickel arsenide and uranium silicate (probably coffinite) form the latest sulphide-arsenide alteration. These arsenides with minor sulphides also cement discrete growth bands of the "fish-eye" concretion in sample B1. These preserve an open-packed framework of included detrital grains, and pre-dates major compaction of the enclosing sediment. As discussed above (Section 6.1), these concretions formed early in the burial history of the Littleham Mudstone Formation, before the end of the Lower Jurassic and possibly during the Triassic. By implication, the alteration of the native copper to this assemblage of arsenides and sulphides is geologically very old (i.e. >176 Ma).

Extensive late-stage alteration to complex intergrowths of copper oxides, copper sulphates and malachite was evident in only one sample (block e4). However, traces of blue surface staining by secondary copper carbonates is seen in hand specimen on the exposed copper surfaces of the other samples. In block e4, the oxide-sulphate alteration partly replaces earlier cuprite as well as affecting the native copper, and is at least partly related to the oxidation of copper sulphide (?chalcocite). Secondary U arsenate and U-Ca-phosphate minerals occur in the adjacent host rock in close association with the late-stage copper oxide-sulphate alteration. Late malachite is present as late alteration in all

samples, mostly minor but in Block b4 (new sample) it is quite extensively developed. This was a block found loose on the surface of the recent mudflows and, therefore, has been subject to recent weathering. Extensive copper carbonate staining and impregnation of malachite was also observed on exposed surfaces of bleached sandstone and siltstone horizons at outcrop. Most of this alteration probably relates to late-stage weathering processes. Some of this alteration includes the formation of copper chlorides, which would be consistent with interaction with recent seawater at outcrop.

All of the native copper plates from Littleham Cove are composites of very thin sheets of copper typically only 1–2 mm thick. Although all the sheets display alteration, and in some cases are completely breached by corrosion, most sheets still preserve a significant thickness (i.e. 30–80%) of the original thickness of the copper. Relatively few of the individual sheets within the composite plates are completely replaced by copper oxides or other alteration products. It demonstrates that even thin sheets of copper can remain intact within a compacted clay matrix for many millions of years. A peculiar phenomenon of the alteration is that corrosion largely affects only one surface of the copper sheets, and in many cases the opposite surface of the metal remains fresh and intact. Furthermore, individual thin copper sheets within the composite copper plates typically display alteration on the same surface which implies a strong directional control on the alteration and mineralisation on the copper surfaces. However, no obvious differences in the nature of the enclosing sediment either side of the copper sheets could be found that could explain the difference in alteration between opposite surfaces. Possibly the alteration is controlled by some sort of electrolytic process, but this is difficult to envisage since the copper sheets display no obvious features that could explain either passivation of one surface of the copper sheet, or for electrochemical differences between the opposing sheet surfaces.

7 Conclusions

- Native copper occurs as thin plates, up to 160 mm in diameter, which are parallel to bedding in the Permian Littleham Mudstone Formation at Littleham Cove (near Budleigh Salterton) in south Devon. The copper is very pure (>99.4% Cu) but is accompanied by minor amounts of native silver (also pure - >99%) which occurs as small inclusions within the native copper.

- The native copper plates are made up of composite stacks of individual thin copper sheets each 1–2 mm thick.

- The native copper mineralisation has a close temporal association with the formation of uraniferous and vanadiferous concretions ("fish-eyes") in the same rocks. Petrographical relationships indicate that both the copper and the "fish-eye" concretions formed during burial diagenesis but before the maximum compaction of the host mudstone and siltstone. The regional burial history of the Wessex Basin /Chadwick, 1985/, indicates that the maximum compaction of the Permian strata would have been achieved by at least the end of the Lower Jurassic (possibly even in the Triassic). Therefore, the native copper sheets are older than 176 Ma.

- The native copper sheets display a complex sequence of alteration and subsequent mineral growth of minerals on their surfaces. The earliest alteration was to copper oxides – principally cuprite with minor tenorite, indicating a change to more oxidising groundwater conditions. This was followed by the dissolution of native silver and the growth of fringes of copper arsenides, nickel arsenides and chalcocite, associated with the precipitation of uranium silicates in the later stages of alteration. This suggests a return to a more reducing porewater environment. Again, petrographical relationships indicate that this alteration and subsequent mineralisation is geologically old (i.e. Lower Jurassic or older).

- Secondary malachite, intimately intergrown copper sulphate and copper oxides, copper chloride, copper-uranium arsenate and uranium vanadates have formed as late-stage alteration products of the native copper and earlier diagenetic cuprite, chalcocite, copper-nickel arsenide and uranium silicate alteration and mineralisation. This late-stage alteration is most probably attributable to near-surface weathering processes.

- Although the native copper is affected by corrosion, the study has shown that a significant proportion (30–80% of the original thickness) of the copper sheets has been preserved in the saturated compacted clay environment of the Littleham Mudstone for many millions of years, at least since the end of the Lower Jurassic. Apart from the recent weathering effects due to exposure at outcrop, most of the observed corrosion and alteration of the native copper is geologically old and also occurred before the end of the Lower Jurassic. This demonstrates that the native copper can remain stable in a saturated and compacted clay environment for geological timescales (over 176 Ma) well in excess of the timescales considered for Performance Assessment. Since the copper sheets found in the Littleham Mudstone Formation are very thin (1–2 mm) and have survived over this long time, waste

canisters – which will be made from much thicker copper – would be expected (by comparison) to show greater performance.

8 Acknowledgements

The authors thank Dr Lars Werme of SKB and Dr Virginia Oversby for their valuable discussions and for their review comments which improved the original manuscript. Dr Richard Scrivener (BGS, Exeter) is thanked for his useful advice in support of the field work undertaken for this project, and Dr Andrew Chadwick is thanked for providing helpful information on the burial history and timing of compaction of the Permian strata in the Wessex Basin.

References

Allen D J, Holloway S, 1984. The Wessex Basin. Investigation of the Geothermal Potential of the UK. British Geological Survey Report.

Barker A J, 1990. Introduction to metamorphic Textures and Microstructures. Blackie & Son Limited, Glasgow & London.

Bateson J H, 1987. Geochemical and geophysical investigations of the Permian (Littleham Mudstone) sediments of part of Devon. British Geological Survey, Mineral Reconnaissance Programme Report, 89.

Beddoe-Stephens B, 1980. Uraniferous “fish-eyes” in the Upper Carboniferous red marls from Warwickshire. British Geological Survey, Mineralogy & Petrology Brief Report, Report No. 258.

Bresle Å, Saers J, Arrhenius B, 1983. Studies in pitting corrosion on archaeological bronzes. SKBF/KBS TR 83-05, Swedish Nuclear Fuel and Waste Management Co.

Burley S D, 1984. Patterns of diagenesis in the Sherwood Sandstone Group (Triassic), United Kingdom. Clay Minerals, 19, 403–440.

Carter G E L, 1931. An occurrence of vanadiferous nodules in the Permian beds of south Devon. Mineralogical Magazine, 22, 609–613.

Carus-Wilson C, 1913. Cupriferous sandstones at Exmouth. Nature, 91, 530.

Chadwick R A, 1985. Permian, Mesozoic and Cenozoic structural evolution of England and Wales in relation to the principals of extension and inversion tectonics. In: Whittaker A (editor). Atlas of Onshore Sedimentary Basins in England and Wales: Post-Carboniferous Tectonics and Stratigraphy, Blackie & Sons Limited, Glasgow.

Chapman N J, McKinley I G, 1987. The Geological Disposal of Nuclear Waste. John Wiley & Sons, Chichester, United Kingdom.

Craik-Smith B, 1999. “Glow in the dark” fish eyes from the Devon coast. Russell Society Newsletter, 35, 42–43.

Durrance E M, 1978. Radon in the stream waters of East Devon. Proceedings of the Ussher Society, 4, 220–228.

Durrance E M, George M C, 1976. Metatyuyamunite from the uraniferous-vanadiferous nodules in the Permian marls and sandstones of Budleigh Salterton, Devon. Proceedings of the Ussher Society, 3, 435–440.

Durrance E M, Meads R E, Ballard R R B, Walsh J N, 1978. Oxidation state of iron in the Littleham Mudstone Formation of the New Red Sandstone Series (Permian-Triassic) of south east Devon. Bulletin of the Geological Society of America, 89, 1231–1240.

Durrance E M, Meads R E, Brindley R K, Stark A G W, 1980. Proceedings of the Ussher Society, 5, 81–88.

Hallberg R, Engvall A-G, Wadsten T, 1984. Corrosion of copper lightning plates. British Corrosion Journal, 19, 85–88.

Hallberg R O, Östlund P, Wadsten T, 1988. Inferences from a corrosion study of a bronze cannon, applied to high level nuclear waste disposal. Applied Geochemistry, 3, 273–280.

Harrison R K, 1975. Concretionary concentrations of the rarer elements in Permo-Triassic red beds of south-west England. Bulletin of the Geological Survey of Great Britain, 52, 1–26.

Harrison R K, Old R A, Styles M T, Young B R, 1983. Coffinite in nodules from the Mercia Mudstone Group (Triassic) of the IGS Knowle borehole, west Midlands. Institute of Geological Sciences Report, 83/10, 12–16.

Henson M R, 1970. The Triassic rocks of south Devon. Proceedings of the Ussher Society, 2, 172–177.

Hoffman B A, 1990. Reduction spheres in hematitic rocks from northern Switzerland: implications for the mobility of some rare elements. Nagra Technical Report, 89–17.

Hoffman B, Dearlove J P L, Ivanovich M, Lever D A, Green D C, Baertschi P, Peters T J, 1987. Evidence of fossil and recent diffusive element migration in reduction haloes from Permian red-beds of northern Switzerland. Proceedings of the Symposium on Natural Analogues, CEC, Brussels, April 1987.

Johnson L H, Tait J C, Shoesmith D W, Crosthwaite J, Gray M N, 1994. Atomic Energy of Canada Limited Report, AECL-10718.

King F, 1995. A natural analogue for the long-term corrosion of copper nuclear waste containers – reanalysis of a study of a bronze cannon. Applied Geochemistry, 10, 477–487.

Marcos N, 1989. Native copper as a natural analogue for copper canisters. Nuclear Waste Commission of Finnish Power Companies, Technical Report, YJT-89-18.

Miller W, Alexander R, Chapman N, McKinley I, Smellie J, 1994. Natural analogue studies in the geological disposal of radioactive wastes. Nagra Technical Report, 93-03.

Nancarrow P HA, 1985. Vanadiferous nodules from the Littleham Marl near Budleigh Salterton, Devon. British Geological Survey, Mineralogy & Petrology Report, 85/12.

Perutz M, 1939. Radioactive nodules from Devonshire, England. Mineralogische und Petrographische Mitteilungen, 51, 141–161.

Plant J A, Jones D G, Haslam H W (editors), 1999. The Cheshire Basin. Basin Evolution, Fluid Movement and Mineral Resources in a Permo-Triassic Rift Setting. British Geological Survey, Keyworth, Nottingham, United Kingdom.

Ponsford D R A, 1955. Radioactivity studies of some British sedimentary rocks. Bulletin of the Geological Survey of Great Britain, 10, 24–44.

Ramsey J G, 1980. The crack-seal mechanism of rock deformation. Nature, 284, 135–139.

Shearman D J, Mossop G, Dunsmore H, Martin M, 1972. Origin of gypsum veins by hydraulic fracture. Transactions of the Institute of mining and Metallurgy (Section B), 93, 149–155.

Smith D B, Brunstrom R G W, Manning P I, Simson S, Shotton F W, 1974. A correlation of Permian rocks in the British Isles. Journal of the Geological Society of London, 130, 1–45.

Stonely R, 1983. Fibrous calcite veins overpressures and primary oil migration. American Association of Petroleum Geologists, 67, 1427–1428.

Strong G E, Milodowski A E, 1987. Aspects of diagenesis of the Sherwood Sandstones of the Wessex Basin and their influence on reservoir characteristics. In: Marshall, J.D. (editor), Diagenesis of Sedimentary Sequences, Geological Society Special Publication, 36, 325–337.

Strong G E, Milodowski A E, Pearce J M, Kemp S J, Prior S V, Morton A C, 1994. The petrology and diagenesis of Permo-Triassic rocks of the Sellafield area, Cumbria. Proceedings of the Yorkshire Geological Society, 50, 77–89.

Tandy B C, 1973. A radiometric and geochemical reconnaissance of the Permian outcrop and adjacent areas in south-west England. Radioactive & Metalliferous Minerals Unit Report, Institute of Geological Sciences, Report No. 315.

Tandy B C, 1974. New radioactive nodule and reduction feature occurrences in the Littleham-Larkbeare area of Devon. Radioactive & Metalliferous Minerals Unit Report, Institute of Geological Sciences, Report No. 316.

Tylecote R F, 1979. The effect of soil conditions on the long-term corrosion of buried tin-bronzes and copper. British Nuclear Fuels Limited Report, Risley, Warrington, October 1979.

Underhill J R, Stonely R, 1998. Introduction to the development, evolution and petroleum geology of the Wessex Basin. In: Underhill, J.R. (editor). Development, Evolution and Petroleum Geology of the Wessex Basin, Geological Society, London, Special Publication, 133, 1–18.

Werme L, 1998. Design premises for canister for spent nuclear fuel. SKB TR-98-08, Swedish Nuclear Fuel and Waste Management Co.

Ziegler P A, 1990. Geological Atlas of Western and Central Europe. Shell Internationale Petroleum Mij Elsevier, Amsterdam.